MULTIPLE POLLUTANT REMOVAL USING THE CONDENSING HEAT EXCHANGER

DOE/PC/95255--T6

Phase I Final Report OCDO--99000515

Start Date: October, 1995
End Date: July, 1997
Issue Date: June, 1998

This report contains no trade secret information

Principal Authors

R. T. Bailey
B. J. Jankura
G. A. Kudlac

McDermott Technology, Inc.
1562 Beeson Street
Alliance, Ohio 44601

This project was sponsored by the U. S. Department of Energy,
the Ohio Coal Development Office (Department of Development, State of Ohio),
the Electric Power Research Institute, and Babcock & Wilcox

US DOE-FETC Contract:	DE-AC22-95PC95255	Ralph T. Bailey
OCDO Grant Agreement:	CDO/D-94-1	FAX: 330-829-7283
McDermott Technology, Inc. Contract:	CRD 1337	Phone: 330-829-7353

McDermott Technology, Inc. assumes no liability with respect to the use of, or for damages resulting from the use of, or makes any warranty or representation regarding any information, apparatus, method, or process disclosed in this report.

McDermott Technology, Inc. expressly excludes any and all warranties either expressed or implied, which might arise under law or custom or trade, including without limitation, warranties of merchantability and of fitness for specified or intended purpose.

DISCLAIMER

DISCLAIMER

Portions of this document may be illegible in electronic image products. Images are produced from the best available original document.

MULTIPLE POLLUTANT REMOVAL USING THE CONDENSING HEAT EXCHANGER

Phase I Final Report

Start Date: October, 1995
End Date: July, 1997
Issue Date: June, 1998

This report contains no trade secret information

Principal Authors

R. T. Bailey
B. J. Jankura
G. A. Kudlac

McDermott Technology, Inc.
1562 Beeson Street
Alliance, Ohio 44601

This project was sponsored by the U. S. Department of Energy,
the Ohio Coal Development Office (Department of Development, State of Ohio),
the Electric Power Research Institute, and Babcock & Wilcox

US DOE-FETC Contract: DE-AC22-95PC95255
OCDO Grant Agreement: CDO/D-94-1
McDermott Technology, Inc. Contract: CRD 1337

Ralph T. Bailey
FAX: 330-829-7283
Phone: 330-829-7353

McDermott Technology, Inc. assumes no liability with respect to the use of, or for damages resulting from the use of, or makes any warranty or representation regarding any information, apparatus, method, or process disclosed in this report.

McDermott Technology, Inc. expressly excludes any and all warranties either expressed or implied, which might arise under law or custom or trade, including without limitation, warranties of merchantability and of fitness for specified or intended purpose.

RC-447

Customer Feedback Questionnaire

Please help us do a better job for you.

11-14-96

Report Title: Multiple Pollutant Removal Using the Condensing Heat Exchanger - Phase I Final Report

Report No.: RDD:98:43456-400-400:01R

Author: R.T. Bailey, B.J. Jankura, G.A. Kudlac Manager: G.A. Farthing

Customer feedback on our work is important to us. We would like to have your comments concerning this report. Your cooperation in completing this form and returning it to the address shown will assist us in improving our service to you.

Do the contents of this report meet your needs? ☐ YES

Not entirely because:

_____

_____

_____

Was this report provided in an acceptable time frame? ☐ YES ☐ NO

Comments:

_____

_____

_____

How could this report have been more useful to you?

_____

_____

_____

_____

Are you the primary recipient of this report? ☐ YES ☐ NO

Thank you.

Name: _____ Date: _____

Organization: _____

Return to: Rodger W. McKain, Vice President
McDermott Technology, Inc.
Research & Development Division
1562 Beeson Street
Alliance, OH 44601

ABSTRACT

The Integrated Flue Gas Treatment (IFGT) system is a new concept whereby a Teflon® covered condensing heat exchanger is adapted to remove certain flue gas constituents, both particulate and gaseous, while recovering low level heat. The pollutant removal performance and durability of this device is the subject of a USDOE sponsored program to develop this technology. The program was conducted under contract to the United States Department of Energy's Fossil Energy Technology Center (DOE-FETC) and was supported by the Ohio Coal Development Office (OCDO) within the Ohio Department of Development, the Electric Power Research Institute's Environmental Control Technology Center (EPRI-ECTC) and Babcock and Wilcox - a McDermott Company (B&W).

This report covers the results of the first phase of this program. This Phase I project has been a two year effort. Phase I includes two experimental tasks. One task dealt principally with the pollutant removal capabilities of the IFGT at a scale of about 1.2MW_t. The other task studied the durability of the Teflon® covering to withstand the rigors of abrasive wear by fly ash emitted as a result of coal combustion.

The pollutant removal characteristics of the IFGT system were measured over a wide range of operating conditions. The coals tested included high, medium and low-sulfur coals. The flue gas pollutants studied included ammonia, hydrogen chloride, hydrogen fluoride, particulate, sulfur dioxide, gas phase and particle phase mercury and gas phase and particle phase trace elements. The particulate removal efficiency and size distribution was investigated. These test results demonstrated that the IFGT system is an effective device for both acid gas absorption and fine particulate collection. Although soda ash was shown to be the most effective reagent for acid gas absorption, comparative cost analyses suggested that magnesium enhanced lime was the most promising avenue for future study.

The durability of the Teflon® covered heat exchanger tubes was studied on a pilot-scale single-stage condensing heat exchanger (CHX®). This device was operated under typical coal-fired flue gas conditions on a continuous basis for a period of approximately 10 months. Data from the test indicate that virtually no decrease in Teflon® thickness was observed for the coating on the first two rows of heat exchanger tubes, even at high inlet particulate loadings. Evidence of wear was present only at the microscopic level, and even then was very minor in severity.

TABLE OF CONTENTS

TABLE OF CONTENTS (Cont'd)

Section **Page**

TABLE OF CONTENTS (Cont'd)

LIST OF FIGURES

TABLE OF CONTENTS (Cont'd)

LIST OF FIGURES

Figure **Page**

TABLE OF CONTENTS (Cont'd)

LIST OF TABLES

EXECUTIVE SUMMARY

McDermott Technology Inc., Research and Development Division entered into contract with the United States Department of Energy (DOE) in September 1995 to study "Multiple Pollutant Removal Using the Condensing Heat Exchanger" under Contract DE-AC22-95PC95255. The program was conducted under contract to the United States Department of Energy's Fossil Energy Technology Center (DOE-FETC) and was supported by the Ohio Coal Development Office (OCDO) within the Ohio Department of Development, the Electric Power Research Institute's Environmental Control Technology Center (EPRI-ECTC) and Babcock and Wilcox - a McDermott Company (B&W). The guidance and support of the project managers from the sponsoring organizations, Thomas J. Feeley III of DOE-FETC, Richard Chu of the OCDO, and Gerry B. Maybach of the EPRI-ECTC, is gratefully acknowledged.

This contract includes two phases with the second phase to be proposed after completing the first phase. Phase I testing was completed at a scale of about 1.3 MW_t. By comparison, the Phase II work will be proposed at a scale of about 10 MW_t. The purpose of this report is to present the results of the Phase I tests.

The purpose of Phase I of this contract was to determine the pollutant removal performance and the anticipated wear life of an Integrated Flue Gas Treatment (IFGT) system using flue gas from coal combustion. The project was divided into four tasks. These included:

Task 1: Project Management,
Task 2: Pollutant Removal tests at ARC
Task 3: Wear tests at ECTC
Task 4: Reporting

Two topical reports have been prepared for this project. The topical reports cover Tasks 2 and 3. The Task 2 Topical Report covers the pollutant removal portion of Phase I. The Task 3 Topical Report covers the wear life segment of this Phase I. The two topical reports will be issued under separate cover. However, since these reports include details that are not present in the main body of this Final report, the technical content of the two topical reports are also included as addenda to the Final report.

In addition to these planned activities, a preliminary economic comparison was made of two versions of the IFGT system versus a conventional limestone forced oxidation scrubbing process that dominates the flue gas desulfurization market. The results of that activity are also reported here.

Integrated Flue Gas Treatment uses two Condensing Heat Exchangers (CHX®) to recover waste heat from the flue gas and remove a variety of pollutants from combustion flue gas. The Teflon® covered internals of the CHX® permits heat recovery at temperatures below the sulfuric acid dew point of the flue gas.

Condensing Heat Exchangers using Teflon® covered heat exchanger tubes are used in the industrial market to recover energy from flue gas, thereby improving the overall thermal efficiency of the combustion process. More than 110 commercial units are in service, with

operating life up to 14 years. These industrial installations have been exclusively gas and oil-fired. Prior to this work, only limited data existed on the pollutant removal efficiency of the IFGT process. Also, the effects of long-term exposure to abrasive fly ash on the integrity of the Teflon® covered heat exchanger tubes was unknown.

Task 2 Overview

Task 2 of this contract was conducted at McDermott Technology's Research Center in Alliance, Ohio. Flue gas was generated using a 1.75 MW_t (6 million Btu/hr) coal-fired Small Boiler Simulator (SBS) combustor. A pilot Integrated Flue Gas Treatment System rated at 1.2 MW_t (4 million Btu/hr) was located downstream of the SBS. The pollutant removal characteristics of the IFGT system were measured over a wide range of operating conditions in four series of tests. Flue gas pollutants of interest included:

- particulate
- sulfur dioxide, chlorides and fluorides
- gas phase mercury, arsenic, and selenium
- particle phase mercury and other particle phase trace elements
- ammonia

The four test series investigated pollutant removal performance using three different coals and three different sulfur scrubbing reagents. The coals tested included a high sulfur coal (Ohio), a medium sulfur coal (Pittsburgh #8) and a low sulfur coal (Powder River Basin). The first three series of tests used sodium carbonate (soda ash) as the scrubbing reagent for each of the three different coals. The fourth test used high sulfur Ohio coal with soda ash, lime and magnesium-lime as the scrubbing reagents.

Lime and magnesium-lime scrubbing reagents were investigated as possible alternatives to sodium carbonate. Soda ash is significantly more expensive than lime per pound of SO_2 removed and can pose a difficult disposal problem if not reclaimed or recycled. Limestone was not tested because a more reactive reagent is needed for the IFGT process to achieve high SO_2 removal with low liquid-to-gas ratios.

Pollutant removal efficiencies were determined by simultaneous measurements of concentration at the inlet and outlet of the IFGT system. The test program investigated the effect of various operating conditions and coal type on pollutant removal. IFGT operating conditions that were varied during the tests included:

- Reagent liquid-to-gas ratio
- Reagent pH
- Flue gas flow rate and outlet temperature
- Fly ash concentration in the flue gas

Comparison of Measured Data to Target Goals

In the Phase I Management Plan, pollutant removal goals were established for the IFGT system to provide a basis for comparison to actual measurements. The goals established in the Management Plan are presented below along with a summary of actual achievements.

SO_2 Removal

Goal	Actual (soda ash)	Actual (mag-lime)
> 95% with a liquid-to-gas ratio (L/G) < 1.34 l/m^3 (10 gal/1000 ft^3)	97% at L/G = 0.60 l/m^3 (4.5 gal/1000 ft^3)	88% at L/G = 0.88 l/m^3 (6.6 gal/1000 ft^3)

The SO_2 removal goal was easily achieved at the targeted test conditions using sodium carbonate reagent. As indicated in the table, the target SO_2 removal was also achieved at a lower L/G than originally specified. This is significant since operation at a lower L/G represents a less costly operating condition in terms of pump power and gas-side pressure drop. Using a mag/lime reagent, an SO_2 removal of 88% was achieved at a low L/G. This is sufficiently high to be considered promising. An SO_2 removal of 95% could be achieved with an increase in L/G or by allowing more time for the buildup of magnesium salts in the recirculating liquid.

Particulate Removal

Particle Size Range	Removal Efficiency Goal (%)	Actual Removal Efficiency (%) (100% Load)	Actual Removal Efficiency (%) (65% Load)
>10 µm	90%	98.7%	97.6%
5 µm to 10 µm	80%	98.8%	96.0%
2 µm to 5 µm	60%	97.1%	79.7%
< 2 µm	25%	76.4%	51.9%

The IFGT system, while not designed to be a primary particulate removal device, does provide substantial particle removal. The targeted particulate removal efficiency is based on a range of particle size, rather than an average over all particle sizes so that the comparisons are not biased by the effect of particle size distribution. At full load, the actual particle removal efficiency exceeded the goal in each of the targeted size fractions. As indicated in the table, the particle removal efficiency decreased with load, as expected, but still exceeded the targeted removal efficiencies.

Chloride and Fluoride Removal

Removal Goal	Actual
> 95% with a liquid-to-gas ratio < 1.34 l/m^3 (10 gal/1000 ft^3)	Chloride: ~98% at L/G= 0.67 l/m^3 (5 gal/1000 ft^3) Fluoride: 83%-99% at L/G = 0.67 l/m^3 (5 gal/1000 ft^3)

As was expected, the removal of chlorides and fluorides with soda ash was as great or greater than the SO_2 removal at similar operating conditions. Hydrogen chloride and hydrogen fluoride are generally more soluble in aqueous solutions than SO_2, and so are preferentially absorbed. This is in agreement with historical performance of wet scrubbers using limestone, lime, or soda ash.

Gas Phase Mercury Removal

Mercury Form	Removal Goal	Actual
Ionic	> 95% for a liquid-to-gas ratio of 1.34 l/m^3 (10 gal/1000 ft^3)	Averaged about 80%
Elemental	+50%	Averaged -23.3% with wide variations

The measured average removal efficiencies for three of four test series show that the goals for gas phase elemental and ionic mercury removal were not achieved. Ionic mercury removal averaged about 80% for the three test series. This is consistent with ionic mercury removal efficiencies measured by others.* Rather than removing any elemental mercury, these tests indicated in most cases that some of the ionic mercury was being reduced to elemental mercury in the IFGT. Whether this phenomenon is actually occurring in the IFGT is uncertain. This trend was consistent in all of the tests during which two different sampling procedures were employed. There exists some concern that this phenomenon is an artifact of the sampling techniques. Regardless, the goal for elemental mercury removal was not achieved. This indicates that the lower operating temperature does not appreciably enhance elemental mercury removal and may, in fact, enhance the reduction of oxidized mercury in the liquid phase.

* Noblett, J.G., "Control of Air Toxics from Coal-Fired Power Plants Using FGD Technology," EPRI Second International Conference on Managing Hazardous Air Pollutants, Washington, D.C., July 13-15, 1993.

Particle Phase Mercury Removal

Goal	Measured Total Particulate Removal (%)	Measured Particulate Mercury Removal (%)
Same total removal as particulate	Pitt #8 coal* : 94.9% PRB coal : 88.9% Ohio coal : 94.1%	Pitt #8 coal : 73.6 ±11.1% PRB coal : 43.8 ±28.2% Ohio coal : 80.0 ±11.0%

As indicated, the removal efficiency for particulate mercury was less than the removal efficiency for the total particulate. The reason for this anomaly is that the particulate mercury is concentrated in the smallest particles (< 2 μm), which are less effectively removed by the IFGT process than the larger particles (> 2 μm). Typically, the mercury concentration in the fly ash at the outlet of the IFGT system was 5 to 10 times greater than the concentration of mercury in the fly ash at the inlet to the IFGT.

For the tests with Pittsburgh #8 and the Ohio #6/#5 coals, the particulate mercury removal averaged about 75%, while the measured removal efficiency for particulate less than 2 micrometers was 76.4%. This indicates that essentially all of the particulate mercury may be contained in the particulate that is less than 2 micrometers.

Vapor Phase Trace Element Removal

No goal was specified for trace element removal other than for mercury, since few of these elements exist in the vapor state in significant quantities. Measurements showed significant vapor phase concentrations of arsenic and selenium for the Ohio and Pittsburgh coals. For these coals, the removal efficiency for vapor phase selenium ranged from 50% to 98%, and the arsenic removal efficiency was greater than 98%. These are significant reductions in the concentrations of these elements.

Particle Phase Trace Element Removal

A goal was not established for particle phase trace elements other than mercury, since these other elements are not at this time considered for regulation. On average, the removal of particle phase trace elements followed the same pattern as for particle phase mercury. The trace elements were concentrated in the fine particulate, and the total particle phase element removal averaged about 80%.

Ammonia and Oxides of Nitrogen Removal

A goal was not established for ammonia (NH_3) and nitrogen oxides (NO_x) removal. For ammonia, the objectives were to evaluate the potential of operating an IFGT in conjunction with an SCR or SNCR system to achieve higher NO_x removal rates by addressing the problem of

* Pitt #8 = Pittsburgh #8; PRB = Powder River Basin; Ohio = 80% Ohio #6 and 20% Ohio #5

ammonia slip. Therefore, tests were conducted to measure ammonia removal through the IFGT system, and estimate the amount of ammonia that reacts with SO_3 before the IFGT system. The inlet ammonia concentration ranged from 31 ppm to 94 ppm and removal efficiency ranged from 57% to 93%. All ammonia tests were conducted at full load. The amount of ammonia that reacts with SO_3 before the IFGT system was estimated by comparing the measured and calculated ammonia concentration at the IFGT inlet based on the ammonia injection rate. The ammonia reduction attributable to ammonia-sulfur reactions ranged from 27% to 45%, and averaged 36%.

The absorption of NO_x as expected, was not significant. The initial measurements of NO_x at the inlet and outlet of the IFGT indicated that NO_x removals were too small to quantify.

Task 3 Overview

Task 3 of this contract was conducted at the Electric Power Research Institute's (EPRI) Environmental Control Technology Center (ECTC) near Barker, New York. A single-stage CHX® unit was installed downstream of the ECTC electrostatic precipitator. The unit was operated as a heat recovery unit to determine the effects of long-term exposure to fly ash under typical flue gas conditions.

Standard operating parameters (flue gas flows and temperatures, cooling water temperatures, etc.) were monitored and recorded by the ECTC data acquisition system over the course of the program. In addition, periodic visual inspections and Teflon® film thickness measurements were performed to determine the amount of wear. Finally, replications of the Teflon® film surface were made to both document the general physical condition of the Teflon® surface and allow for detection of wear at the microscopic level. Surface replications are made by moistening a strip of cellulosic film in acetone, laying the strip on the tube surface, and allowing to dry. The physical characteristics of the tube surface are thus exactly duplicated on the cellulosic film.

The wear test unit was operated for over 6,200 hours during the test program. A summary of the operating conditions is shown in the table below.

Summary of CHX® Operating Conditions at the ECTC

Time of Operation	6,240 hours
Inlet Gas Flow	1,275 scmh (750 scfm)
Inlet Gas Temperature	150°C (300°F)
Inlet Water Temperature	55 to 60°C (130 to 140°F)
Outlet Gas Temperature	82 to 93°C (180 to 200°F)
Outlet Water Temperature	76 to 80°C (170 to 175°F)
Inlet Particulate Loading (average)	25 mg/dscm (0.02 lb/10^6 Btu) 2,060 hours 400 mg/dscm (0.35 lb/10^6 Btu) 4,180 hours
Tube Wash Cycle	20 minutes every 8 hours

Five inspection trips were made over the course of the test program. During each trip, visual inspections, Teflon® thickness measurements and surface replications were performed.

No visible signs of wear were evident over the course of the test program. Minor amounts of fly ash deposition, not removed by the normal wash cycle, were detected after 5,000 hours of operation. These deposits were located several rows down from the top of the tube manifold and were attributed to inadequate wash water flow rates. A new wash nozzle manifold (3 nozzles vs. 1 nozzle) was installed following the 5,000 hour inspection. The end of test inspection revealed virtually no ash deposition.

Data from the Teflon® thickness measurements indicated no significant decrease in the tube film thickness. Measurements were made at several locations on each of the tubes in the top two rows of the tube bank. Over the course of the test program, the Teflon® film thickness increased approximately 7-10% (30.5 to 50.8 μm [0.0012 to 0.002 inch] of a nominal 508 μm [0.020 inch] film) after roughly 2,000 hours of operation then showed no subsequent signs of decrease. This initial thickness increase has been attributed to a relaxation of surface stresses in the Teflon®. These surface stresses are a result of the manufacturing process, and stress relaxation occurs when the Teflon® film is heated. A graphical summary of the Teflon® thickness measurements is given for the first row of tube in the figure below.

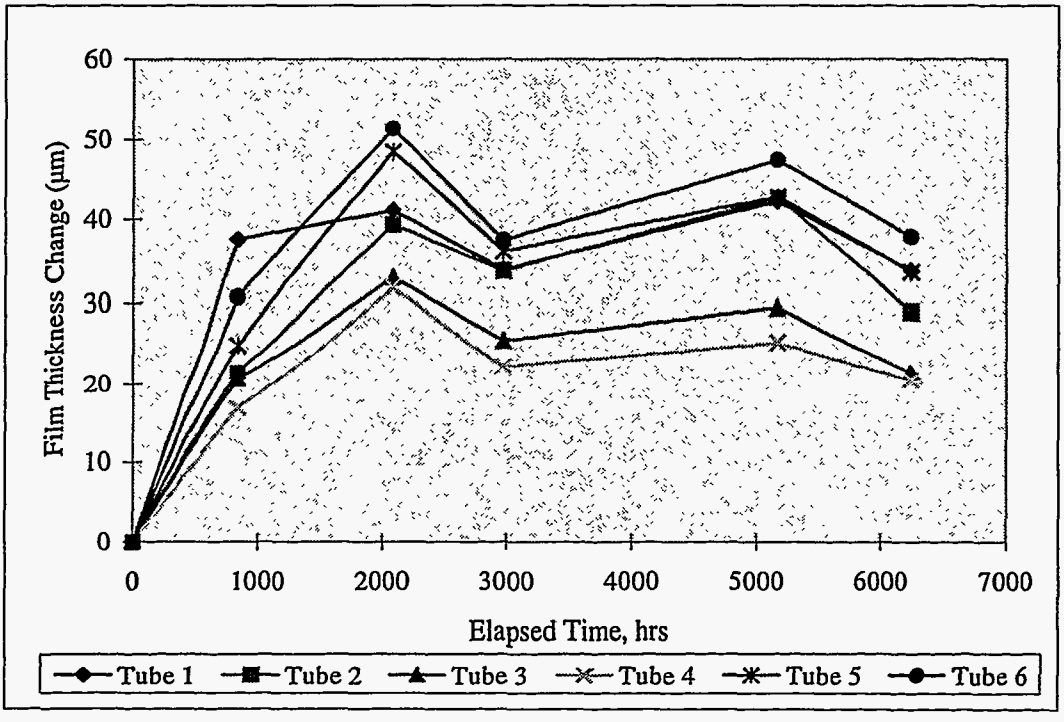

Cumulative Change in Teflon® Film Thickness as a Function of Time for Tubes 1 through 6

Evaluation of the film surface replications revealed no significant wear damage to the Teflon® covering. Very minor wear damage was visible on tube 6, which was subject to the highest flue gas flow rate. This damage, however, was on the μm scale and is of the same magnitude as the

surface striations created during manufacture and should pose no problems for extended operation.

Preliminary Comparative Economic Analysis

A comparative economic analysis was performed of the IFGT system against the conventional limestone forced oxidation (LSFO) system. Two versions of the IFGT system were considered. The first employed soda ash as the reagent and the second used magnesium promoted lime. The analysis was based on a plant life of 30 years, a 70% load factor and a capital levelization factor of 15.2%. The analysis was based on a plant size of 100 MW_e. The comparative annualized costs are presented here as follows:

Limestone Forced Oxidation:	$3,620,000
Soda Ash based IFGT:	$3,635,000
Mg Lime based IFGT:	$2,689,000

While the comparative costs of the soda ash based IFGT are essentially equivalent to the conventional LSFO system, the mag-lime based IFGT compares very favorably. This economic advantage, though based on many assumptions and of a very preliminary nature, offers sufficient advantage to warrant further detailed study.

Conclusions

Task 2

The Task 2 goals for the project were met or exceeded in all cases except for vapor phase mercury removal. The goals for mercury removal were based, in part, on the relatively high gas-liquid contact area of the condensing heat exchanger, the high reactivity of the sodium reagent, and the relatively lower operating temperature of the IFGT process compared with other flue gas clean-up technologies. That this goal - for vapor phase mercury removal - was not realized indicates that temperature and surface area by themselves will not provide reductions in elemental mercury at typical flue gas concentrations. Other methods of promoting elemental mercury capture were beyond the scope of work for this project.

The Task 2 results show that the IFGT process is an effective multiple pollutant removal system that can also provide an improvement in thermal efficiency. The data measured in this Task provides the basis for predictions of the performance of an IFGT system for both utility and industrial applications. This data is needed to provide performance guarantees as well as to evaluate the economic cost and benefit of an IFGT system.

Task 3

Based on the operational and inspection data collected over the course of the test program, the following conclusions are drawn:

- No significant wear was observed for any of the Teflon® tube coverings. Minor microscopic wear detected on some tubes is insignificant and should pose no problems for extended operation.
- Particulate deposition can be a problem, especially at higher particulate loadings and insufficient wash water flows. Increasing the wash water flow rate by modifying the wash nozzle manifold essentially eliminated particulate deposition.
- Teflon® life expectancy should be greater than 10 years. Tube replacement will more likely be required due to operational problems other than abrasive wear.

Economic Comparison

The IFGT system offers sufficient economic advantage to warrant further experimental and engineering study, especially with respect to the mag-lime based system.

1.0 INTRODUCTION

1.1 Background

The 1990 Clean Air Act Amendments address the need to reduce the quantity of pollutants released to the atmosphere. Some pollutants are currently regulated and additional species are targeted for control in the near future. The emission of SO_2 and particulate from electric utilities is currently regulated under the Phase I and Phase II requirements defined in Title IV. An additional 189 substances, classified as hazardous air pollutants, have been identified for regulation under Title III of the Clean Air Act Amendments. The Title III requirements will be imposed across approximately 750 source categories. Cluster rules are also being established to set emission standards for specific industries. Many state and local agencies are already imposing stringent regulations on hazardous pollutants, such as mercury. There is a need for equipment to remove the pollutants of concern in a cost-effective manner. Most of the commercial pollutant removal equipment suffers from three major drawbacks:

1) Commercially available pollution removal equipment is parasitic, that is, they consume energy during operation. A typical coal-fired power plant will have a 2-4% or more reduction in power generation capacity when commercial SO_2 and particulate removal equipment is added for gas clean up.

2) Commercially available flue gas clean up equipment generally treats only one pollutant at a time. Separate units are installed for each pollutant to be removed.

3) Most of the commercial flue gas clean up equipment used in the electric utility industry cannot be economically scaled down for industrial coal-fired applications. Capital cost and operating cost of these units are often prohibitive for the smaller energy producer.

1.1.1 Commercial Condensing Heat Exchanger

An untapped source of energy from coal-fired units is the waste heat in the flue gas released to the stack. The efficiency of a boiler can be significantly increased by decreasing the flue gas exit temperature. One means of lowering the exit temperature is to use a condensing heat exchanger to recover both sensible and latent heat from the flue gas. Condensing Heat Exchangers (CHX®) using Teflon®-covered internals are widely used to recover waste heat from flue gases. The Teflon® covering protects the heat exchanger components from corrosion as the temperature of the flue gas drops below the acid dew point. The most common applications to date, are boilers firing oil or natural gas. Single-stage commercial condensing heat exchangers have provided satisfactory performance and lifetimes for more than one hundred industrial installations for the past fourteen years.

Commercial condensing heat exchangers remove both sensible and latent heat from the flue gas in a single unit. Figure 1.1 is a drawing of a typical condensing heat exchanger application. It shows the heat exchanger along with the support equipment provided for a retrofit application.

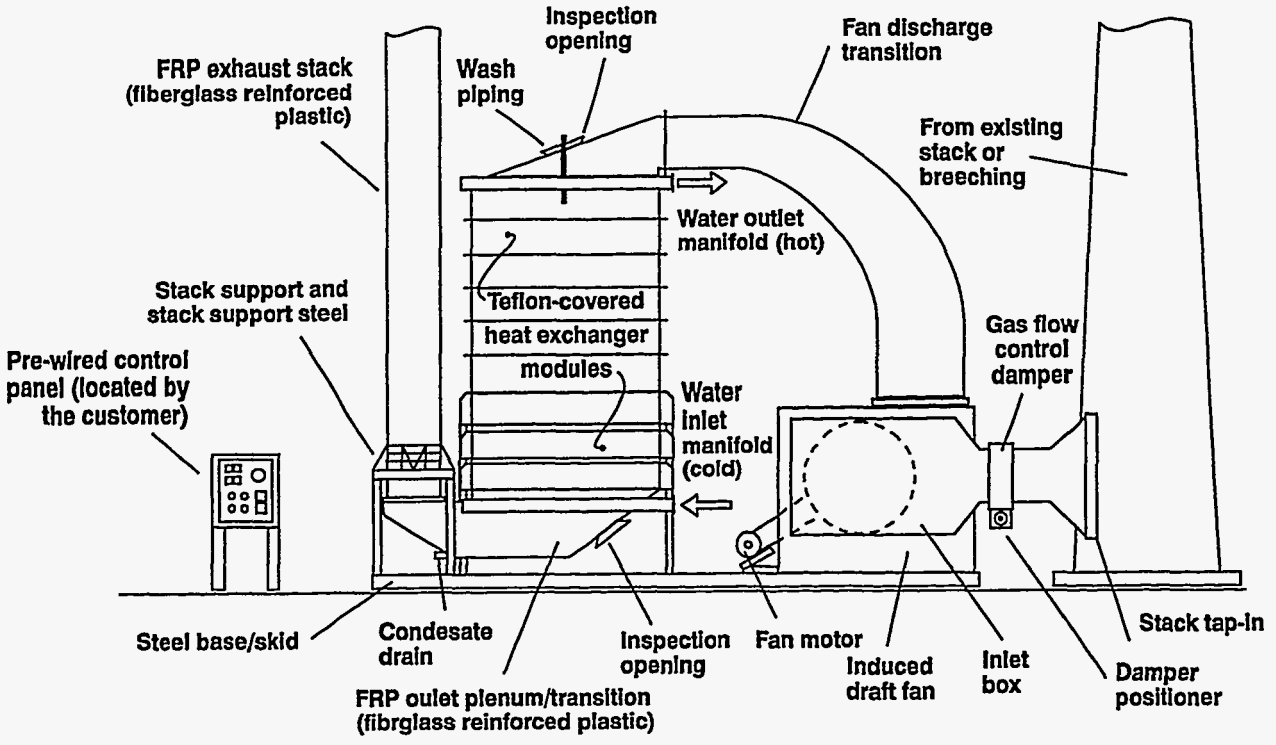

Figure 1.1 Condensing Heat Exchanger of the CHX® Design

The flue gas passes down through the heat exchanger while the water passes upward in a serpentine path through the tubes. Condensation occurs within the heat exchanger as the gas temperature at the tube surface is brought below the dew point. The condensate falls as a constant rain over the tube array and is drained at the bottom. Some cleaning of the gas can occur within the heat exchanger as the particulate impact the tubes and acid gas condensation occurs.

Commercial designs are optimized for removing heat and ensuring adequate lifetime of the unit. Heat exchanger tubes are made of Alloy 706 (10% nickel and 90% copper), a material commonly used in boiler water applications. Each tube is covered with Teflon® extruded over the outside of the tube. Since Teflon® is hydrophobic, condensation on the surface of the tube occurs in drops rather than in a film. This allows continuous exposure of most of the surface and improves heat transfer.

Teflon® is also durable and resistant to abrasion by solid particles in the gas. Fly ash will not stick to the Teflon® tubes. The inside surfaces of the heat exchanger shell are covered with Teflon® sheets. During fabrication, the Teflon®-covered tubes are pushed through the Teflon® tube sheet lining to form a Teflon®/Teflon® seal, ensuring that all heat exchanger surfaces exposed to the flue gas are protected against acid corrosion. Interconnections between the heat exchanger tubes are made outside the tube sheet and are not exposed to the corrosive flue gas stream.

A commercial condensing heat exchanger is made up of heat exchanger modules that can be stacked in series in the gas stream. This modular design allows the size of the unit to be optimized for each application at minimum cost. To ensure the lifetime of the Teflon® covering

on the tubes, the inlet gas temperature is limited to 260°C (500°F), a condition easily satisfied in most flue gas waste heat recovery applications.

1.1.2 Integrated Flue Gas Treatment System

A recent innovation to the commercial condensing heat exchanger design, called the Integrated Flue Gas Treatment (IFGT) system, exhibits improved pollutant removal from the flue gas while recovering waste heat. The IFGT system is a two-stage condensing heat exchanger. Most of the sensible heat is removed from the gas in the first heat exchanger stage. The second heat exchanger stage can be operated in a condensing mode, recovering latent heat from the gas while removing pollutants. The top of the second heat exchanger stage is equipped with an alkali reagent spray system to enhance SO_2 and particulate removal. Pollutant removal mechanisms in the IFGT include condensing (for water, some organic compounds, and some acid gases and trace metals), impaction (for particulate), and gas absorption (for removal of SO_2, and other acid gases). In an IFGT, several pollutants are treated using a single device - while recovering waste heat. Because of its modular design, it can be easily built for a wide range of applications. An additional benefit realized by using the IFGT system is the proportional reduction in carbon dioxide released per MW of generated electricity because of the increase in plant efficiency.

The IFGT condensing heat exchanger is expected to effectively remove air toxics still present in the flue gas that penetrate upstream pollution removal devices (i.e., baghouse or electrostatic precipitator). The vapor phase air toxics that routinely pass through these removal devices include mercury, selenium and arsenic. Low temperature operation and gas-liquid contact inherent to the IFGT promotes the removal of air toxics in the gas phase and present on the fine particulate.

It has been proposed to use an IFGT system downstream of a selective catalytic reduction (SCR) or selective non-catalytic reduction (SNCR) unit to remove the remaining ammonia in the flue gas. SCR and SNCR devices utilize the injection of ammonia into the flue gas upstream of the SCR/SNCR zones. The ammonia is the reducing agent. Invariably, excess ammonia is injected. The excess that remains in the flue gas is referred to as ammonia slip. NO_x removal can be increased by increasing the ammonia injected into the flue gas, but because of ammonia slip, local atmospheric emission limits may be exceeded for ammonia. By capturing the excess ammonia in the IFGT, higher concentrations of ammonia can be injected upstream of the SCR thereby increasing NO_x removal without increasing ammonia emissions to the atmosphere.

1.2 Phase I Technical Program

In the Phase I Proposal, two primary technical issues were identified that needed to be resolved to bring the IFGT Process to commercial practice for coal-fired applications;

1) The pollutant removal performance of the IFGT system, and

2) The expected lifetime for the Teflon®-covered tubes that comprise the heat exchanger surface when exposed to flue gas containing fly ash from coal combustion.

Item 1 has been addressed in Phase I and is reported in the Task 2 Topical Report for this project. The Task 2 Topical Report provides the results of pollutant removal tests conducted at McDermott Technology Inc.'s, Alliance Research Center. Task 2 investigated the removal performance of the IFGT process for a variety of flue gas pollutants. These included SO_2, NO_x, particulate, mercury and other trace elements, chloride and fluoride compounds, and ammonia.

Four series of tests (series I through IV) were conducted using four coals and three reagents. The coals included two blends of Ohio #5 and Ohio #6 coals, a Powder River Basin coal, and a Pittsburgh #8 coal. The different coals were selected to represent high, medium, and low sulfur content and also represent several different classifications of coal used by the utility industry. The Pittsburgh coal was selected for its sulfur content and also because this coal is used at the Kintigh Station, the site of the Environmental Control Technology Center (ECTC) and the planned location for Phase II testing.

The reagents tested included sodium carbonate, lime and magnesium enhanced lime (mag-lime*). The IFGT process was originally designed for the industrial market, and the sodium-based reagent provided a highly reactive reagent that required a minimum of preparation before use. For utility applications, sodium reagents are costly and represent a significant disposal problem if not reclaimed or recycled. Although sodium-based regenerable scrubbing systems have been used in the utility industry (Wellman Lord and dual alkali systems) they are not widely accepted. Lime and magnesium-lime reagents are typically less reactive than sodium, but are less costly and pose a much simpler disposal problem.

The goal of Task 2 was to determine the pollutant removal efficiencies of the IFGT process and the functional dependence on process parameters so that reliable predictions of performance can be made for commercial coal-fired applications.

The Task 3 Topical Report deals primarily with erosive wear. One of the major questions that must be addressed before the IFGT can be considered viable for coal-fired applications is the expected material lifetime for the Teflon® covering on the tubes. Commercial condensing heat exchangers with Teflon®-covered parts have exhibited lifetimes of over 14 years, but these have been clean fuel (oil or natural gas) applications. Tests on coal-fired units have been limited in duration.

To address the material lifetime issue for coal-fired applications, a long-term wear test was included in Phase I of this project as Task 3 -- "Long-Term Wear Testing". The specific goal of this task is to determine the amount of wear, if any, on the Teflon®-covered internals of the heat exchanger. The location of maximum material wear in an IFGT will be at the inlet of the first heat exchanger stage. This is where the flue gas and Teflon® coverings are the hottest, the flue gas velocity and particulate loading the highest, and where the particulates first impact the Teflon®-covered tubes. It is expected that the top rows of tubes in an IFGT will experience the maximum wear due to fly ash abrasion. A single-stage condensing heat exchanger unit was used for the material lifetime demonstration since the inlet conditions will be the same as for an IFGT.

---

* Mag lime is a physical mixture of magnesium oxide and calcium oxide. It is typically manufactured from Dolomite. The MgO is usually less than 6% by weight of the total.

Visual and physical examinations were performed on the top rows of tubes at periodic intervals during the one-year demonstration.

1.3 Preliminary Economic Comparison

To provide guidance for the continued development of the IFGT system, an economic comparison was made with the base technology used in the Flue Gas Desulfurization (FGD) industry on utility scale boilers. That base technology is "Limestone Forced Oxidation Wet Scrubbing (LSFO)". The comparative cost analysis was performed by the B&W Company, the Company's manufacturer of LSFO systems. The cost comparison was made with two versions of the IFGT system. The first uses soda ash and the second uses mag-lime. The results of this analysis are presented here as part of the section titled Results and Discussion.

2.0 FACILITIES

2.1 Integrated Flue Gas Treatment System

The IFGT condensing heat exchanger, shown schematically in Figure 2.1 is designed to enhance the removal of pollutants from the flue gas stream. The IFGT design uses many of the same heat exchanger components found in the commercial CHX® design, so unit lifetimes are expected to be comparable to current commercial units. The pilot facility at B&W's Alliance Research Center is essentially full scale in the vertical direction, with a stack of seven heat exchanger modules in the first stage and a stack of eight modules in the second heat exchanger stage. The cross-sectional area of the heat exchanger shell is 0.3 m by 0.46 m (1 ft. X 1.5 ft).

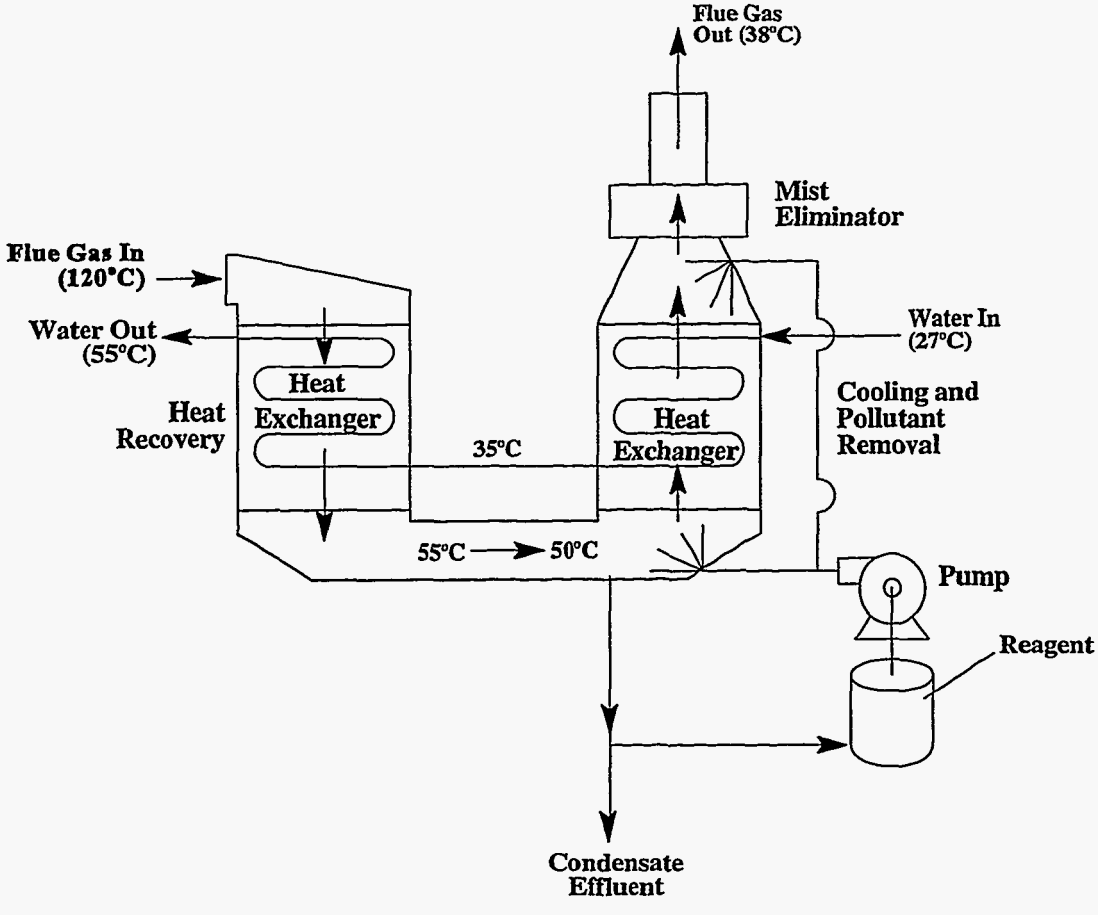

Figure 2.1 Schematic of an Integrated Flue Gas Treatment System

The IFGT system consists of four sections: the first heat exchanger stage, the interstage transition region, the second heat exchanger stage, and the mist eliminator. The major differences between the integrated flue gas treatment design and the conventional condensing heat exchanger design are:

1) the integrated flue gas treatment design uses two heat exchanger stages instead of one,

2) the interstage transition region, located between the two heat exchanger stages, is used to direct the gas to the second heat exchanger stage, acts as a collection tank, and allows treatment of the gas between the stages,

3) the gas flow in the second heat exchanger stage is upward, rather than downward,

4) the top of the second heat exchanger stage is equipped with an alkali reagent spray system, and

5) the mist eliminator is used to remove any alkali spray and condensed droplets from the flue gas.

Most of the sensible heat is removed from the gas in the first heat exchanger stage of an IFGT system. The transition region can be equipped with water or alkali sprays to saturate the flue gas with moisture and assist removal of pollutants and particulate from the gas. The inter-stage transition piece is made of corrosion resistant fiberglass-reinforced plastic. Usually, the second heat exchanger stage is operated in the condensing mode, removing latent heat from the gas along with pollutants. The gas in this module flows upward and countercurrent to the liquid. This provides a scrubbing mechanism that enhances particulate impaction and gas absorption. The dimensions and spacings of the heat exchanger tubes ensures that the particulate impact wet tubes where droplet condensation is taking place. Sub-micron size particles act as condensation sites in the gas. This enhances collection by impaction. These small particles also come into contact with the wetted tubes by Brownian diffusion.

The mechanisms described above primarily address the removals of particulate and condensible vapors. Additional flue gas processing is still needed, however, to provide adequate removal of SO_2 from the flue gas. To achieve this, the top of the second heat exchanger module is equipped with an alkaline spray system. The condensed gases, particulate, and alkaline spray are collected at the bottom of the transition section. The condensate from the flue gas provides a portion of the water requirements for the spray system. In some applications, all of the water requirements can be met with condensate, thereby reducing or eliminating fresh water demands. This improves the attractiveness of the process by reducing the fresh water requirements. A condensate/reagent blow down stream is used to maintain the process chemistry.

The spray/disengagement region consists of three plastic sections installed above the second heat exchanger stage. Each section is about 0.46 m (1.5 ft) in height. The three plastic sections contain the second-stage reagent spray nozzles and two sets of chevron style mist eliminators. They also provide a disengagement zone for liquid drops entrained in the flue gas as it exits the second heat exchanger stage. The mist eliminators are designed to capture any droplets entrained by the flue gas as it passes upwards through the counter flowing liquid.

An alkali reagent tank is used to mix fresh reagent with the recirculating solution/slurry. For example, sodium carbonate is added to the solution in the tank with a pH controlled variable speed screw feeder. A mixer stirs the solution in the tank to dissolve the sodium carbonate. The scrubbing solution and condensate collected at the bottom of the interstage transition during operation is gravity fed to the reagent tank. As originally constructed, and during initial testing, the reagent tank was equipped with an overflow drain to remove accumulated water and dissolved solids inventory due to condensation, makeup water addition, and the accumulated reaction products. To improve reagent utilization, the overflow connection was later moved - after Test Series I - to the reagent return line from the interstage transition.

The scrubbing solution can be directed to the top of the second stage heat exchanger or to the transition section. The fiberglass interstage transition located between the two heat exchanger stages is equipped with six spray nozzles.

2.2 SBS/IFGT Pilot Plant Facility

Flue gas for the pollutant removal test was provided by a pilot scale furnace designated as the Small Boiler Simulator (SBS). This 1.75 MW_t (six million Btu/hr) combustion research facility includes fuel preparation and handling equipment, a furnace and convection pass that provided a typical flue gas time-temperature history, a heat exchanger, dry scrubber module and a bag house. Figure 2.2 shows an isometric view of the major components of the SBS facility and how they are connected to the pilot IFGT condensing heat exchanger. The IFGT facility is in a bypass loop downstream of the SBS induced draft fan.

The coal burner used for these tests is a low NO_x burner equipped with dual air zones. The same burner with the same nominal air register settings was used for all of the test coals. Although designed as a Low NO_x burner, it was not operated as such during these tests. NO_x concentrations typically ranged from 300 ppm to 400 ppm. The furnace load was set to provide the required flue gas flow rate and was essentially constant at 1.3 MW_t (4.4 million Btu/hr) for all tests.

The heat exchanger downstream of the SBS convection pass is a two-pass shell and tube construction with cooling water in the shell and flue gas passing through the tubes. The heat exchanger is used to reduce the flue gas temperature at the outlet of the SBS convection pass from a temperature of about 370°C (700°F) to a temperature of about 150°C (300°F). The 150°C flue gas temperature is an upper limit for the bag house, and is also the typical operating temperature of the dry scrubber when in service.

The SBS bag house typically removes 99.9+% of the particulate from the flue gas leaving the furnace. For these tests a measurable particle loading at the IFGT unit was needed to characterize the particle removal efficiency of the IFGT system. To provide a measurable particle loading at the CHX® facility, approximately 10% to 20% of the flue gas from the SBS

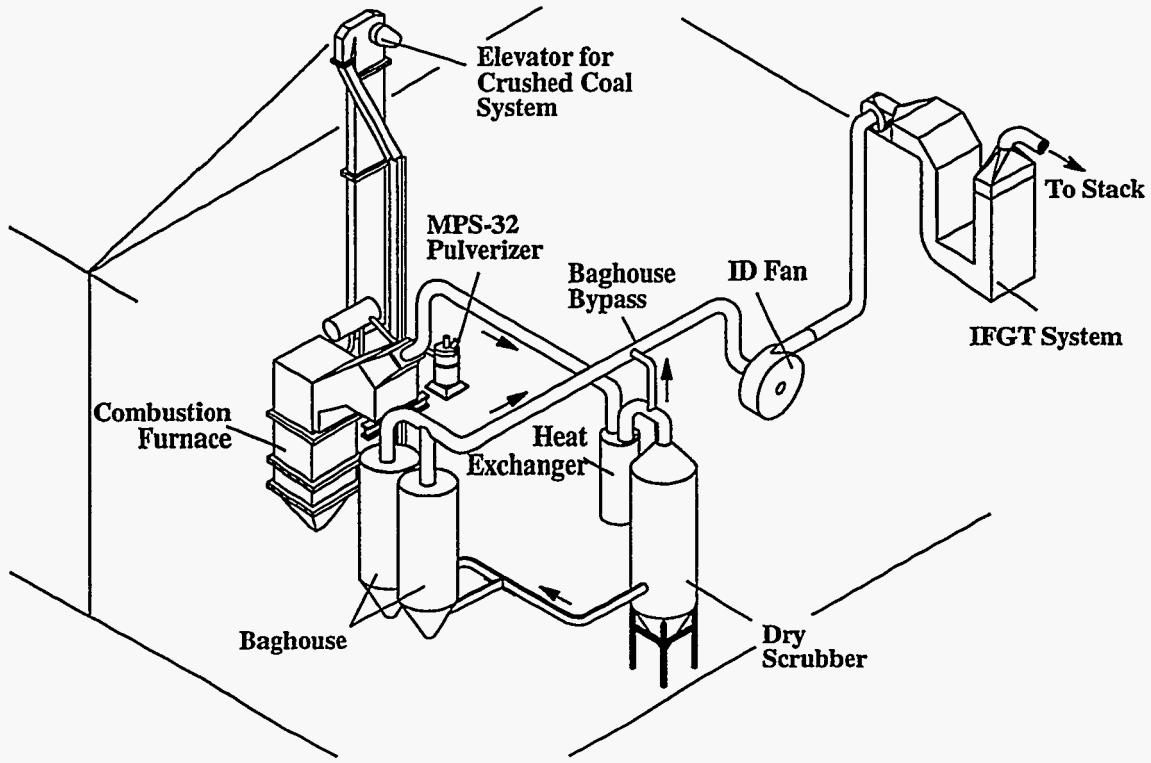

Figure 2.2 SBS/IFGT Pilot Plant Facility

furnace was bypassed around the bag house. The dry scrubber module was not used for these tests, but provided the gas path from the heat exchanger to the bag house. Heat loss and air infiltration downstream of the bag house limited the flue gas temperature at the inlet of the IFGT system to about 120°C (250°F).

Flue work brings the exhaust gas from the SBS to the pilot IFGT. The 305 mm (12 inch) insulated flue is tied into the exhaust of the SBS downstream of the baghouse and I.D. fan. The flue gas enters at the top of the first heat exchanger stage and exits out the top of the second heat exchanger stage. A 305 mm non-insulated PVC flue is installed at the exit of the pilot IFGT to an exhaust stack placed outside the building.

Gas sampling lines and 102 mm (4 inch) ports for in-situ sampling are located at the inlet and outlet of the IFGT facility. The heated gas sample lines provide a continuous flow of flue gas for the on-line gas analyzers. One gas sample line is in the inlet duct just upstream of the first heat exchanger stage. The other gas sample line is in the PVC outlet duct. Heat-traced lines are used to transport the flue gas samples from the ducts to the gas analyzers. Two 102 mm (4-inch) ports are installed both in the inlet and in the outlet flue gas ducts for particulate sampling and other gas sampling as required by the test program.

The facility is equipped with instrumentation to measure the flow rate and temperatures of the IFGT process streams, including the flue gas, cooling water, reagent flow rate to the nozzles, blowdown stream and make up water.

2.3 ECTC/CHX® Pilot Plant Facility

The Environmental Control Technology Center (ECTC) was used to provide the flue gas to the wear test CHX® unit for this test program. The ECTC is a comprehensive test facility for evaluating advanced emissions control technologies applied to high sulfur coals. The test facility utilizes about one percent of the flue gas available from the 662 MW Kintigh Station, a pulverized coal boiler operated by the New York State Electric and Gas Corporation (NYSEG) near Barker, New York.

A flow schematic of the ECTC facility is shown in Figure 2.3. The facility is operated 24 hours a day, allowing long-term continuous tests to be performed. The pilot CHX® unit was installed in

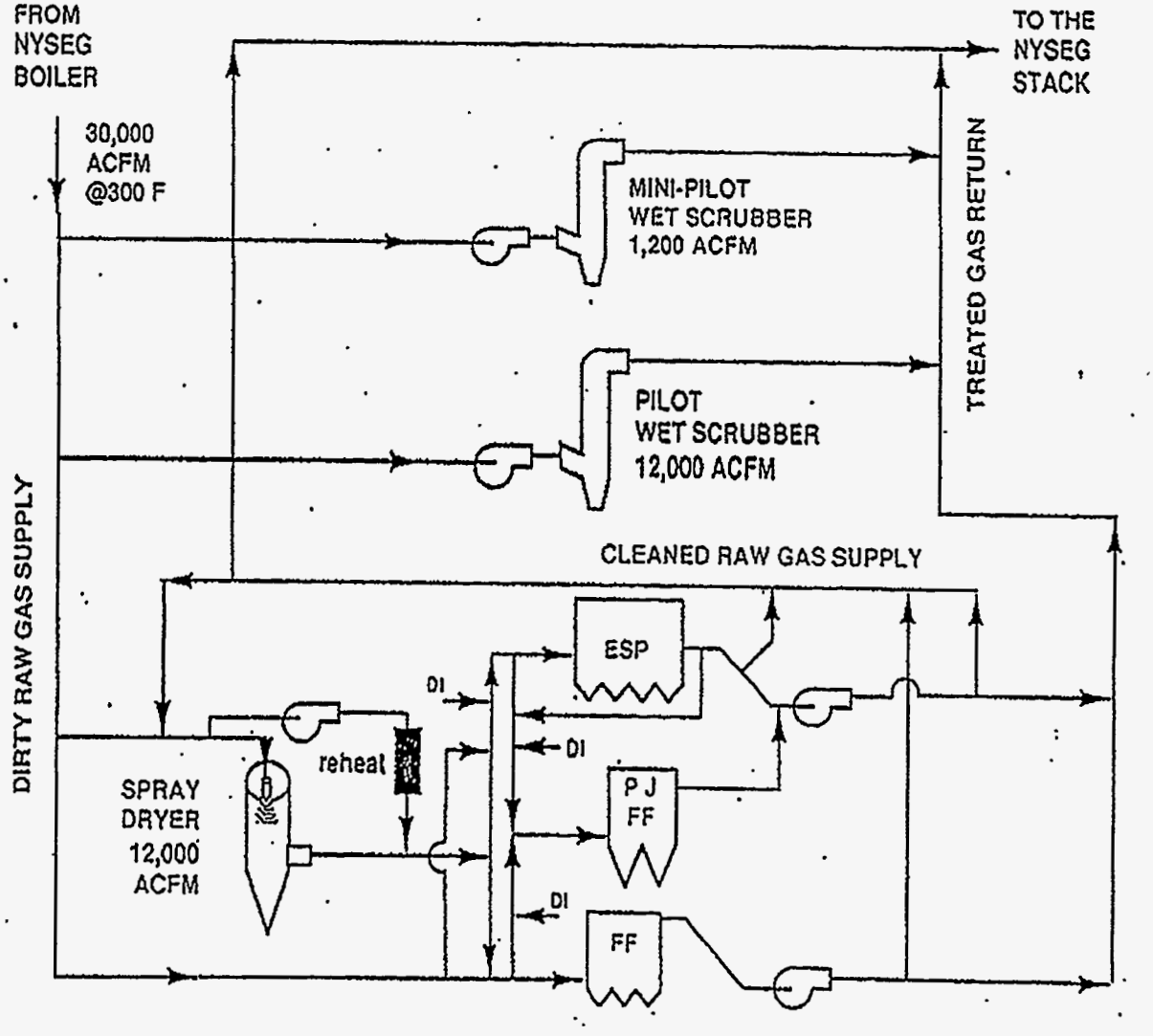

Figure 2.3 Gas Flow Schematic of the ECTC Facility

the mini-pilot wet scrubber sub-loop of the ECTC. This loop has a flue gas flow capacity of 2040-2550 acmh (1200-1500 acfm), sufficient to provide the "design" flue gas velocity of 12.2 m/sec (40 ft/sec) between the tubes at the inlet of the heat exchanger. To reproduce expected commercial conditions, the unit used a slipstream from the flue gas after it exits the electrostatic precipitator (ESP). The pilot CHX® test unit was located downstream of the ESP in place of the mini-pilot wet scrubber.

The CHX® unit used for the wear test is a skid-mounted, single-stage unit as shown in Figure 2.4. In addition to the heat exchanger, the unit is also equipped with a flue gas inlet control damper, water pump, and water circulation tank. The internal dimensions of the heat exchanger are 30.87 cm by 36.51 cm (12 5/32 inches by 14 3/8 inches). There are six heat exchanger tubes in each

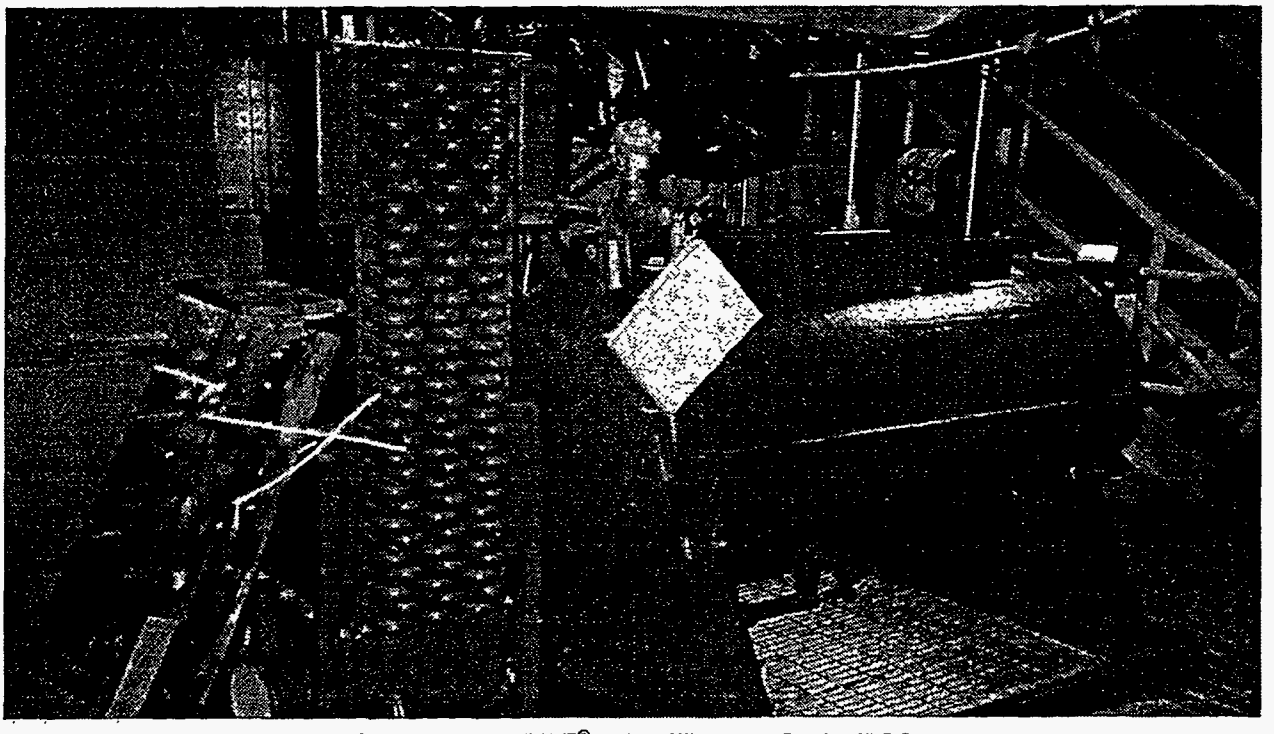

Figure 2.4 CHX® Pilot Unit at the ECTC

row and 32 rows of tubes. The heat exchanger tube rows are staggered from each other (triangular pitch) so that there is no open line of sight from the top to the bottom of the heat exchanger. The CHX® pilot test unit heat exchanger is operated with countercurrent flow, with the flue gas entering the top of the heat exchanger and exiting at the bottom, and the cooling water entering the bottom row of tubes and exiting the top row. The flue gas inlet plenum is removable, allowing access to the top of the heat exchanger for inspection of the Teflon® film on the top rows of tubes.

Data from the CHX® pilot test unit and ECTC equipment was collected and recorded by the ECTC data acquisition system. In addition, ECTC personnel maintained an hourly log of the major test parameters, including gas and water flows and temperatures, and ESP operating conditions.

3.0 TEST DESCRIPTION

3.1 Pollutant Abatement

The experimental test program completed for the SBS/IFGT facilities was designed to investigate the effect of the primary system operating parameters on pollutant removal and is discussed below. The SBS/IFGT facilities were operated from 5 to 12 days on each coal to characterize the performance of the IFGT system. Four coals were tested. These coals are described in Table 3.1. The Pittsburgh #8 coal was also used at the ECTC for the wear tests. Tests using that coal will provide a link to the 5.0 MW IFGT tests at the ECTC scheduled for Phase II.

Table 3.1 Coal Analyses

Coal		80% Ohio #5 20% Ohio #6 Test Series I	Pittsburgh # 8 Test Series II	Powder River Basin Test Series III	80% Ohio #6 20% Ohio #5 Test Series IV
C	% by wt.	69.15	75.08	58.74	75.58
H_2	% by wt.	5.03	5.09	4.05	5.24
S	% by wt.	3.85	2.58	0.44	3.07
O_2	% by wt.	7.01	5.45	14.48	8.79
N_2	% by wt.	1.37	1.5	0.96	1.41
H_2O	% by wt.	6.93	0.92	15.12	2.83
Ash	% by wt.	6.66	9.38	6.21	5.08
Heating Value - wet basis (Btu/lb)		12538	13438	10049	13320
Arsenic	ppm_m	12.43	7.92	1.59	7.47
Barium	ppm_m	3.24	25.26	493.50	3.85
Beryllium	ppm_m	0.15	0.63	0.11	0.83
Cadmium	ppm_m	0.70	0.05	0.09	0.19
Cobalt	ppm_m	0.78	0.91	1.43	0.53
Chromium	ppm_m	46.58	0.34	9.26	1.23
Manganese	ppm_m	15.75	9.29	28.20	6.19
Nickel	ppm_m	22.11	18.93	13.14	42.70
Lead	ppm_m	5.71	2.58	3.05	6.01
Selenium	ppm_m	1.56	1.17	0.12	1.90
Mercury	ppm_m	0.43	0.10	0.41	0.13
Chlorides	ppm_m	2200	123	134	1900
Fluorides	ppm_m	25.8	<11	46	25.6

Tables 3.2 through 3.5 summarize the completed test matrix for test series I, II, III, and IV. Each matrix is grouped according to the different types of pollutant removal under study. The first three test series evaluated removal efficiencies for various gas phase, and particulate phase species with different coals and soda ash. The fourth test series evaluated the ability of the soda ash, lime and mag-lime to capture SO_2, mercury, and heavy metals, and investigated the use of mesh pads for providing fine particulate control. The HCl and HF measurements conducted in test series IV repeated measurements that were made earlier in the program and showed relatively poor HCl removal efficiencies compared to all other test data. Mesh pads were also used in test series IV for assisting fine (submicron) particulate removal. The mesh pads were positioned in the interstage of the IFGT system. Particle loading and size distribution measurements were made at the inlet and outlet of the IFGT system.

During each test series, several large samples of blowdown waste water were collected in 35 gallon drums. This condensate waste will be used to evaluate disposal methods in Phase II of the program. Additionally, smaller samples of the blowdown were collected to determine the chemistry of the waste water and to test for mercury, particulate, and other heavy metals.

3.1.1 Acid Gas Absorption

In these tests, SO_2 and NO_x removal, and HCl and HF removal were evaluated. SO_2, HCl, and HF removal was evaluated during all four test series. Numerous tests were conducted on each coal so that sufficient data was collected to determine the removal characteristics of the IFGT for these gas phase pollutants.

At high pH with Na_2CO_3, or $Ca(OH)_2$, the rate controlling resistance to mass transfer of SO_2 is from the gas phase to the liquid surface. Above a pH of about 6.5, the vapor pressure of SO_2 in the liquid is negligible. Under these conditions, the major factors for SO_2 removal performance are the amount of gas-liquid surface area in the 2nd stage of the IFGT and flue gas velocity. When the pH of the absorbing solution falls below about 6.5, the liquid phase SO_2 vapor pressure increases which contributes to a measurable reduction in the absorption of SO_2. To investigate these effects, the test matrix included conditions at a variety of pH, flue gas inlet velocity, and liquid-to gas ratio (L/G). The SO_2 tests were conducted with continuous gas concentration monitors at the IFGT inlet and outlet. Therefore, the test durations were relatively short. Once the inlet and outlet SO_2 levels stabilized, approximately 10 to 20 minutes was required to collect operating data from the Data Acquisition System and other instruments, and to collect process stream samples.

The absorption of NO_x occurs by mechanisms similar to SO_2. However, approximately 95% of NO_x is in the form of NO with the remaining being principally NO_2. The solubility of NO is less SO_2 by a factor of about 1300. As will be described later, NO_x absorption proved at the outset of testing to be negligible and testing for NO_x absorption was curtailed for subsequent tests.

The test matrix for each test series included one test to investigate HCl and HF removal. The HCl and HF removal efficiency was quantified across the IFGT utilizing EPA methods and required approximately two hours to complete a single test.

Table 3.2 Test Series I Completed Test Matrix

Test ID	pH	Flue Gas Outlet Temperature (°C)	Flue Gas Inlet Velocity (m/s)	Stage 2 L/G Ratio (l/m^3)	Particulate Loading (mg/dscm)	IFGT Inlet NH3 Concentration (ppm_v)	Stage 2 Steam Injection (kg/hr)
SO_2 and NO_x Removal and Heat Recovery							
1	8	Dewpoint	12	0.07	<14 to 420		
2	8	Dewpoint	12	0.13	<14 to 420		
3	8	Dewpoint	12	0.27	<14 to 420		
4	8	Dewpoint	12	0.67	<14 to 420		
5	8	Dewpoint	12	1.07	<14 to 420		
7	8	Dewpoint	6	2.14	<14 to 420		
8	8	Dewpoint	6	0.27	<14 to 420		
9	8	Dewpoint	6	0.67	<14 to 420		
10	8	Dewpoint	6	1.07	<14 to 420		
11	8	Dewpoint - 11	12	0.07	<14 to 420		
12	8	Dewpoint - 11	12	0.13	<14 to 420		
13	8	Dewpoint - 11	12	0.27	<14 to 420		
14	8	Dewpoint - 11	12	0.67	<14 to 420		
15	8	Dewpoint - 11	12	1.07	<14 to 420		
16	7	Dewpoint	12	0.07	<14 to 420		
17	7	Dewpoint	12	0.27	<14 to 420		
18	7	Dewpoint	12	1.07	<14 to 420		
19	6	Dewpoint	6	0.07	<14 to 420		
20	6	Dewpoint	6	0.27	<14 to 420		
21	6	Dewpoint	6	1.07	<14 to 420		
22	7	Dewpoint - 11	6	1.88	<14 to 420		
23	7	Dewpoint - 11	6	1.34	<14 to 420		
24	7	Dewpoint - 11	6	0.40	<14 to 420		
25	7	Dewpoint - 11	6	0.67	<14 to 420		
26	7	Dewpoint - 11	6	1.07	<14 to 420		
HCl and HF Removal							
4A	8	Dewpoint	12	0.67	420		
Hg and Heavy Metals Metals Removal							
4B	8	Dewpoint	12	0.67	420		
4C	8	Dewpoint	12	0.67	<14		
14D	8	Dewpoint - 11	6	0.67	420		
Ammonia Removal							
4	8	Dewpoint	12	0.67	420	50	
4F	8	Dewpoint	12	0.67	420	10	
14G	8	Dewpoint - 11	12	0.67	420	50	
Particulate Removal							
4J	8	Dewpoint	12	0.67	0.3	---	45.3
Particulate Removal - Cascade Impactor							
4L	8	Dewpoint	12	0.67	0.3	---	0
14M	8	Dewpoint - 11	12	0.67	0.3	---	0
4N	8	Dewpoint	12	0.67	0.3	---	45.3

Table 3.3 Test Series II Completed Test Matrix

Test ID	pH	Flue Gas Outlet Temperature (°C)	Flue Gas Inlet Velocity (m/s)	Stage 2 L/G Ratio (l/m^3)	Particulate Loading (mg/dscm)	IFGT Inlet NH3 Concentration (ppm_v)
SO_2 Removal and Heat Recovery						
1	8	Dewpoint	12	0.07	<14 to 28	
2	8	Dewpoint	12	0.13	<14 to 28	
3	8	Dewpoint	12	0.27	<14 to 28	
4	8	Dewpoint	12	0.67	<14 to 28	
5	8	Dewpoint	12	1.07	<14 to 28	
6	8	Dewpoint	6	0.27	<14 to 28	
7	8	Dewpoint	6	0.67	<14 to 28	
8	8	Dewpoint	6	1.07	<14 to 28	
9	6	Dewpoint	12	0.07	<14 to 28	
10	6	Dewpoint	12	0.27	<14 to 28	
11	6	Dewpoint	12	0.67	<14 to 28	
12	7	Dewpoint	12	0.07	<14 to 28	
13	7	Dewpoint	12	0.27	<14 to 28	
14	7	Dewpoint	12	0.67	<14 to 28	
16	6	Dewpoint	6	0.67	<14 to 28	
17	6	Dewpoint	6	0.27	<14 to 28	
18	6	Dewpoint	6	1.07	<14 to 28	
19	6	Dewpoint	6	0.80	<14 to 28	
20	7	Dewpoint	6	0.27	<14 to 28	
21	7	Dewpoint	6	0.67	<14 to 28	
22	7	Dewpoint	6	1.07	<14 to 28	
23	7	Dewpoint - 11	6	0.47	<14 to 28	
24	7	Dewpoint - 11	6	1.27	<14 to 28	
25	7	Dewpoint - 11	6	0.27	<14 to 28	
26	7	Dewpoint - 11	6	0.67	<14 to 28	
27	7	Dewpoint - 11	6	1.07	<14 to 28	
HCl and HF Removal						
4B	8	Dewpoint	12	0.67	<14 to 28	
Hg and Heavy Metals Metals Removal						
4A	8	Dewpoint	12	0.67	<14 to 28	
4C	8	Dewpoint	12	0.67	42 to 420	
Ammonia Removal						
4D	8	Dewpoint	12	0.67	<14 to 28	50
4E	8	Dewpoint	12	0.67	<14 to 28	20
4F	8	Dewpoint - 11	12	0.67	<14 to 28	50
Particulate Removal						
4F	8	Dewpoint - 11	12	0.67	<14 to 28	50
Particulate Removal - Cascade Impactor						
4G	8	Dewpoint	12	0.67	42 to 420	---

Table 3.4 Test Series III Completed Test Series

Test ID	pH	Flue Gas Outlet Temperature (°C)	Flue Gas Inlet Velocity (m/s)	Stage 2 L/G Ratio (l/m^3)	Particulate Loading (mg/dscm)	IFGT Inlet NH3 Concentration (ppm_v)
SO2 Removal and Heat Recovery						
1	NC	Dewpoint	12	0.00	420 to 830	
2	NC	Dewpoint	12	0.40	420 to 830	
3	4	Dewpoint	12	0.40	420 to 830	
4	4	Dewpoint	12	0.20	420 to 830	
5	5	Dewpoint	12	0.40	420 to 830	
6	5	Dewpoint	12	0.20	420 to 830	
7	6.5	Dewpoint	12	0.40	420 to 830	
8	6.5	Dewpoint	12	0.20	420 to 830	
9	8	Dewpoint	12	0.40	420 to 830	
10	8	Dewpoint	12	0.20	420 to 830	
11	8	Dewpoint	6	0.80	420 to 830	
12	8	Dewpoint	6	0.40	420 to 830	
13	5	Dewpoint	6	0.80	420 to 830	
14	6.5	Dewpoint	6	0.40	420 to 830	
15	nc	Dewpoint - 11	12	0.40	420 to 830	
16	6.5	Dewpoint - 11	12	0.40	420 to 830	
17	6.5	Dewpoint - 11	12	0.20	420 to 830	
15R	NC	Dewpoint - 11	12	0.20	420 to 830	
HCl and HF Removal						
7A	6.5	Dewpoint	12	0.40	420 to 830	
Hg and Heavy Metals Metals Removal (See Note 1)						
9A	8	Dewpoint	12	0.40	420 to 830	
12A	8	Dewpoint	6	0.40	420 to 830	
Ammonia Removal						
7B	6.5	Dewpoint	12	0.40	420 to 830	20
9B	8	Dewpoint	12	0.40	420 to 830	50
18	8	Dewpoint - 11	12	0.40	420 to 830	50
Particulate Removal						
9B	8	Dewpoint	12	0.40	420 to 830	20
12C	8	Dewpoint	6	0.40	420 to 830	----
Particulate Removal - Cascade Impactor						
12B	8	Dewpoint	6	0.40	420 to 830	----
12D	8	Dewpoint	6	0.40	420 to 830	----

Table 3.5 Test Series IV Completed Test Matrix

Test ID	Feed pH	Return pH	Flue Gas Outlet Temperature (°C)	Flue Gas Inlet Velocity (m/s)	Stage 2 L/G Ratio (l/m^3)	Particulate Loading (mg/dscm)	Reagent	Mesh Pad
SO_2 Removal and Heat Recovery								
1	8	--	Dewpoint	12	0.53	420 to 830	Sodium Carbonate	
2	8	--	Dewpoint	6	0.53	420 to 830	Sodium Carbonate	
3	8	--	Dewpoint	12	0.80	420 to 830	Hydrated Lime	
4	10	--	Dewpoint	12	1.07	420 to 830	Hydrated Lime	
5	10	--	Dewpoint	12	0.53	420 to 830	Hydrated Lime	
6	8	--	Dewpoint	12	0.53	420 to 830	Hydrated Lime	
7	8	--	Dewpoint	12	1.07	420 to 830	Hydrated Lime	
8	6	--	Dewpoint	12	0.80	420 to 830	Hydrated Lime	
9	6	--	Dewpoint	12	0.53	420 to 830	Hydrated Lime	
10	6	--	Dewpoint	12	1.07	420 to 830	Hydrated Lime	
12	--	8	Dewpoint	12	0.13	420 to 830	Mag-Hydrated Lime	
13	--	8	Dewpoint	12	0.27	420 to 830	Mag-Hydrated Lime	
14	--	7	Dewpoint	12	0.53	420 to 830	Mag-Hydrated Lime	
14R1	--	6	Dewpoint	12	0.53	420 to 830	Mag-Hydrated Lime	
15	--	7	Dewpoint	12	1.07	420 to 830	Mag-Hydrated Lime	
16	--	6	Dewpoint	12	0.27	420 to 830	Mag-Hydrated Lime	
HCl and HF Removal								
1A	8	--	Dewpoint	40	0.53	420 to 830	Sodium Carbonate	
Hg and Heavy Metals Metals Removal								
14A	8	7	Dewpoint	12	0.53	420 to 830	Mag-Hydrated Lime	
Particulate Removal								
2A	8	--	Dewpoint	6	0.53	420 to 830	Sodium Carbonate	None
Particulate Removal - Cascade Impactor								
1B	8	--	Dewpoint	12	0.53	420 to 830	Sodium Carbonate	Interstage
2B	8	--	Dewpoint	6	0.53	420 to 830	Sodium Carbonate	None

3.1.2 Mercury and Heavy Metals Removal

The ability of the IFGT to remove mercury and heavy metals from the flue gas and the fate of the mercury was also determined. A total of eight test conditions were completed. Mercury speciation measurements were conducted at both the inlet and outlet of the IFGT to quantify total, elemental, and oxidized mercury removal for each of the coals evaluated. Quantifying the individual specie is important since each species has different chemical and physical properties. The main forms of mercury emitted in flue gas are elemental (Hg^o) and oxidized (Hg^{++}). Previous SBS measurements indicate that the total mercury emissions were within the expected range of 1-10 $\mu g/m^3$ (0.7 to 7 lb/trillion Btu) for coal-fired boilers.

Mercury species are removed from the flue gas by either condensation of Hg^o or absorption of Hg^{++} into the liquid. Condensation of Hg^o is usually not complete as the trace metal

concentration is relatively low. However, this test series was based on the hope that the lower outlet flue gas temperature of the IFGT (35°C, 90°F) compared to a commercial wet scrubber (50°C, 122°F) may provide for higher levels of elemental mercury condensation.

Mercury concentration measurements were conducted on the following process streams:

- coal feed
- IFGT inlet and outlet gas flows and particulate
- IFGT condensate/blowdown
- baghouse ash

Under steady-state operating condition, measurements were conducted in triplicate for all eight test conditions to determine the repeatability of the data. Each test required approximately two hours of sample time. Blanks were also run in order to assess the uncertainty in the measurements and to detect unknown sources of contamination.

3.1.3 Ammonia Removal

During ammonia removal tests ammonia was injected upstream of the IFGT system at a constant measured flow rate. Below 230°C (450°F) ammonia reacts with sulfur trioxide (SO_3) in the flue gas, so that some of the ammonia may be removed from the flue gas upstream of the IFGT. Ammonia removal tests were conducted only during the first three test series. A matrix of 3 tests was completed during each test phase for a total of nine tests. For all of these tests, removal efficiency was based on measurements at the inlet and outlet of the IFGT. A Severn Sciences continuous ammonia analyzer was used to sequentially measure the ammonia concentration upstream and downstream of the IFGT. Differences between the measured and calculated concentration based on the injection rate of ammonia at the IFGT inlet were used as a measure of the ammonia-sulfur reactions.

3.1.4 Particulate Removal

These tests determined the overall particulate removal efficiency of the IFGT facility and the removal efficiency as a function of particle size. The particulate loading to the IFGT facility consisted of the fugitive emissions from the SBS baghouse, and a portion of the flue gas from the SBS that was diverted around the baghouse and fed directly to the IFGT. Approximately 20% of the flue gas bypassed the SBS baghouse.

A total of eight cascade impactor tests were completed to measure the particulate size distribution. Andersen Mark III cascade plate impactors were utilized for all particulate sizing tests. Additional total particulate measurements were obtained as part of the sampling for mercury and acid gases. For those measurements, the sampling technique requires collection of particulate as well as the gas sample. Thirty-one total particulate concentration measurements were completed.

The effect of steam injection on particulate removal was investigated in this test program. It has been postulated that the addition of steam to flue gas can enhance the removal of fine particulate. Supersaturating the flue gas causes condensation to occur on particulate, resulting in particle

growth. As the smaller submicron size particles increase in diameter they may become easier to remove from the flue gas stream. Saturated plant steam was injected between the first and second stage of the IFGT and particulate loading measurements were conducted at the inlet and outlet to the IFGT.

The effect of mesh pads on particulate removal was investigated. Several layers of mesh pads were placed in the horizontal transition just before entering the second stage. The particulate removal efficiency was measured by cascade impactor tests at the 1st stage inlet and outlet. Mesh pads provide a target surface for impaction of fine particulate that passes through the first stage.

3.1.5 Heat Recovery

The heat recovery provided by the IFGT was an integral part of the standard data acquisition, and was recorded continuously for all of the tests. In addition to this standard data, the following tests were conducted to investigate specific heat transfer mechanisms.

- *Onset of 1st Stage Condensation* - For this test, cooling water passed only through the 1st stage heat exchanger. The cooling water flow rate was increased until condensate initially formed on the tubes. The data was compared to heat transfer models to better understand the conditions that initiate condensation.

- *Onset of 1st Stage Measurable Condensate Flow* - This was an extension of the previous test, where the cooling water flow rate is sufficient to produce a continuous flow of condensate that can be collected and weighed. The data was compared to heat transfer models to better understand the conditions that initiate condensation.

3.1.6 Calcium Reagents

After a preliminary analysis of the data collected through the third test phase, the database for a sodium carbonate reagent was deemed sufficient to meet the project goals and objectives. The remaining tests conditions for the fourth test phase were modified to include reagents other than sodium carbonate.

Effective reagents for the fourth test series must supply a source of alkalinity in the liquid phase that can then readily react with the SO_2 absorbed from the flue gas. The dissolved alkalinity produced by the reagent defines the SO_2 absorption capacity of the liquor, and includes all dissolved species more alkaline than the bisulfite ion (HSO_3^-). Flue Gas Desulfurization (FGD) systems have primarily relied on highly soluble reagents containing sodium carbonate and slurry reagents containing calcium hydroxide and magnesium hydroxide, or calcium carbonate that slowly dissolve into alkaline anions. The two additional reagents selected for the fourth test series derive their alkalinity from calcium and magnesium hydroxide compounds. The first reagent, calcium hydroxide is widely used in commercial FGD systems and dissolves into highly alkaline hydroxide (OH^-) anions. The second reagent, magnesium promoted calcium hydroxide is also widely used in commercial FGD systems and in addition to (OH^-) anions also produces high dissolved concentrations of alkaline sulfite ($SO_3^=$) anions. The SO_2 removal performance of the these reagents was expected to be sufficient enough to justify their use in commercial

applications. The calcium hydroxide reagent was expected to have lower SO_2 removal capabilities as the reagent does not produce as high dissolved alkalinity as sodium carbonate or magnesium promoted calcium hydroxide.

3.1.7 Reporting Basis

The concentration of compounds, elements, and particulate in the flue gas are on a dry basis, corrected to 3% excess oxygen. The units used in this report are micrograms per dry standard cubic meter (µg/dscm),* milligrams per dry standard cubic meter (mg/dscm), and parts per million on a volume basis (ppm_v). The concentration of compounds and elements in the solid phase are reported as parts per million on a mass basis (ppm_m).

3.2 Wear Assessment

3.2.1 Unit Operation

The ECTC pilot facility and the pilot condensing heat exchanger were operated so that the wear test was conducted under conditions representative of commercial operation at the flue gas inlet of an IFGT condensing heat exchanger. Specifically, this required:

- A flue gas with a representative particulate loading, temperature, and flow for a commercial coal-fired application. For example, the inlet particulate loading was to be maintained at 34 mg/dscm (0.03 lbs/10^6 Btu) or greater during the test period.

- Controlling the temperature and flow rate of the cooling water for the condensing heat exchanger to provide the Teflon® film temperature expected at the flue gas inlet of a full-scale IFGT unit.

- Operation of the CHX® unit on a continuous basis, whenever possible, to maximize the Teflon® exposure to flue gas.

The design operating conditions used as a basis for operation of the CHX® pilot unit are shown in Table 3.6. All major operating parameters were monitored by ECTC personnel (and recorded by the ECTC data acquisition system) to ensure that the CHX® test unit was operating within the desired conditions.

To achieve the desired particulate loading at the inlet to the condensing heat exchanger, the test unit was located downstream of the ECTC ESP. An opacity meter was used to monitor the flue gas particulate loading downstream of the ESP. In addition to the opacity meter, an Environmental Systems P-5A *in-situ* particulate monitor was used as a qualitative indicator for the particulate loading level to aid ECTC personnel in maintaining a steady particulate loading. Finally, EPA Method 5 particulate loading measurements were made at various times during the test to confirm the opacity readings and the particulate loading to the unit.

---

* Standard conditions are 20 C and 1 atm.

Table 3.6 Design Operating Conditions for the CHX® Pilot Unit -- One Year Wear Test

Parameter	Nominal Value	Range
Inlet Flue Gas Temperature	160 °C (320 °F)	+/- 17 °C (30 °F)
Outlet Water Temperature	77 °C (170 °F)	+/- 11 °C (20 °F)
Cooling Water Supply	11.4 lpm {3.0 gpm (est.)}	---
Flue Gas Velocity, between tubes	12.2 m/sec (40 ft/sec)	+/- 1.5 m/sec (5 ft/sec)
Inlet Flue Gas Flow	1,275 scmh (750 scfm)	+85 -0 scmh (+50 -0 scfm)
Inlet Particulate Loading	representative of poor to good particulate cleanup from a commercial cleanup device.	34 to 340 mg/dscm (0.03 to 0.30 lbs/10^6 Btu)

3.2.2 Inspection Measurements

In order to determine the amount of wear, if any, on the Teflon® covered internals of the heat exchanger, and specifically the tubes, three types of measurements, in addition to a visual inspection, were performed during each of the five inspection trips conducted during the course of the test program. These measurements included:

- Vertical and horizontal tube dimensions
- Eddy current Teflon® film thickness determination
- Teflon® film surface replications

A fourth type of surface measurement utilizing a surface profilometer, which was originally specified as a test program measurement, was not used due to damage to the Teflon® film caused by the profilometer probe during use.

Each measurement was performed at several locations on the top two rows of tubes. A graphical representation of the measurement locations is shown in Figure 3.1. Tubes 1 through 6 are located in the top row of the heat exchanger and tubes 7 through 12 in the second row. Flue gas flow with respect to the diagram is from the left and then into the page. Each of the dimensional measurements (horizontal, vertical, and film thickness) were performed in triplicate at each location and the values averaged. These location values were then averaged to obtain an average tube value. Single surface replications were made at each of the indicated locations. Three replications were performed on tube 6 since the greatest potential for abrasive wear was expected on this tube. Descriptive summaries of each of the three measurement techniques may be found in the following paragraphs:

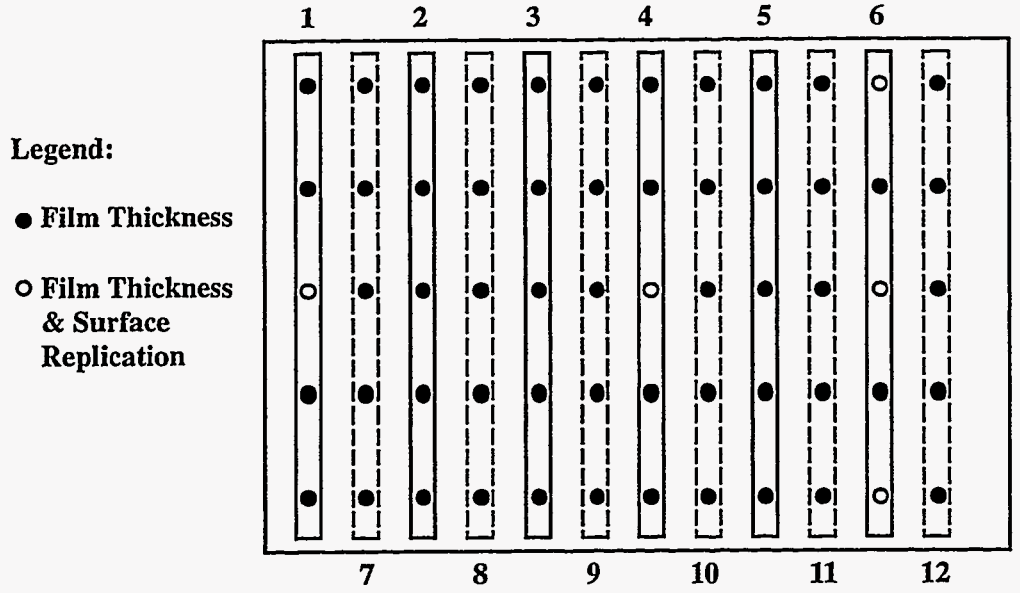

Figure 3.1 Location of Film Thickness and Surface Replication Measurements

Tube Dimensions: Micrometers were used to measure the top-to-bottom and side-to-side dimensions of the top row of tubes at each of the locations shown in Figure 3.1 (locations labeled "Film Thickness" on tubes 1 through 6). A digital caliper micrometer was used for the horizontal diameter measurements and a standard micrometer was used for the vertical diameter measurements. The overall accuracy of the horizontal diameter measurement was 25.4 μm (0.001 inches) and the overall accuracy of the vertical diameter measurement was 12.7 μm (0.0005 inches). After two sets of dimensional measurements were obtained, it was discovered that the Teflon® tube surfaces were being damaged by the micrometers. This was most likely due to the tight tube spacing, which complicated the insertion and removal of the calipers. Evaluation of the two sets of measurements indicated that any change in film thickness would be more evident from the eddy current measurements, so this procedure was dropped from subsequent inspection trips.

Film Thickness: An Elcometer 300 Coating Thickness Gage, which uses an eddy current measurement principle, was used to make the film thickness measurements. The instrument has a range of 25.4 to 1,016 μm {0.001 to 0.040 inches (1 to 40 mils)} and an accuracy of ±1% of its reading. Teflon® thickness measurements were made for the top surface of the first and second row of heat exchanger tubes. Thickness measurements were also made at specified angles from vertical (0 + 45 and 0 - 45 degrees) for the top row of tubes. In relation to the diagram in Figure 3.1, "vertical" may be thought of as a line coming straight out of the paper, "+45" angled towards tube 1 and "-45" angled towards tube 6. Thickness measurements could not be made for these angles for the second row of tubes because of the staggered array (overlap of the tubes for adjacent rows) of the tubes. Measurements were made at the locations indicated in Figure 3.1. As mentioned above, these measurements were made in triplicate at each location and angle and then averaged. These location average values were then averaged for each tube to obtain a tube average. Each data set was then normalized based on 1) the calibration data for that particular set, and 2) the film thickness data from a "reference" tube measured at the same time using the same calibration as the inspection.

Surface Roughness: A cellulosic film surface replication technique was used to obtain a physical replicate of the Teflon® tube surfaces. The goal of making the surface replications was to record and observe any microscopic changes to the Teflon® tube surface. The replications were made during each inspection trip at the locations indicated in Figure 3.1. After cleaning the Teflon® tube surfaces, a strip of cellulosic film tape was moistened with acetone and laid on the surface of the tube. Upon drying, the tape was lifted from the tube and mounted on a glass side, replicate side up. This procedure was then repeated for the remaining sample locations. The tapes were then viewed under a microscope and photographed at magnifications of 25X and 200X for comparison with the replications made prior to exposing the heat exchanger to flue gas.

4.0 RESULTS AND DISCUSSION

4.1 Heat Recovery

One principal benefit of the IFGT process compared with other gas clean up technologies is the capability to recover waste heat from the flue gas. The heat recovery capability can be a substantial benefit provided there is a use for the recovered heat. The quantity of heat that can be recovered from the flue gas is dependent on several factors including the temperature of the flue gas, the sink temperature for the cooling water, and the flue gas water vapor dew point. In an open cycle industrial system the heat recovery can amount to 10% to 12% of the furnace heat release.

For coal combustion, the flue gas dew point is typically about 38°C (100°F), which is substantially less than for oil and gas combustion. In addition, the sink temperature at electric utility generating plants that use a closed steam cycle is typically higher than the sink temperature associated with open cycle processes. The combination of low dew point temperature and high sink temperature reduces the quantity of heat than can be recovered, but this heat can still have a significant impact on the cost of operation.

4.1.1 Measured Heat Recovery

Temperatures and flows of cooling water and flue gas were monitored continuously during these tests, primarily as a means to control the operating conditions of the IFGT. The flue gas inlet temperature was maintained at 120°C (250°F) for all tests. Flue gas outlet temperature was maintained either at the water vapor dew point, or 8°C to 12°C (14°F to 22°F) below the dew point. The 120°C inlet temperature is lower than the 150°C (300°F) that is typical of the inlet temperature to most flue gas desulfurization systems. At the ARC pilot IFGT, the baghouse is limited to a 150°C temperature, and heat loss and air infiltration reduces the temperature to well below 150°C. A 120°C inlet temperature was selected because it was quickly attainable at startup, and could be controlled regardless of the gas flow or ambient conditions.

Since the water and gas-side temperatures and flows were nearly the same for all tests, the heat recovery (as a percentage of furnace heat release) was also nearly the same. Figure 4.1 shows the components of heat recovery expressed as a percentage of the furnace heat release for an outlet flue gas temperature at the dew point (Test I-5) and 10°C (18°F) below the dew point (Test I-14D). For a condensing mode of operation, the heat recovery is equally split between the first and second heat exchanger stages, and the latent heat recovery (2%) accounts for about 1/3 of the total heat recovery (6%). In Test I-5 (non-condensing) the stage 1 heat recovery is nearly the same as for test I-14D, while the second stage heat recovery is less, because of the absence of condensation.

Although net condensation does not occur in Test I-5, both evaporation and condensation occur in the second heat exchanger stage. The flue gas enters the second stage at a temperature greater than the dew point by about 17°C (30°F). The flue gas is then evaporatively cooled to the adiabatic saturation temperature. As the flue gas moves through the second stage, the water initially evaporated to cool the flue gas is condensed as the flue gas temperature is reduced to the

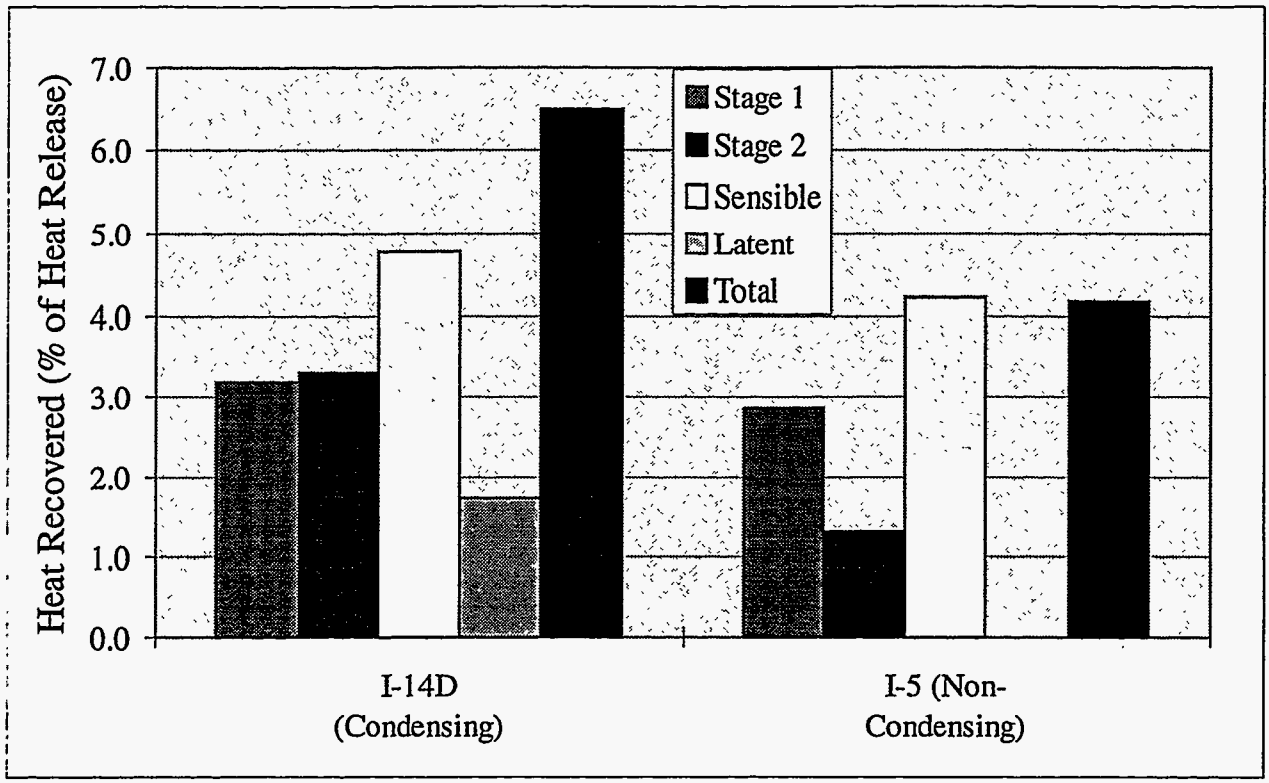

Figure 4.1 Components of Heat Recovery in the IFGT Process

original dew point temperature. This reflux process does not affect the net heat transfer, but it may influence the removal of pollutants.

4.1.2 Predictions of Heat Recovery and Gas Side Pressure Drop

CHX's® are sized with the assistance of a computer program that determines the physical size of the heat exchanger for the required gas flow and predicts heat recovery and gas side pressure drop through the unit. Several tests were conducted to determine the accuracy of these predictions.

Heat Recovery - Heat transfer tests were conducted using only the first heat exchanger stage so that the effect of water flow rate and water temperature could be closely controlled, and condensate flow rates could be accurately measured. Table 4.1 lists the operating conditions for these tests, which were designed to vary the condensation in the heat exchanger in a step wise fashion. As shown in Table 4.1, the energy balance for the measured data varied between about ±5%.

Figure 4.2 shows the percent error between the measured and predicted heat recovery for the five tests. As shown, the errors are all negative indicating that the model consistently predicts a slightly greater energy recovery than was measured.

Figure 4.3 is a comparison of measured and predicted condensate flows for the five tests. As expected, based on the energy balance error, the program predicts a slightly greater condensate flow rate than was measured. Although the predictions show a fixed bias, the difference between

Table 4.1 Summary Operating Conditions and Comparison to Predicted Heat Recovery for the Five Heat Transfer Tests

		CASE 1 II-HX1	CASE 2 II-HX2	CASE 3 II-HX3	CASE 4 II-HX4	CASE 5 II-HX5
Cooling Water Flow Rate (Corr)	(kg/min)	15.7	15.3	22.6	22.9	21.8
Cooling Water Inlet Temperature	(°C)	18.1	12.3	11.3	22.4	11.4
Cooling Water Outlet Temperature	(°C)	62.1	60.0	47.9	54.2	43.6
Water Energy Gain, Stage 1	(kw)	48.3	50.9	57.6	50.9	48.9
Flue Gas Flow (Wet)	(kg/min)	39.2	39.0	39.1	38.8	27.7
Gas Temperature @ Module 1 Inlet	(°C)	120.7	123.3	123.7	124.1	120.9
Inlet Dew Point Temperature	(°C)	35.5	35.3	36.1	36.0	34.5
Humidity at CHX inlet	(gm/gm)	0.036	0.036	0.038	0.037	0.035
Flue Gas Flow (dry)	(kg/min)	37.9	37.6	37.7	37.4	26.8
Gas Temperature @ Module 1 Outlet	(°C)	53.0	51.3	47.7	52.8	41.7
Flue Gas Total Energy Loss	(kw)	48.4	54.4	60.9	49.7	49.6
Condensate Flow Rate	(gm/min)	85.4	165.0	249.9	71.5	293.8
Condensation Heat to Water	(kw)	3.5	6.8	10.3	2.9	12.1
Fraction of Water Energy Gain	%	7.3%	13.3%	17.8%	5.8%	24.7%
Overall Water/Gas Energy Balance	%	-3.3%	3.6%	2.9%	-5.9%	-1.7%
PREDICTIONS						
Predicted Water Energy Gain, Stage 1	(kw)	49.1	53.4	60.7	51.6	50.1
Measured - Predicted	(kw)	-0.8	-2.5	-3.0	-0.7	-1.2
Measured - Predicted	%	-1.65%	-4.89%	-5.29%	-1.39%	-2.42%
Predicted condensate flow	(gm/min)	165.7	202.2	300.8	183.9	312.3
Measured - Predicted	(gm/min)	-80.3	-37.2	-51.0	-112.3	-18.5
Predicted flue gas outlet temperature	(°C)	56.2	53.9	49.6	56.0	40.3
Measured - Predicted	(°C)	-3.2	-2.6	-1.9	-3.3	1.4
Predicted water outlet temperature	(°C)	62.8	62.3	49.8	54.6	44.3
Measured - Predicted	(°C)	-0.7	-2.3	-1.9	-0.4	-0.8

measured and predicted energy recovery are quite small. Likewise, the differences between measured and predicted condensate flows and water and gas temperatures are all on the order of experimental error.

Gas Side Pressure Drop - The gas side pressure drop through the first heat exchanger stage was measured as a function of air flow rate for isothermal operation and is shown in Figure 4.4. Also shown in this figure, is the predicted gas side pressure drop for the first stage. The predicted pressure drop is less than the measured pressure drop by about 8% over the entire range of flows.

Part of the error in the predicted pressure drop is likely due to differences in the geometry of the pilot CHX® unit compared with a full scale unit. The "near wall" area in the pilot unit represents a larger fraction of the total flow area than a commercial sized unit. Pressure drop predictions are based on data for commercial sized units that closely simulate an infinite array of tubes.

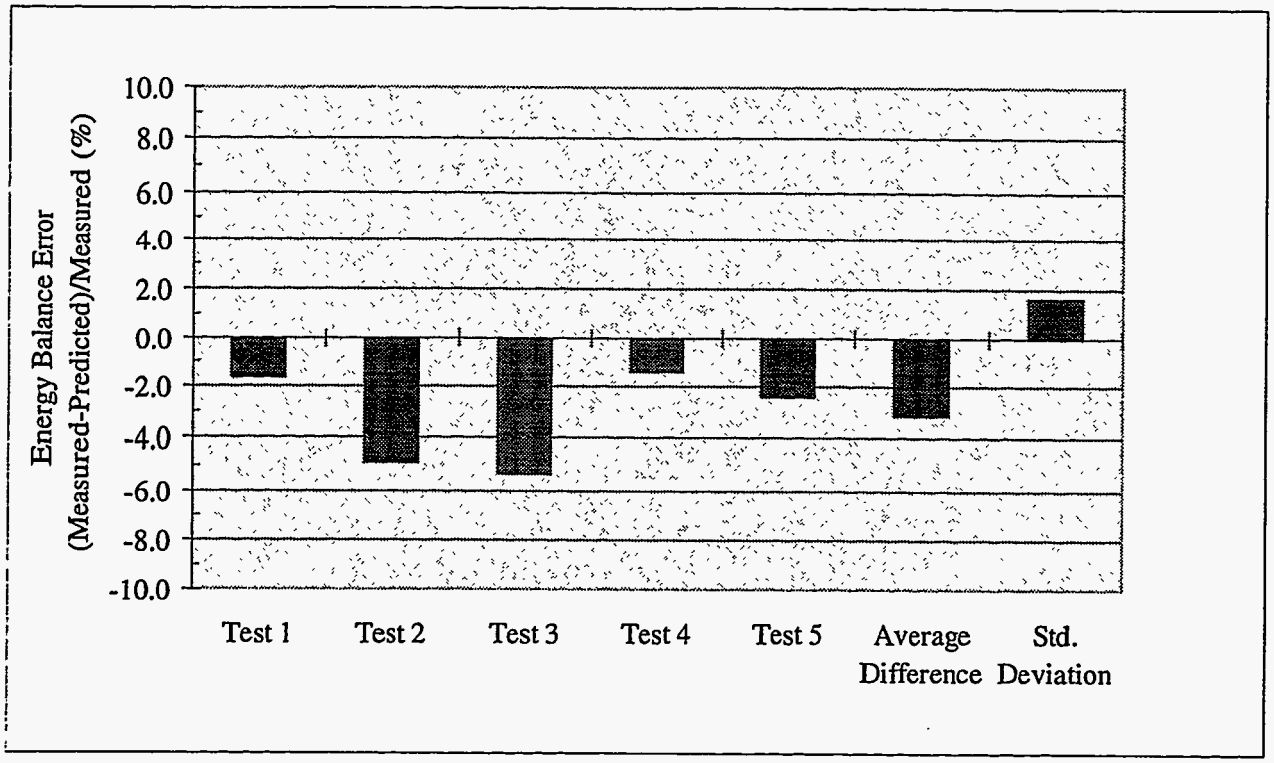

Figure 4.2 Percent Difference Between the Measured and Predicted Heat Recovery for the Five Heat Transfer Tests

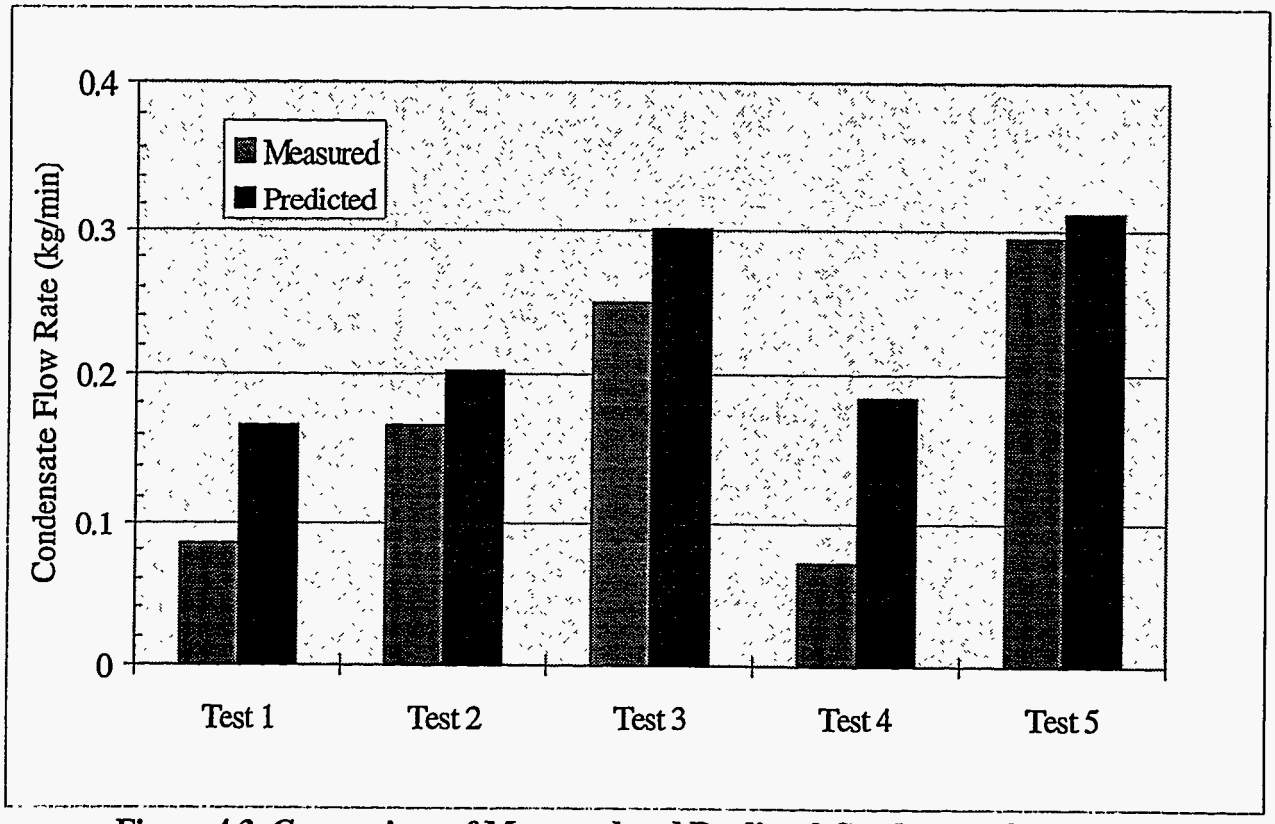

Figure 4.3 Comparison of Measured and Predicted Condensate Flow Rates

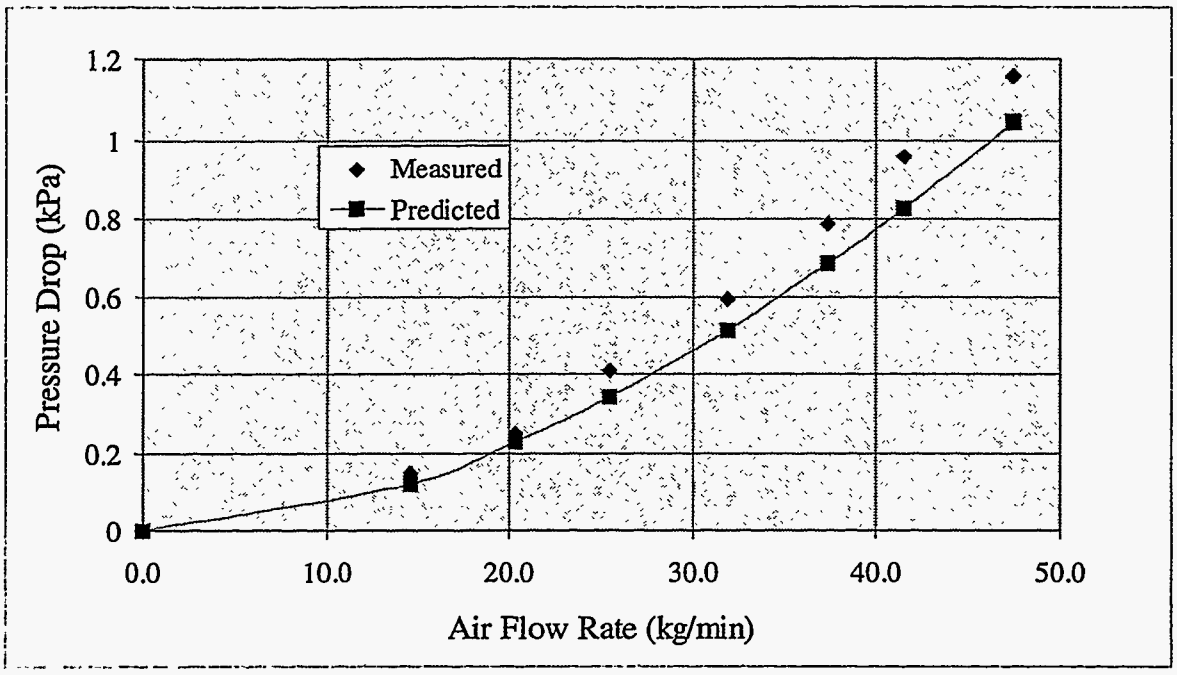

Figure 4.4 Measured and Predicted Pressure Drop Across the First Heat Exchanger Stage as a Function of Air Flow Rate

4.2 SO_2 Removal

SO_2 absorption in the IFGT was studied as a function of L/G, pH, load, reagent type, outlet temperature, and coal type. Overall SO_2 removal performance can be expressed in terms of percent removal or in terms of "number of transfer units". Although in chemical engineering parlance N_g is defined rigorously as $dN_g = dy/(y - y_i)$, it has become common practice in the FGD industry to define N_g as follows:

$$N_g = -\ln(1 - \epsilon) \quad (1)$$

where

$$\epsilon = 100\left(1 - \frac{y_{outlet}}{y_{inlet}}\right) \quad (2)$$

ϵ = SO_2 removal efficiency, %

y_{inlet} = Inlet SO_2 concentration (ppm_v)

y_{outlet} = Outlet SO_2 concentration (ppm_v)

y_i = SO_2 vapor pressure at the gas-liquid interface (ppm_v)

Expressing performance in terms of transfer units has two advantages. First, N_g has greater sensitivity to incremental changes than removal percentage when the SO_2 removal efficiency approaches 100%. The effect of operating parameters are more easily visualized in graphical form. Second, transfer units usually produce more linear relationships between SO_2 removal and system parameters. For the plots shown in this section, the left y-axis is given in transfer units and the right y-axis shows the equivalent percent removal.

4.2.1 Test Repeatability

Soda ash reagent testing was carried out for the four test series with 118 individual tests. For selected tests, system operating conditions were repeated to determine the repeatability of SO_2 performance data. A comparison of the repeatability data for all coals is shown in Table 4.2 below. The measure of repeatability used in Table 4.2 is the standard deviation of the SO_2 removal. Overall, the repeatability was good. The average standard deviation in the measurements was ±0.6%, and ranged from 0.2% to 1.4%.

Table 4.2 Repeatability of SO_2 Removal Measurements

Test ID[1]	Number of Measurements	Average SO_2 Removal (%)	Standard Deviation (% of Removal)
I-4	7	97.2	0.5
II-4	5	98.3	0.2
III-7	3	97.1	0.5
IV-2	4	87.2	1.4

(1) "I-4" denotes test series I, test condition 4.

4.2.2 Sodium Reagent Test Results

Effect of L/G

The recirculated liquid flow rate is one of the major process operating factors affecting the SO_2 removal efficiency. For all of the figures that follow, the recirculated liquid flow rate is expressed as the ratio of liquid (or slurry) flowing to the top of the 2nd stage of the IFGT to the flue gas flow leaving the top of the 2nd stage. This quantity is generally referred to as the "Liquid-To-Gas Ratio" (L/G) and is considered one of the major process operating factors specified by Flue Gas Desulfurization (FGD) system designers. When the L/G increases, the qualitative effect is to increase the liquid (or dissolved) alkalinity per unit volume of treated gas. When the gas flow is constant and the reagent flow rate is increased, there is usually an increase in the liquid surface area per unit volume of treated gas, an increase in the amount of liquid in the IFGT system (commonly called the "liquid holdup"), and an increase in the turbulence (or agitation) between the gas and liquid. These effects improve the mass transfer characteristics of SO_2 removal.

The major effect of increasing L/G under typical constant load conditions is to increase the exposed surface area for gas absorption, and to increase the rate of absorption by reducing the resistance for SO_2 transport into the liquid. The SO_2 removal efficiency data shown in Figure 4.5 for Test series I, shows the quantitative effect of L/G at full load. At low L/G in the range of 0.07 to 0.27 l/m^3 (0.5 to 2.0 gal/1000 ft^3), the SO_2 removal efficiency increases rapidly, and reflects the generation of additional surface area from partial to complete liquid coverage of the internal tubes and walls, and an increase in the capacity of the reagent for SO_2 absorption. As the L/G increases above 0.27 l/m^3, more surface area is generated by increasing the number of liquid droplets flowing downward between the tubes. The incremental surface area generated for an L/G > 0.27 l/m^3 is significantly less, and the SO_2 removal efficiency increases only moderately. The qualitative effect of L/G measured for test series I was consistently evident for all of the coals tested.

The data shown in Figure 4.5 for Test Series I, a high-sulfur Ohio Coal, show that 95% SO_2 removal efficiency can be obtained at an L/G between 0.13 and 0.2 l/m^3 (1.0 and 1.5 gal/1000 ft^3). Increasing the L/G by a factor of 4 from 0.27 to 1.07 l/m^3 (2.0 to 8.0 gal/1000 ft^3) only

moderately increases the SO_2 removal efficiency from approximately 96.5% to 98.5%. However, this represents a significant increase in the transfer units from 3.3 N_g to 4.3 N_g.

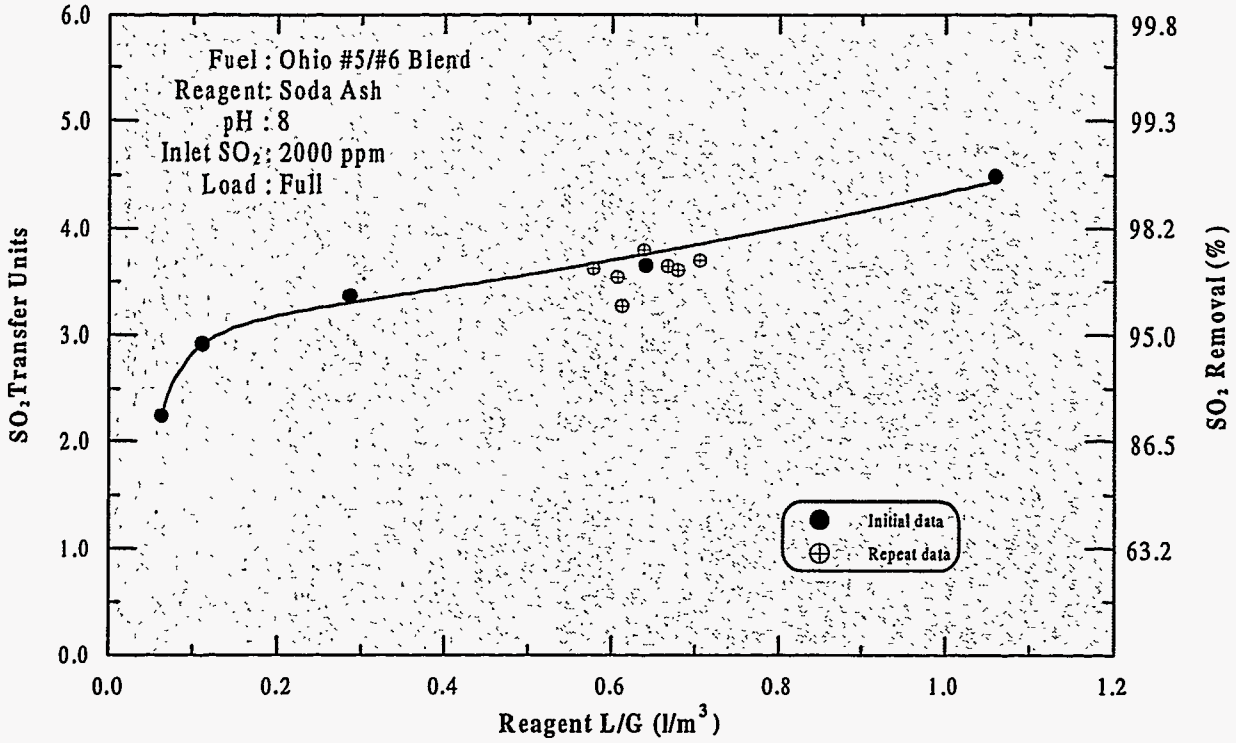

Figure 4.5 Effect of L/G at High pH

Effect of pH

The pH of the recirculating liquid entering the top of the second stage can affect the SO_2 removal efficiency. The effect will only be significant when the pH is sufficiently low that for the specific test conditions, the composition of the liquid flowing down through the IFGT second stage changes significantly. A significant composition change will be evident when the pH of the liquid leaving the bottom of the IFGT is low enough to create significant SO_2 vapor pressure at the gas-liquid interface. When this condition occurs, a sufficient excess of dissolved alkalinity is not present to absorb SO_2 and still maintain the pH at the gas-liquid interface above approximately six. For typical IFGT operating conditions with sodium reagent, operation at a recirculated solution pH greater than approximately 8.0 will usually ensure that the liquid pH leaving the IFGT is above 7.0, with no significant SO_2 vapor pressure.

The SO_2 removal efficiency at a pH of 8 and 7 for Test Series I is shown in Figure 4.6. The SO_2 removal efficiency at a pH of 7 is somewhat lower than with a pH of 8 with good agreement on the incremental effect of L/G. At similar L/Gs, reducing the pH from 8 to 7 lowered the SO_2 removal efficiency by approximately 0.5 transfer units. At the lower pH of 7, the reduced SO_2 removal efficiency reflects sufficient changes in the liquid composition for the generation of a significant SO_2 vapor pressure.

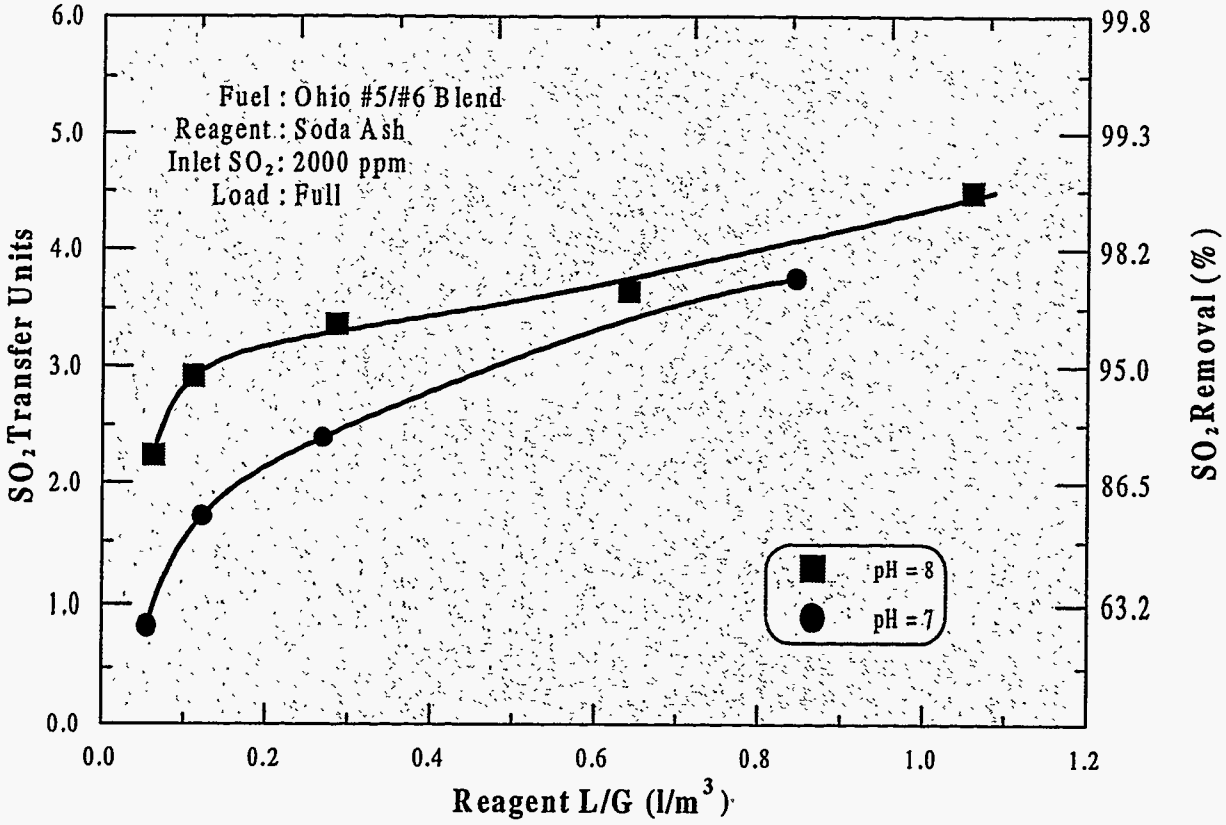

Figure 4.6 Effect of pH on SO_2 Absorption

Effect of Load

The effect of the load on SO_2 removal efficiency is shown in Figure 4.7 along with the effects of L/G and pH. For operation at half load, the SO_2 removal efficiency is significantly less by approximately 1.5 N_g. Two factors are contributing to the reduction in SO_2 removal efficiency at reduced load. First, the reduced load decreases the liquid holdup and its contribution to exposed surface area for gas absorption from droplets traveling downward from tube to tube. Second, is the reduction in turbulence between the liquid and gas. The reduced turbulence decreases the rate of absorption by increasing the resistance in the gas phase for SO_2 transport into the liquid surface.

Effect of Outlet Temperature

The outlet flue gas temperature of the IFGT second-stage is typically adjusted for operation at temperatures ranging from slightly above to several degrees below the dewpoint. The flue gas temperature throughout the IFGT second stage is relatively constant when operating at or below the dewpoint. When the operating temperature of the flue gas within the IFGT second stage changes, physical and mass transfer properties of the flue gas, SO_2, and liquid may also change. The overall effect on the rate of mass transfer is complex, but the net effect on the mass transfer rate may be estimated by combining the individual temperature effects.

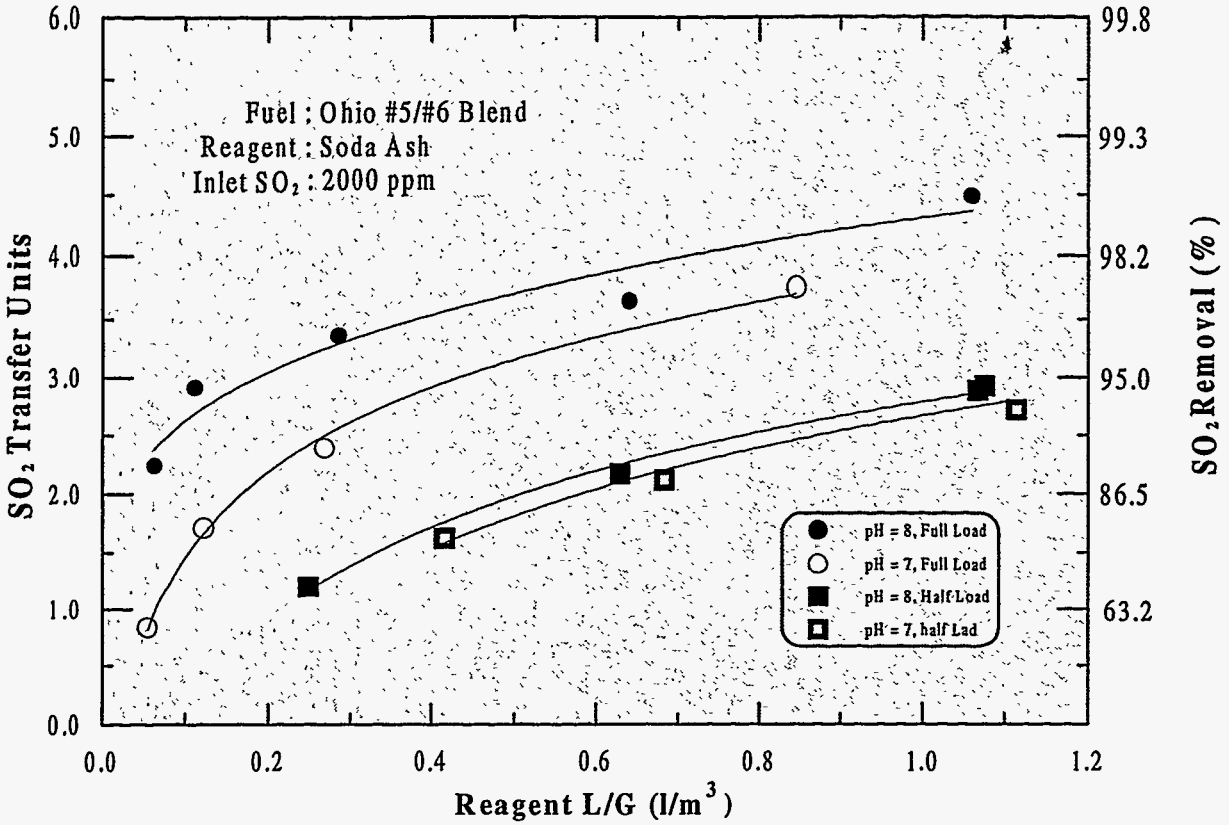

Figure 4.7 Effect of Load on SO_2 Removal

The effect of temperature on the mass transfer rate was measured during Test Series I at a pH of 8 at full load and is shown in Figure 4.8. The data suggests that reducing the operating temperature by 9°C (16°F) reduces the mass transfer rate by approximately 3 to 5%. To estimate the observed effect of temperature, dimensionless empirical power law mass transfer correlations for droplets and cylindrical tubes were evaluated for the effect of temperature dependency. In an attempt to simplify the estimate, the analysis was conducted assuming a high pH in which the liquid phase resistance to mass transfer could be considered insignificant. This was confirmed experimentally as increasing the pH above 8 did not change the difference between the reagent feed pH and the pH at the exit of the IFGT second stage. For the droplets falling between the tubes, the following expression for turbulent mass transfer around a sphere applies.[1]

$$N_{sh} = 2.0 + 0.55 N_{re}^{1/2} N_{sc}^{1/3} \qquad (3)$$

where:

N_{sh} = Sherwood No.
N_{re} = Reynold's No.
N_{sc} = Schmidt No.

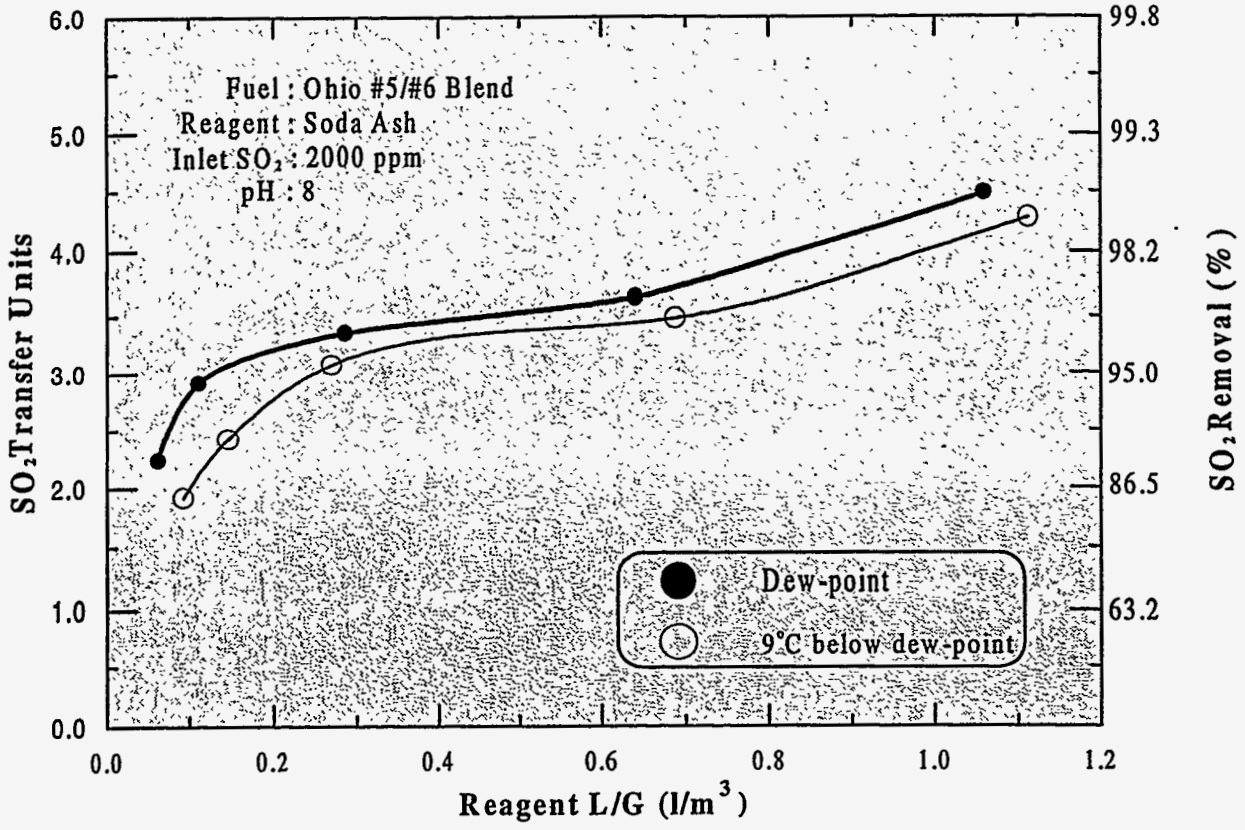

Figure 4.8 - Effect of Outlet Temperature on SO_2 Removal.

For the liquid flowing over the tubes the expression for turbulent mass transfer is[2]

$$N_{sh} = 0.25 N_{re}^{0.6} N_{pr}^{0.38} \quad (4)$$

For both expressions, the factors that are temperature dependant are the flue gas density, flue gas viscosity, and binary diffusion coefficient for SO_2 in flue gas. The dependency of these parameters on temperature was used in Equations 3 and 4, to determine the overall effect of a 9°C (16°F) temperature decrease on the mass transfer rate. For the droplets, the net effect was a decrease in mass transfer rate of approximately 9%. For the tubes, the net effect was a decrease in mass transfer rate of approximately 10%. The total mass transfer in the IFGT second stage is some combination from the droplets and tubes. As the estimated effect of temperature is essentially identical for both the droplets and tubes, the estimated effect of the temperature reduction is approximately 9%. This is consistent with the measured reduction in transfer units of approximately 3% to 5%.

Effect of Coal Type

The primary effect of the coal type is the variation in the coal sulfur content. The coal ash content and coal ash alkali composition have an insignificant effect as essentially all of the fly ash is

collected in the upstream baghouse. For the four coals tested, the flue gas SO_2 concentration ranged from approximately 300 ppm_v to 2000 ppm_v. The SO_2 removal efficiency at full load and solution pH of 8 for various L/Gs is shown in Figure 4.9. At these conditions, no clear effect of the coal sulfur content on SO_2 removal efficiency is evident. This is consistent with operation under gas phase mass transfer limited conditions where the SO_2 removal efficiency is unaffected by variations in the inlet SO_2 concentration.

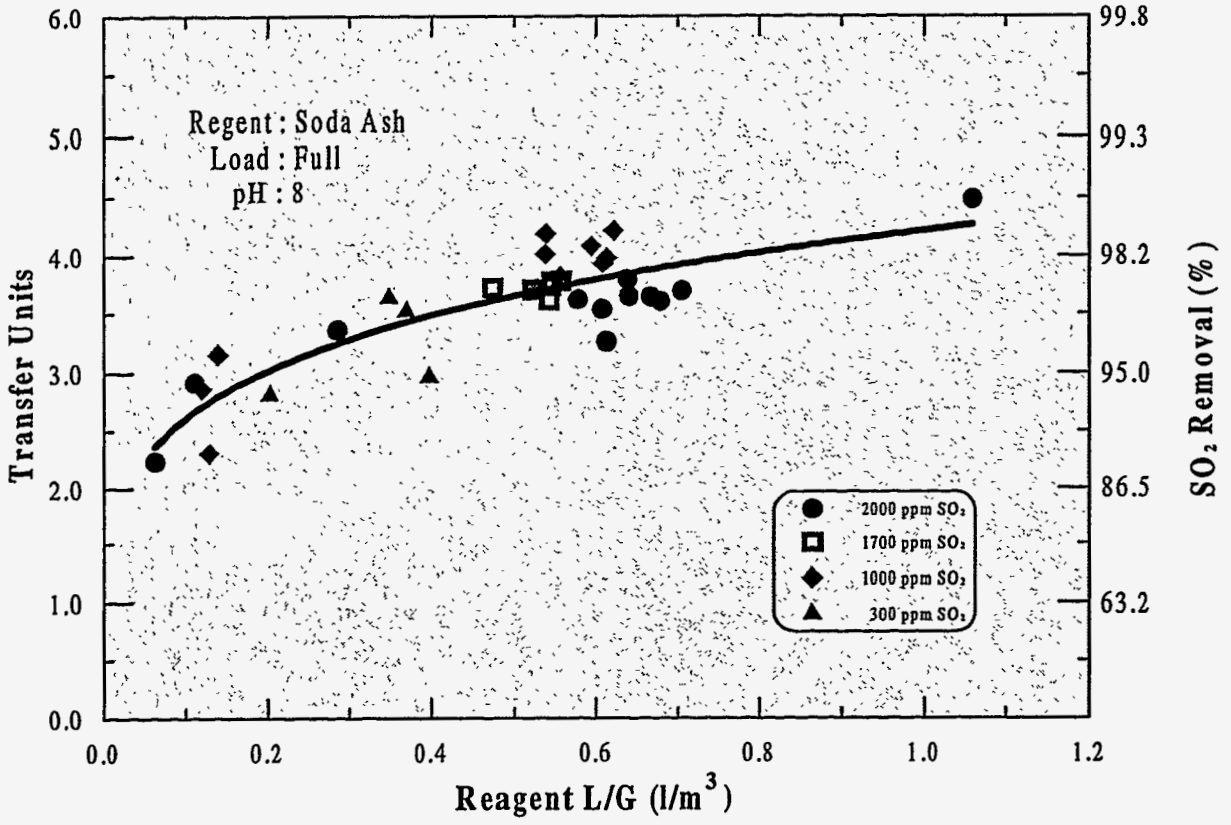

Figure 4.9 Effect of Inlet SO_2 Concentration on SO_2 Removal

As an example, if the inlet SO_2 concentration is reduced by a factor of 2, the SO_2 absorbed will likewise decrease by a factor of 2 and the SO_2 removal efficiency will remain the same. The SO_2 removal efficiency at half load and reagent feed pH of 7 for various L/Gs is shown in Figure 4.10. At these conditions, there was a noticeable effect of the coal sulfur content on SO_2 removal efficiency. It is generally assumed that at pH of 7 or less there will be significant SO_2 back pressure at the gas-liquid interface, causing some liquid phase mass transfer resistance. Under these conditions, reducing the flue gas SO_2 concentration will contribute to higher SO_2 removal efficiency.

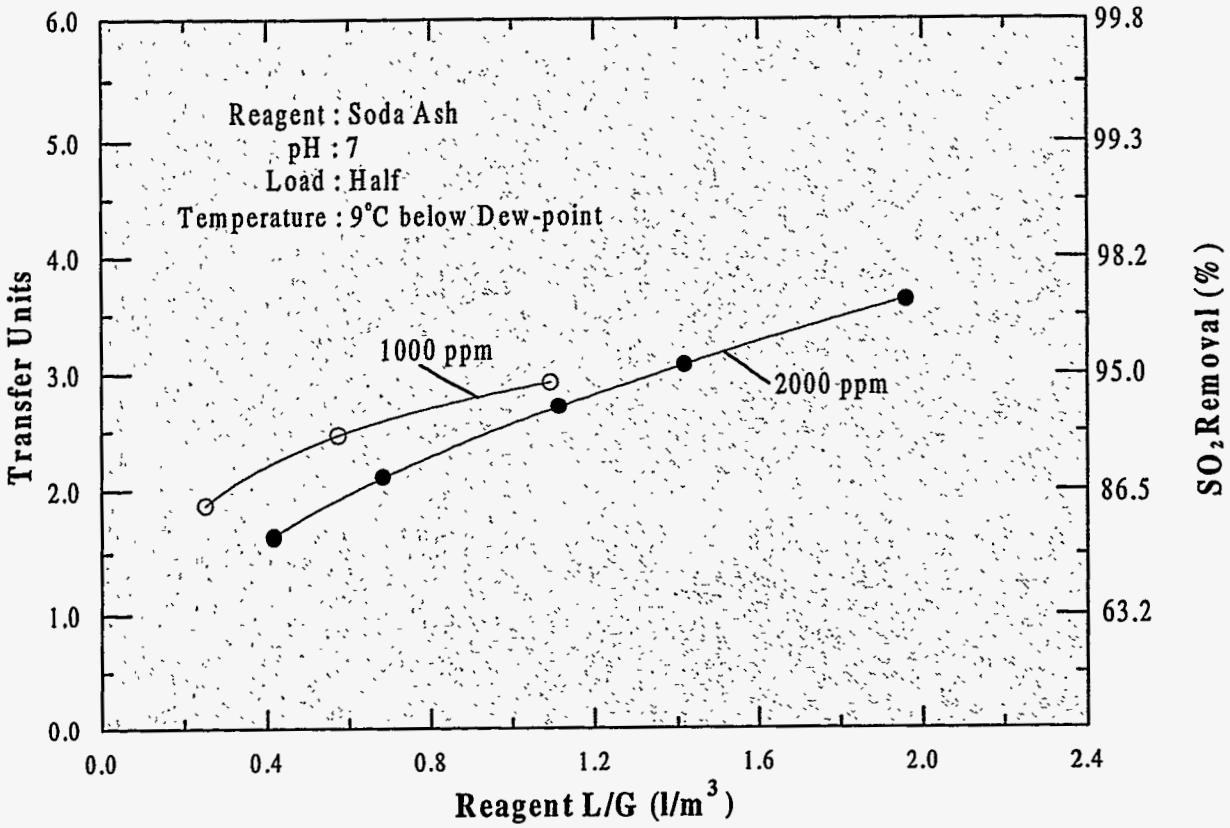

Figure 4.10 Effect of Inlet SO_2 Concentration on SO_2 Removal at Half Load

4.2.3 Lime Reagent

A lime-based reagent differs from soda ash reagent in both the type of alkaline species they generate, and in the amount of dissolved alkaline species produced. With soda ash reagent, the active alkaline species is highly soluble sodium sulfite and bicarbonate. A lime reagent produces relatively low dissolved levels of hydroxide. In a 5% magnesium-95% lime reagent, approximately 5% of the total alkali comes from magnesium sulfite. While the magnesium sulfite is low in total concentration, it is highly soluble and can deliver 10 to 15 times as much dissolved alkalinity as a calcium-based lime reagent.

The effect of reagent type on SO_2 removal efficiency is shown in Figure 4.11 for full load conditions. At an L/G of 0.8 l/m^3 (6 gal/1000ft^3), the SO_2 removal efficiency for the sodium reagent was 98%, and for the mag-lime reagent was 83%. For both reagents the pH measured in the scrubbing solution return line was approximately 7.5. While there was a small reduction in reagent pH of 0.5 across the second stage for the sodium reagent, the mag-lime reagent scrubbing solution pH dropped by approximately four. This is consistent with the lower SO_2 removal

efficiency, and suggests that the mag-lime has insufficient dissolved alkalinity at an L/G of 0.8 l/m^3 to absorb the available SO_2.

When planning the mag-lime tests, it was anticipated that a 5% mag-95% lime reagent would give only slightly less SO_2 removal efficiency than soda ash. The results showed a significant drop in SO_2 removal efficiency. Post test analysis indicated that the actual composition of the mag-lime reagent was 12% magnesium hydroxide and 88% calcium hydroxide. The high magnesium concentration should have allowed sufficient buildup of dissolved magnesium sulfite. However, the dissolved solids for the mag-lime test was unexpectedly low, about 0.4 %, and is the cause for the lower than anticipated removal. Allowing more operation time for the magnesuim sulfite to dissolve or, higher L/G will be required to approach the performance of a sodium reagent.

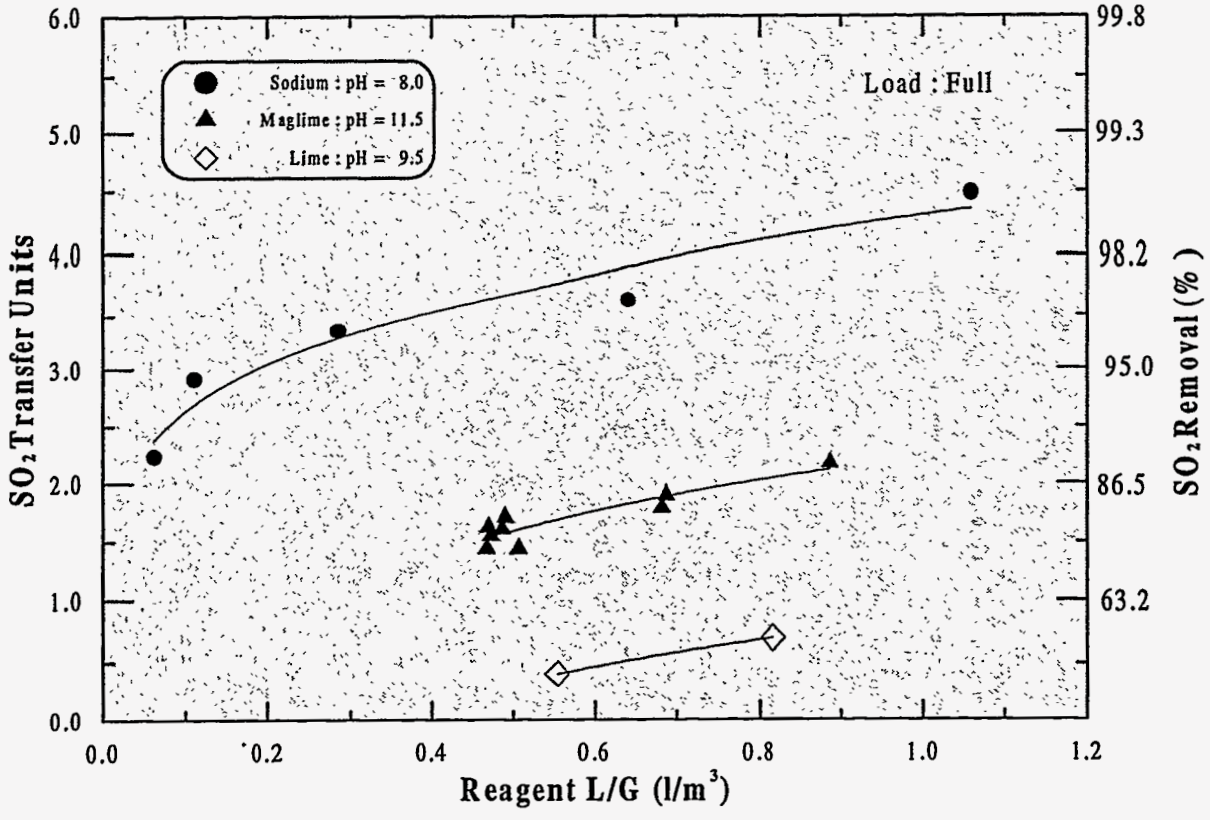

Figure 4.11 Effect of Reagent Type on SO_2 Removal

For the lime reagent, significantly lower SO_2 removal efficiency was anticipated. At an L/G of 0.8 l/m^3 (6 gal/1000 ft^3), the SO_2 removal efficiency for the sodium reagent was 98% for a feed pH of 8.0. For the lime reagent at the same L/G, the SO_2 removal efficiency was approximately 50%, for a feed pH of 9.5. There was a significant reduction in the pH of the scrubbing solution (~5.5 pH units) across the second stage. This was expected, as the lime reagent produces very low dissolved alkalinity in the lime slurry.

4.3 Chloride/Fluoride Removal

Chlorine and fluorine are halogens present in coal and released from combustion as the acid gases hydrogen chloride (HCl) and hydrogen fluoride (HF). Of the four halogens - fluorine (F), chlorine (Cl), bromine (Br), and iodine (I) present in coal, chlorine and fluorine are the most abundant and are present in sufficiently high concentrations to be of concern. Some countries currently require emissions control of these halogens, and new regulations are pending in others. The IFGT system has the capability to absorb these acid gases by mechanisms similar to the capture of SO_2. Generally, HCl and HF will be absorbed at levels equal to or greater than SO_2. This section reports the removal efficiencies of HCl and HF measured across the IFGT for various coals for a wide range of combustion emission concentrations. Although some data are inconsistent, high removals were generally obtained for both HCl and HF.

Chlorine

Chloride emissions are a major contributor to man-made atmospheric acidity. Most of the chloride in coal is in the form of NaCl, which is converted essentially 100% to HCl in the combustion process. The HCl passes completely through the combustion process and particulate collection devices as there is little interaction between the HCl and fly ash. Generally, deposition will only occur in the particulate collection device if the flue gas temperature is below the acid dew point for HCl of 60°C (140°F). While SO_2 and NO_x emissions are greater than emissions of HCl, both the absorption rate and solubility of HCl in water is much higher.

The HCl concentration was measured at the inlet and outlet of the IFGT for each coal. Table 4.3 lists the test conditions and indicates how HCl partitioned to the vapor and particulate phases and the removal efficiency for the particulate and gas phases. More than 99.9% of the HCl entering the IFGT was in the vapor phase with concentrations ranging from 22 mg/dscm to 134 mg/dscm. The HCl concentration in the particle phase was generally much lower than in the vapor phase. As shown in Table 4.3, the HCl concentration in the particulate was generally less than 400

Table 4.3 Vapor and Particle Phase Chloride Concentration and Removal Efficiencies

Test	Scrubbing Solution pH	Location	Conc. in Particulate (ppm_v)	Unit Concentrations			Removal Efficiency			on Filter (%)	Percent in Vapor (%)
				Vapor (ug/dscm)	Particulate (ug/dscm)	Total (ug/dscm)	Vapor (%)	Particulate (%)	Total (%)		
I-4A	7.9	Inlet	134	134430	97	134527				0.07	99.9
		Outlet	8080	44709	209	44919	66.7	-116.3	66.6	0.47	99.5
II-4B	8.3	Inlet	16600	184429	26	184455				0.01	100.0
		Outlet	---	1150	---	1207	99.4	---	99.4	0.00	100.0
III-7A	6.5	Inlet	0.26	21997	0.01	21997				0.00	100.0
		Outlet	0.31	551	0.00	551	97.5	90.3	97.5	0.00	100.0
IV-1A	8.0	Inlet	396	156951	15	156966				0.01	100.0
		Outlet	18600	3628	44	3672	97.7	-184.5	97.7	1.20	98.8

ppm_m. However, for test series II, the HCl concentration in the particulate was very high - 16,600 ppm_m. For test series II, the SBS carbon carryover was also very high, and the baghouse was operated without bypass. The relatively high HCl concentration measured in the

particulate could be due to either excessive carbon carryover from the furnace adsorbing HCl, or HCl being concentrated in the particulate fines that pass through the baghouse. The overall effect indicated an 40-fold increase in the particulate's chloride concentration compared to the other tests.

The HCl removal efficiency for tests I, II, and III, were 66.7%, 99.4%,and 97.5%, respectively. The results for test I, were much lower than anticipated. A review of the analytical methods and procedures followed did not explain the results. The test was repeated in test series IV and the removal efficiency was measured at 97.7%. For test III, the effect of reagent feed pH on HCl removal efficiency was measured by reducing the reagent feed pH from approximately 8.0 to 6.5. The HCl removal efficiency was not significantly reduced and measured 97.5%.

The HCl removal efficiency for the particulate phase indicates large negative efficiencies. This is primarily due to the relatively large measurement uncertainty associated with the small measured concentrations for chloride in the particulate.

Fluorine

Fluoride emissions are a relatively minor component of the acid gases from coal combustion. For the four test series, the concentration of HCl in the flue gas was 40 to 87 times greater than the concentration of HF. Like HCl, the absorption rate and solubility of HF in water is much higher than SO_2 or NO_x. Most of the HF in coal is in the form of the mineral fluorapatite $[Ca_5(PO_4)_3(OH,F,Cl)]$, fluorite (CaF_2), and biotite $[K(Mg,Fe)_3(AlSi_3)O_{10}(OH,F)_2]$. These fluoride compounds are converted essentially 100% to HF in the combustion process. Like HCl, HF also passes completely through the combustion process and particulate collection devices as there is little interaction between the HF and fly ash.

The HF removal efficiency was measured at the inlet and outlet of the IFGT for each coal with sodium reagent. Table 4.4 lists the test conditions and the vapor and particulate phase concentration and removal efficiency. More than 98% of the HF entering the IFGT was in the vapor phase with concentrations ranging from 0.43 mg/dscm to 4.3 mg/dscm. The HF concentration in the particulate was generally less than 700 ppm_m. However, for test series II, the HF concentration in the particulate was relatively high and measured 49,000 ppm_m. For test series II, the SBS carbon carryover was also very high, and the baghouse was operated without bypass. The relatively high HF concentration measured in the particulate could be due to either excessive carbon carryover from the furnace adsorbing HF, or HF being concentrated in the particulate fines that pass through the baghouse. The overall effect indicated an 80-fold increase in the particulate's fluoride concentration compared to the other tests.

Table 4.4 Vapor and Particle Phase Fluoride Concentration and Removal Efficiencies

Test	Scrubbing Solution pH	Location	Conc. in Particulate (ppm_v)	Unit Concentrations			Removal Efficiency			Percent on Filter (%)	Percent in Vapor (%)
				Vapor (ug/dscm)	Particulate (ug/dscm)	Total (ug/dscm)	Vapor (%)	Particulate (%)	Total (%)		
I-4A	7.9	Inlet	37	1655	14	1669				0.87	99.1
		Outlet	560	60	2	62	96.4	85.6	96.3	3.35	96.7
II-4B	8.3	Inlet	48800	4184	65	4249				1.52	98.5
		Outlet	---	22	---	22	99.5	---	99.5	0.00	100.0
III-7A	6.5	Inlet	22	431	1	432				0.24	99.8
		Outlet	241	74	1	75	82.8	9.5	82.7	1.25	98.7
IV-1A	8.0	Inlet	610	1859	24	1883				1.27	98.7
		Outlet	2535	42	6	48	97.8	74.8	97.5	12.62	87.4

As shown in Table 4.3, the HCl concentration in the particulate was generally less than 400 ppm_m. However, for test series II, the HCl concentration in the particulate was very high - 16,600 ppm_m. For test series II, the SBS carbon carryover was also very high, and the baghouse was operated without bypass. The relatively high HCl concentration measured in the particulate could be due to either excessive carbon carryover from the furnace adsorbing HCl, or HCl being concentrated in the particulate fines that pass through the baghouse. The overall effect indicated an 40-fold increase in the particulate's chloride concentration compared to the other tests.

The HF removal efficiency for tests I, II, III, and IV, were 96.3%, 99.2%, 82.7%, and 97.5%, respectively. The results were generally as expected. The HF removal for test III was lower than the other three tests and may be due to the lower reagent pH for this test, or may be due to uncertainty arising from the low concentrations of HF for this test.

4.4 Ammonia Removal

Ammonia has been used extensively in electric utility and industrial catalytic systems to control NO_x emissions. A concern in the operation of these systems is how much ammonia passes through unreacted and is emitted to the atmosphere. These ammonia emissions are commonly referred to as "Ammonia Slip". Currently, the USEPA has not imposed limits on ammonia slip. However, ammonia emission limits have been established by state and local agencies. In California, NO_x emission limits generally range from 2 ppm to 10 ppm. Operators of NO_x control systems must balance between using sufficient ammonia to meet NO_x emissions without exceeding the ammonia slip limits. Excessive ammonia use can also cause ammonia salt formation, which can cause fouling in air heaters and catalyst deactivation in the NO_x control equipment. The ammonia salts are formed by the reaction of ammonia with SO_3 in the flue gas to form ammonium sulfate compounds (NH_4HSO_4 and $(NH_4)_2SO_4$)). With these concerns in mind, operators of ammonia based NO_x control systems could benefit from an IFGT system if the IFGT could demonstrate the ability to absorb a large amount of ammonia. The NO_x system could then be operated at higher ammonia to NO_x ratios without increasing ammonia slip.

One objective for ammonia testing for Task 2 was to measure ammonia removal through the IFGT system. Ammonia removal was based on measurements at the inlet and outlet of the IFGT. Ammonia was injected at a constant measured flow rate upstream of the IFGT inlet, at the inlet to the SBS system ID fan. The ammonia flow rate was measured by a certified rotameter and manually controlled at the rotameter. A continuous ammonia analyzer (Severn Science Instruments Ammonia Analyzer) was then used to sequentially measure the ammonia concentration upstream and downstream of the IFGT. For selected tests, the measurements of the continuous analyzer were verified using USEPA Method 206.

During each of the first three test series, three ammonia removal tests were conducted. Table 4.5, Section A, summarizes the results for all nine test conditions. The inlet ammonia concentration ranged from 31 ppm_v to 94 ppm_v and removal efficiency ranged from 57% to 93%. All ammonia tests were conducted at full load. For test III-9B, the measured inlet ammonia concentration was inconsistent with previous data and was estimated from the rotameter settings and previously measured reductions from ammonia-sulfur reactions. The ammonia removal efficiency for test III-9B was subsequently adjusted from 24% to 57%. The IFGT system outlet flue gas temperature for tests I-14G, II-4F, III-18 were planned to be at 9°C (20°F) below the water vapor dewpoint. However, due to seasonal variations in the process cooling water temperature, the actual outlet temperatures achieved were 9°C (16°F), 7°C (13°F), and 4°C (7°F), respectively, below the water vapor dewpoint.

The ammonia removal data in Table 4.5 indicates that the major factors effecting ammonia removal include the IFGT outlet temperature, L/G, the level of dissolved solids in the recirculating liquid, and liquid pH. The effect of outlet temperature is shown for three pair of data sets in Table 4.5, Section B. As with SO_2, the solubility of ammonia in aqueous solution is strongly affected by temperature. The solubility of ammonia increases as the temperature of the liquid decreases. The equilibrium solubility of ammonia in contact with air containing 100 ppm ammonia is approximately 65 mg/l at 38°C (100°F) and increases to 100 mg/l at 27°C (80°F). On average, the data suggests that the ammonia removal efficiency improved by approximately 0.75 N_g for a 6°C (11°F) reduction in outlet temperature.

The effect of inlet ammonia concentration is shown for two pair of data sets in Table 4.5, Section C. There was essentially no measured improvement in ammonia removal efficiency in Test Phase I, when the inlet ammonia concentration was reduced from 94 ppm_v to 68 ppm_v. In Test Phase II the ammonia removal efficiency improved somewhat from 73% to 83% when the inlet ammonia concentration was reduced by almost half from 68 ppm_v to 31 ppm_v.

In the third test phase, the reagent feed total dissolved solids, or "TDS", was reduced from approximately 12% to 4% to reflect the relatively low sulfur content of powder river basin coal. Reducing the TDS reduces the ionic strength in the reagent feed and increases the solubility of ammonia in the liquid. For Test Phase III, the lower TDS enhanced the ammonia solubility by approximately 30%. As shown in Table 4.5, Section D, high TDS test (I-4F) is compared to a low TDS test (III-18). The measured ammonia removal efficiency for both tests was 76%. As previously discussed, the slightly lower flue gas ammonia concentration will not significantly a affect the ammonia removal efficiency. Therefore, the data suggests that the ammonia removal efficiency can be held constant while reducing the L/G from 0.67 l/m^3 (5.0 gal/1000 ft^3) to 0.39 l/m^3 (2.9 gal/1000 ft^3) by lowering the TDS from approximately 12% to 4%.

Ammonia, being an alkaline gas, is better absorbed by liquids with lower pH. The effect of pH on ammonia removal efficiency was investigated in Test Phase III, see Table 4.5, Section E. For the indicated tests, two factors were varied. The inlet ammonia concentration was reduced from 70 pm to 31 ppm, and the reagent feed pH was reduced from 8.2 to 6.8. Based on the previous data, the estimated effect of lowering the inlet ammonia concentration would be a reduction in ammonia removal efficiency of approximately 0.4 N_g. However, by also reducing the pH from 8.2 to 6.8, the ammonia removal efficiency **increased** from 57% to 87%, or a net increase of 1.1 TU. These results suggest that for the operating conditions used in test phase III, reducing the liquid pH from 8.2 to 6.8 improved the ammonia removal efficiency by approximately 1.5 N_g.

Another objective for ammonia testing for Task 2 was to estimate the amount of ammonia that reacts with SO_3 before the IFGT system. Below 230°C (450°F), ammonia reacts with sulfur trioxide (SO_3) in the flue gas, so that some of the gaseous ammonia will be removed from the flue gas upstream of the IFGT. Differences between the measured and calculated ammonia concentration at the IFGT inlet based on the ammonia injection rate determined the amount of the ammonia-sulfur reactions. For the nine completed ammonia tests, the ammonia reduction attributable to ammonia-sulfur reactions ranged from 27% to 45%, and averaged 36%. The ammonia reduction for test III-9B was measured at 75%, and was considered inconsistent with the other test results.

Table 4.5 Summary of Ammonia Removal Measurements

Test	NH_3 At CHX Inlet (ppm_v, wet)	NH_3 At CHX Outlet (ppm_v, wet)	NH_3 Removal (%) / (TU)	Outlet Gas Temp. (°C)	Feed pH	L/G l/m^3
Section A - Data Summary						
I - 4G	70	5	93 / 2.69	27.2	7.9	0.67
I - 4F	94	22	76 / 1.43	36.1	7.9	0.67
I - 4E	68	16	76 / 1.42	36.1	7.9	0.68
II - 4D	68	12	83 / 1.76	36.0	8.2	0.66
II - 4F	64	7	88 / 2.16	29.3	8.2	0.64
II - 4E	31	8	73 / 1.30	36.3	8.2	0.64
III - 18	84	20	76 / 1.45	38.0	7.9	0.39
III - 9B	70	30	57 / 0.86	42.3	8.2	0.35
III - 7B	31	4	87 / 2.02	42.3	6.8	0.34
Section B - Effect of Lower Outlet Temperature.						
I - 4E	68	16	76 / 1.42	36.1	7.9	0.68
I - 14G	70	5	93 / 2.69	27.2	7.9	0.67
II - 4D	68	12	83 / 1.76	36.0	8.2	0.66
II - 4F	64	7	88 / 2.16	29.3	8.2	0.64
III - 9B	70	30	57 / 0.86	42.3	8.2	0.35
III - 18	84	20	76 / 1.45	38.0	7.9	0.39
Section C - Effect of Lower Inlet NH_3 Concentration.						
I - 4F	94	22	76 / 1.43	36.1	7.9	0.67
I - 4E	68	16	76 / 1.42	36.1	7.9	0.68
II - 4D	68	12	83 / 1.76	36.0	8.2	0.66
II - 4E	31	8	73 / 1.30	36.3	8.2	0.64
Section D - Effect of Reduced L/G and Total Dissolved Solids.						
I - 4F	94	22	76 / 1.43	36.1	7.9	0.67
III - 18	84	20	76 / 1.45	38.0	7.9	0.39
Section E - Effect of pH.						
III - 9B	70	30	57 / 0.86	42.3	8.2	0.35
III - 7B	31	4	87 / 2.02	42.3	6.8	0.34

4.5 Particulate Removal

The IFGT system is effective at removing particulate from a flue gas stream because of the serpentine gas flow path around the Teflon®-covered tubes in the heat exchangers. The primary removal mechanism is inertial impaction of the larger particles on the tube surface. Previous testing conducted using oil-fired flue gas indicated that removal extends to smaller particles in which inertial effects are minimal.

Although effective at removing particulate, the CHX® design is not intended to handle the full particle load from a coal-fired boiler. Collected particulate must be rinsed from the tubes and flushed from the system at regular intervals to prevent plugging between tubes. However, since the measurement of particle loading, particle removal efficiency, and trace element concentrations in particulate are all more easily made if the particle loading to the IFGT inlet is relatively large, the particle loading to the IFGT system inlet was set to about 500 to 900 mg/dscm (0.4 to 0.6 lb/MBtu) for most of the tests. This particle loading represents about 10% of the ash in the coal. In the SBS combustor about 50% of the fly ash is retained in the furnace/convection pass as bottom ash and ash deposits and so the loading to the IFGT system was about 20% of the normal ash loading to the baghouse.

To achieve the targeted particle loading, the baghouse bypass valve was opened so that the baghouse pressure drop was reduced about 20%, indicating a bypass gas flow of about 20%. Once set, the valve position was maintained for the duration of a test. The normal bag cleaning cycle based on baghouse pressure drop was suspended during a test day. Likewise, soot blowing of the convection pass tubes was delayed until the end of a test day. These precautions prevented upsets in the particle loading at the IFGT during testing. Soot blowing and bag cleaning was performed at the end of a test day. Similarly, particulate was permitted to accumulate in the first stage of the IFGT system during a test day and was rinsed after daily testing was completed.

Using this procedure, the particle loading to the IFGT system was lowest at the start of the day when the baghouse pressure drop was lowest. Later in the day, as the filter cake on the bags caused the baghouse pressure drop to increase, a larger fraction of the gas flow was bypassed and so the particle loading at the IFGT system inlet increased. These mild changes in particle loading did not influence the results as the particle loading changed only slowly with time, and removal efficiencies were always based on simultaneous measurements at the inlet and outlet of the IFGT system.

Raw coal for the SBS furnace was crushed, dried and stored in a bunker. The crushed coal was then ground in an MPS pulverizer and stored in a second bunker. All of the coals used on these tests was ground to the same nominal coal fineness of 70% through a 200 mesh screen (70% < 75 micrometers).

The particle size distributions of the fly ash at the inlet to the IFGT system for the four test series are shown in Figure 4.12. The cumulative percent of the mass is shown as a function of the flyash aerodynamic particle size. These size distributions were measured with the cascade

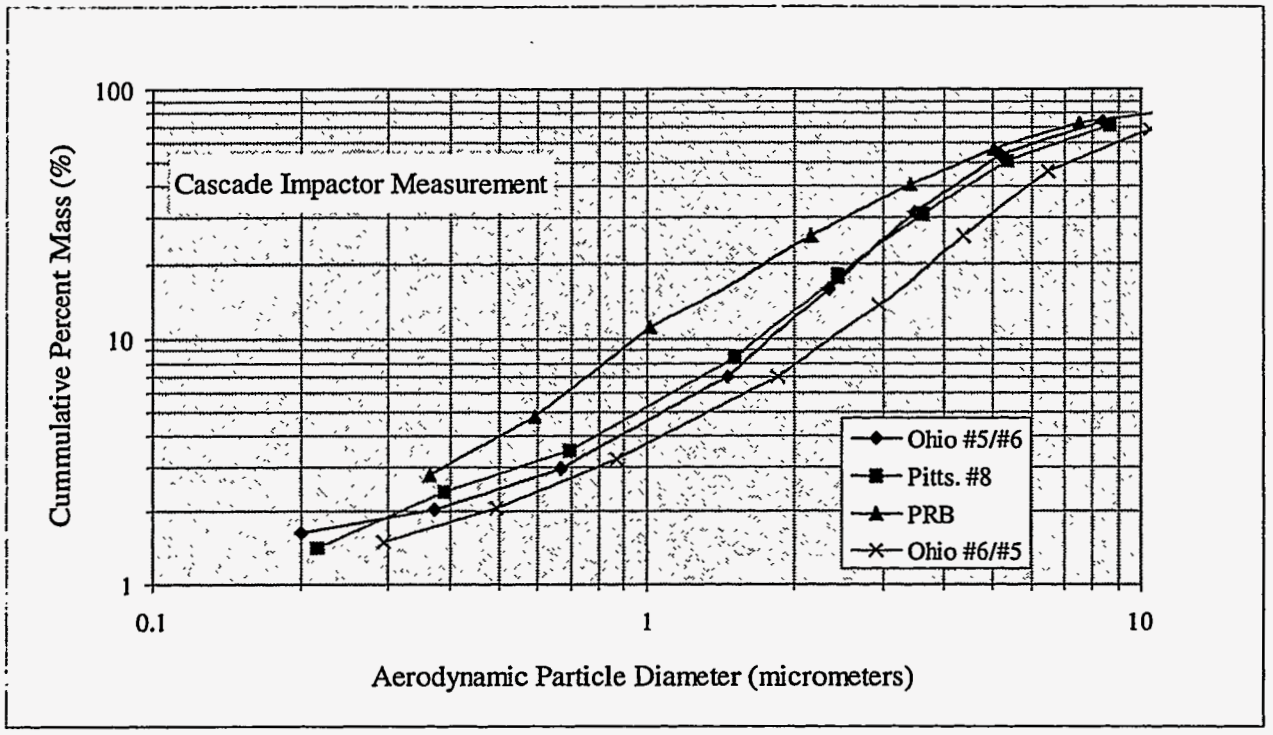

Figure 4.12 Fly Ash Particle Size Distribution at the IFGT Inlet for Each Coal Tested

impactor at the inlet to the IFGT system. As shown in the figure, the flyash size distribution for test series I and II (Ohio 5/6 and Pittsburgh coals) are nearly identical. The size distribution for test series IV (Ohio 6/5) is slightly larger, and the size distribution for test series III, Powder River Basin coal, is smaller. The mass median diameters for the four test series range from 4 μm to about 7 μm, which is in the range of that for coal-fired utility power plants.

4.5.1 Particle Removal Efficiency as a Function of Particle Size

Cascade impactor measurements were made for selected tests to determine the fly ash particle size distribution measurements at the inlet and outlet of the IFGT system. The particle size distribution combined with the measured particle loading at the inlet and outlet was used to determine the particle removal efficiency as a function of particle size.

Removal efficiencies calculated in this manner are subject to errors because of the small amount of mass collected on some of the filters (< 1 mg), and because the different flue gas conditions at the inlet and outlet flues result in slightly different cut sizes for the impactor plates. To minimize these errors, the following approach was used to determine removal efficiencies:

- The aerodynamic particle diameter cut size of the cascade impactor stages were calculated based on the flue gas properties, temperature and sample flow rate through the cascade impactor. The procedure followed was that recommended by Southern Research Institute[3]:

- The cumulative percent of mass and the particle loading were used along with the calculated particle diameter cut sizes to determine the cumulative mass loading (mg/dscm) as a function of particle size at the inlet and outlet.

- Linear interpolation of the cumulative mass loading data was used to determine the slope of the curve (dm/dlog[D]) at a set of diameters, D. Removal efficiency was calculated at each D as the percent change in (dm/dlog[D]) from the inlet to the outlet.

Cascade impactor measurements were made for seven different tests which spanned the four test series and included two different inlet gas velocities (loads). Table 4.6 provides a listing of the cascade impactor tests cross referenced to the test at which total removal measurements were also made. Five tests were conducted at full load and two tests were conducted at partial load.

Table 4.6 List of Cascade Impactor Tests

Cascade Impactor Test ID	Total Removal Test ID	Inlet Gas Velocity (m/s)	L/G (l/m^3)	Gas Outlet Temperature Difference From Dew-Point (°C)	Comments
I-4L	I-4B	11.77	0.64	0.0	
I-14M	I-14D	12.05	0.70	-9.0	
I-4N	I-4J	11.79	0.64	1.0	Inter-stage Steam Injection
II-4G	II-4C	11.78	0.63	0.0	
III-12B	III-12A	7.10	0.36	0.0	Partial Load
IV-1B	IV-1A	11.14	0.52	0.0	Mesh Pad
IV-2B	IV-2A	7.02	0.47	0.0	Partial Load

Figure 4.13 shows the cumulative mass distribution at the inlet and outlet of the IFGT for test I-14. The data is presented as the cumulative mass as a function of fly ash aerodynamic particle size. The data in this figure shows that the mass median diameter (50% mass) at the inlet to the IFGT is about 5 μm, and is about 1 μm at the outlet.

Figure 4.14 shows the particle removal efficiency as a function of particle size calculated from the data presented in Figure 4.13. This curve has several general characteristics that are evident in all of the data:

- The removal efficiency is greatest at the largest particle size and then decreases rapidly with particle size below 3 μm.

- The removal efficiency decreases to a minimum value at about 0.6 μm.

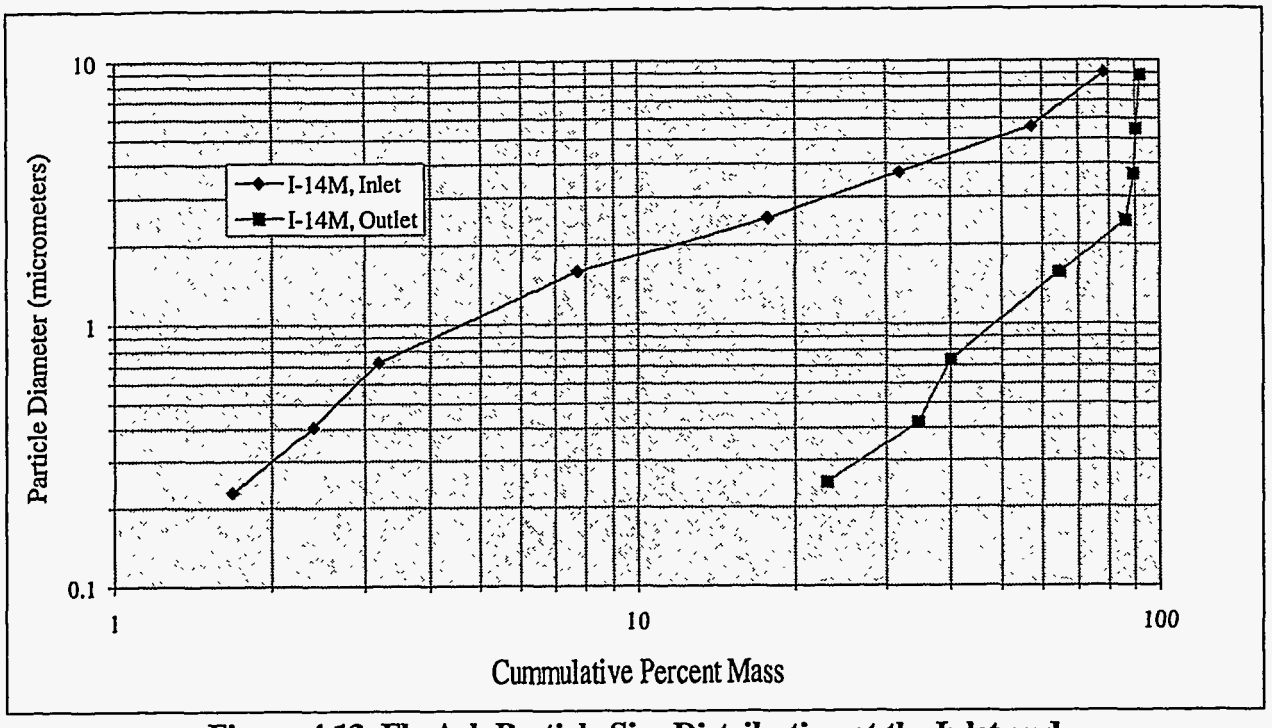

Figure 4.13 Fly Ash Particle Size Distribution at the Inlet and Outlet of the IFGT System for Test I-14M

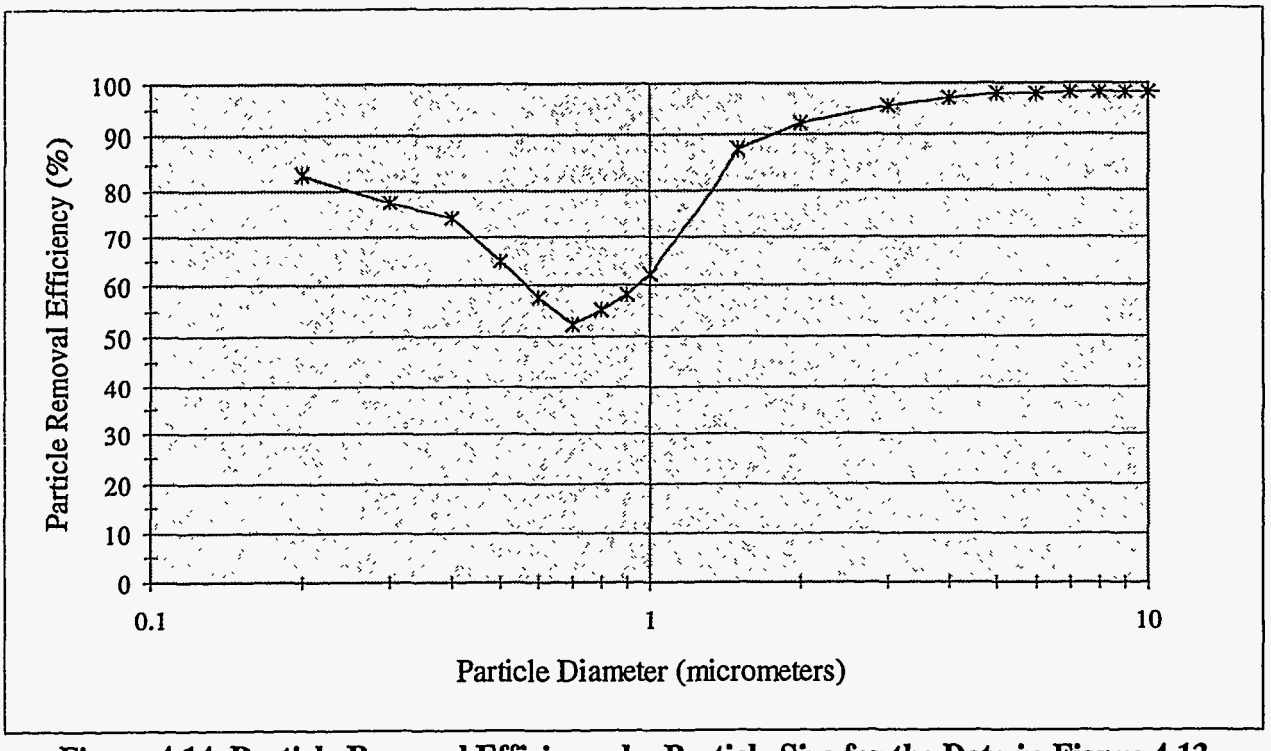

Figure 4.14 Particle Removal Efficiency by Particle Size for the Data in Figure 4.13

- the removal efficiency increases as particle diameter decreases for diameters below about 0.6 μm.

The removal efficiencies for particle sizes greater than 1 μm have the least uncertainty because they represent the greatest amount of mass collected on the filters. Similarly, the removal efficiencies for particulate less than 1 μm have the greatest uncertainty because they represent only a small fraction of the mass collected. Typically, the mass collected on the filters in this size range was less then .5 mg, and represented less than 5% of the total mass collected.

The decrease in removal efficiency with particle size is expected since the primary particle removal mechanism is inertial impaction, which is less effective as particle size decreases. The cause for the increase in removal efficiency for diameters less than ~0.5μm is not known. In this size range diffusion and thermophoresis may become important mechanisms and enhance particle removal.

Figure 4.15 shows the removal efficiency as a function of particle size for the five full-load tests, and the average for the five tests. The data show that the average removal efficiency for particles greater than 1μm is in excess of 90%, while the average removal for particles smaller than 1μm is about 60%.

The removal efficiency as a function of particle size for the two partial load tests are shown in Figure 4.16. The two data curves have the same general shape as the data for full load, but with lower overall removal efficiencies. This again is not unexpected since the effect of inertial impaction is diminished as gas velocity is decreased.

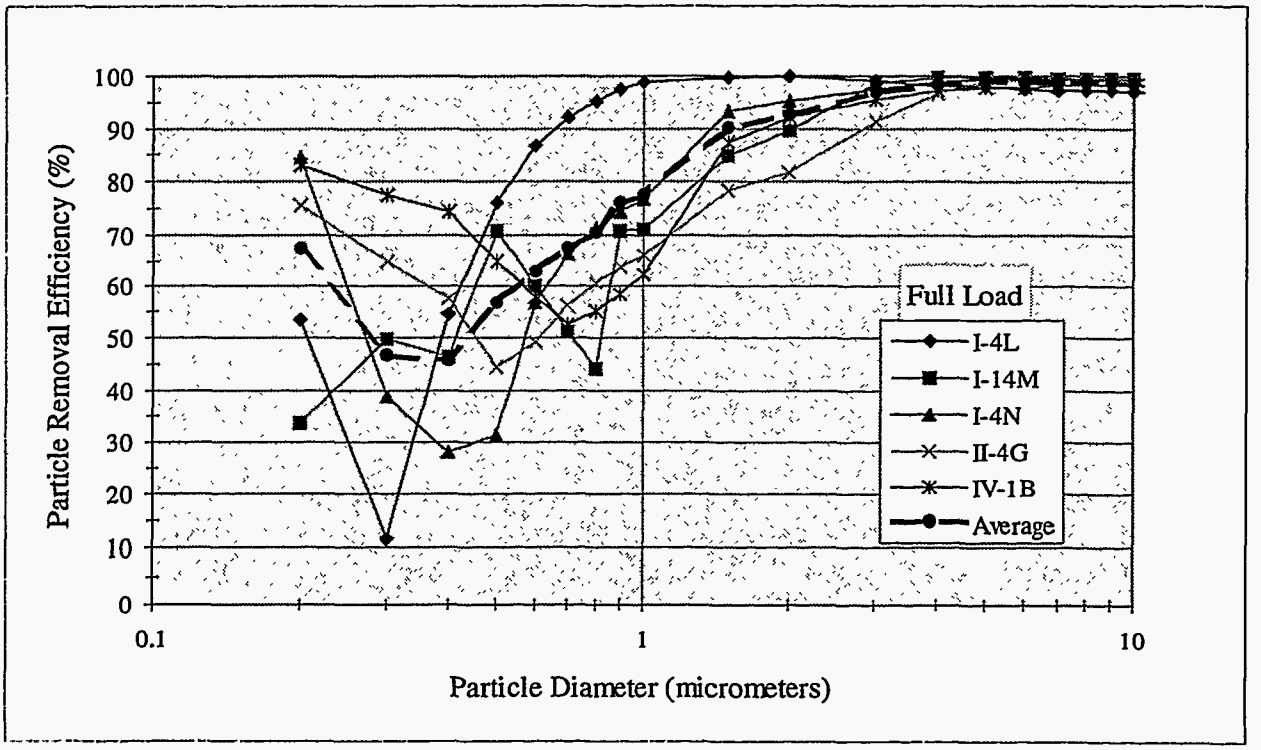

Figure 4.15 Particle Removal Efficiency by Particle Size for All Full Load Tests

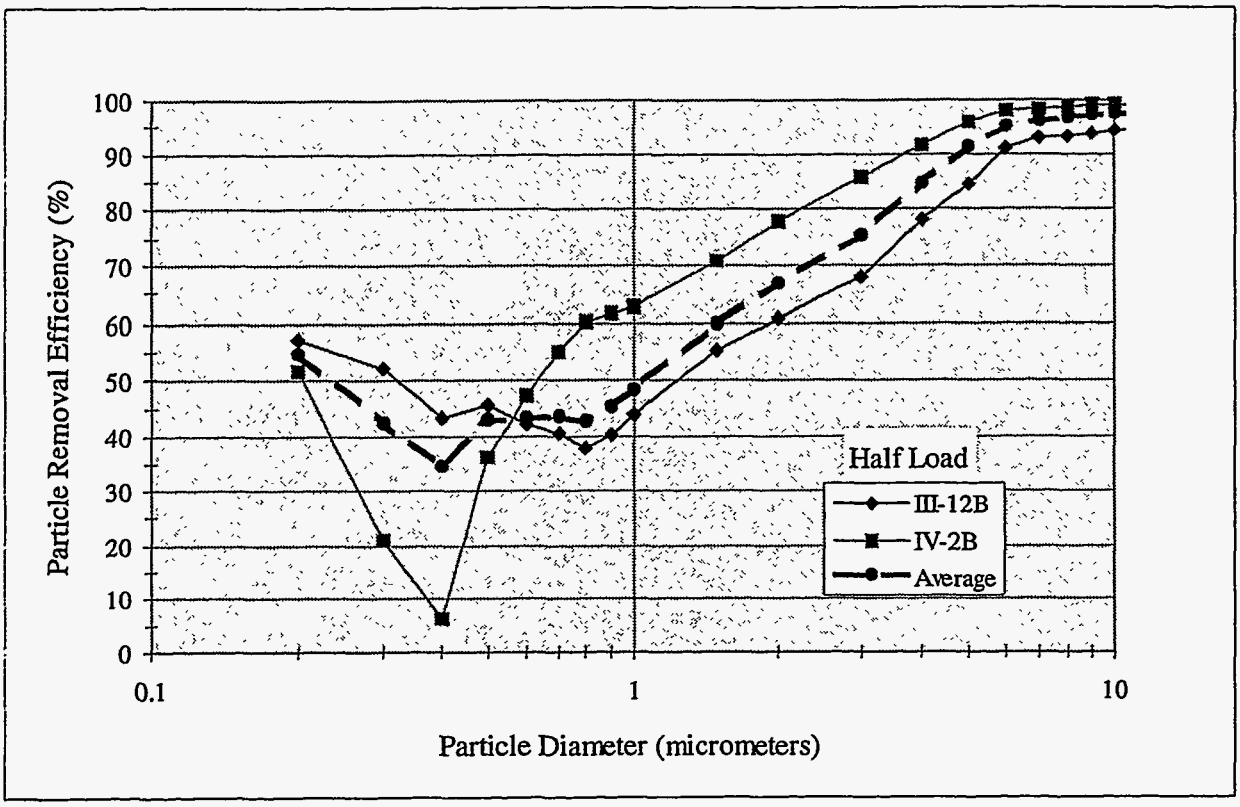

Figure 4.16 Particle Removal Efficiency by Particle Size For Partial Load Tests

4.5.2 Total Particle Removal

Particle loading at the inlet and outlet of the IFGT facility was made during all of the sampling for mercury/trace metals, chloride/fluoride, and ammonia, along with several dedicated Method 5 samples.

The only abnormal occurrence in the particle loading data occurred in test series II using the Pittsburgh #8 coal. With Method 5 sampling, the total collected particulate consists of the fly ash collected on a filter (filter particulate) and the fly ash that deposits on the sampling probe surfaces and is collected in a rinse (probe rinse particulate). In test series II, the probe rinse particulate was weighed with a scale of insufficient accuracy and resolution. For the test series II tests, particle removal efficiency was calculated based on the filter weights only. This is a conservative approach since for all tests, the probe rinse is a greater fraction of the total particulate collected at the inlet to the IFGT facility than at the outlet.

The particle removal data are shown in Table 4.7. Along with the particle loading and removal efficiency, this table also provides the type of test, sampling time, gas velocity at the CHX® inlet and the reagent liquid-to-gas ratio. For test series I, the particle loading exceeded 400 mg/dscm, and the particle removal efficiency exceeded 95%. For test series II, the inlet particle loading varied from about 0.7 to 400 mg/dscm, and the removal efficiency ranged from 23% to 94%. For tests II-4A and II-4F all of the flue gas was routed through the baghouse. The low inlet particle

loadings of 3.6 and 0.7 mg.dscm are the fugitive baghouse emissions and are well below the NSPS limit of 42 mg/dscm (0.03 lb/million Btu).

Table 4.7 Overall Particulate Removal Data

Test Number	Test Type	Total Sample Time (hrs)	Inlet Gas Velocity (m/s)	Outlet Gas Temperature (°C)[1]	L/G (l/m^3)	Inlet Particle Loading (mg/dscm)	Particle Removal Efficiency (%)
I-14D	M-29 Avg.	6.0	12.05	-9.0	0.70	842.	96.5
I-4A[2]	M-26	1.7	11.87	0.0	0.67	722.	96.4
I-4J[3]	M-5	2.0	11.79	1.0	0.64	711.	95.2
I-4F	M-5/NH3	2.0	11.95	0.0	0.65	644.	95.6
I-4B	M-29 Avg.	6.0	11.77	0.0	0.64	642.	97.2
I-4C	M-29 Avg.	6.0	11.78	0.0	0.63	401.	95.9
II-4C	M-29 Avg.	6.0	11.87	0.0	0.53	655.	93.9
III-7A	M-26	2.0	11.70	0.0	0.38	482.	88.7
III-9B	M-5NH3	1.3	11.60	1.0	0.35	480.	89.7
III-9A	M-29/OH Avg.	6.0	11.53	0.0	0.36	478.	88.4
IV-14A	M-29/OH Avg.	6.0	11.42	-1.0	0.49	296.	95.1
IV-1A	M-26	2.0	11.14	0.0	0.52	40.2	94.3
II-4A	M-29 Avg.	6.0	11.77	0.0	0.61	3.6	71.9
II-4F	M-5/NH3	2.0	11.94	-8.0	0.64	0.7	23.6
IV-2A	M-5	1.3	7.02	0.0	0.47	444.	93.0
III-12A	M-29/OH Avg.	6.0	7.10	0.0	0.36	384.	77.6

1) Gas Temperature Relative to The Water Vapor Dew Point Temperature
2) Woven Mesh Pad Located in the IFGT Interstage
3) Interstage Steam Injection

The removal efficiency for tests III-9A, -9B and -7A averaged about 89%, which is less than other data at comparable particle loadings. The lower overall removal efficiency for these tests is due to the finer fly ash particle size distribution for the Powder River Basin coal and the lower removal efficiency for the fine particulate.

From the data in the table, it is evident that the particle removal efficiency decreases as the particle loading to the CHX® is reduced. This is due to the size distribution of the particulate. The other trend in evidence in Table 4.7 is shown by tests III-9B and III-12A which show a decrease in removal efficiency as the gas velocity (i.e., load) is decreased.

In Test IV-2A, the use of wire mesh pads was investigated as a means of fine particulate removal. For this test four layers of mesh pad were located in the interstage between the first and second heat exchanger stages. The measured removal efficiency of 93% is substantially greater than the 77.5% removal efficiency for test III-12A which was also conducted at partial load, but without the use of a mesh pad. Although this is a substantial difference, most of the difference may be attributable to differences in the inlet particle size distribution.

With the exception of load (gas velocity) and particle loading, the removal efficiency is insensitive to other operating conditions over the range tested.

4.6 Mercury Removal

4.6.1 Measurement Methods and Detection Limits

The mercury content of the vapor and particle phases entering the IFGT facility were measured in each of the four test series. Triplicate two hour tests were conducted at each test condition. In the first two test series, mercury concentrations were measured exclusively using EPA Method 29 sample trains. During the third and fourth test series the triplicate measurements consisted of two Ontario Hydro sample trains bracketing a single Method 29 sample train. The sample time for the mercury measurements were two hours for each triplicate test.

The measurement accuracy of speciated forms of mercury using Method 29 and the Ontario Hydro method have not been resolved, and this issue is beyond the scope of this work. Rather, the concentrations of the speciated forms and the total mercury as determined using the Method 29 and Ontario Hydro are presented in this report with the caution that the absolute accuracy of the speciated concentrations are in question.

The concentration of mercury in the recovered impingers (vapor phase) and the concentration of mercury in the digested particulate samples (particle phase) was measured using Cold Vapor Atomic Absorption (CVAA). The detection for mercury measurements in the laboratory using CVAA is 0.1 parts per billion (ppb) for ionic mercury and 0.5 ppb for elemental mercury when measured in a prepared solution. The solution analyzed in the laboratory is prepared from the impinger and washing solutions gathered from the Method 29 and Ontario Hydro sampling trains. Mercury emissions are normally expressed on terms of micrograms per dry standard cubic meter, (ug/dscm). If the laboratory detection limits of 0.1 to 0.5 ppb are transformed to ug/dscm using typical Method 29 and Ontario Hydro sampling rates and impinger volumes, the detection limits can be compared to actual measurements to insure that these measurements are sufficiently above the detection limits to be meaningful. The estimated detection limits for mercury are summarized in Table 4.8. Also listed in Table 4.8 are the minimum reportable

Table 4.8 Mercury Detection Limits and the Minimum Reportable Concentrations

Mercury Form	Detection Limit in the Flue Gas (ug/dscm)	Minimum Reportable Concentration (ug/dscm)
Ionic Vapor Phase	0.02	0.5
Elemental Vapor Phase	0.20	1.0
Total Vapor Phase	0.22	1.0
Particle Phase	0.01	0.2
Total mercury	0.23	1.0
Mercury in the Coal	2.66	(-)

concentrations that have been used in this report. These minimum reportable concentrations take into account the detector's limits as well as triplicate test repeatability.

4.6.2 Mercury Concentration in the Coal

Typically, the concentration of mercury in the coal was determined from grab samples of the pulverized coal in the coal pipe just upstream of the burner. Grab samples were obtained at the start, middle, and end of a two-hour test period. A composite of the grab samples from the triplicate tests was used to obtain a test average coal sample for analysis.

Not all of the collected samples were analyzed for mercury. Rather, the mercury concentration in the coal provided measurement redundancy and a cross check by which the reasonableness of gas and particle phase measurements could be evaluated.

Figure 4.17 shows the concentration of mercury in the flue gas that would result from 100% emission of the mercury contained in the coal for each coal in the four test series. The error bars indicate the range of multiple measurements. The mercury level from the Ohio #5/#6 coal (Test Series I) and the PRB coal are relatively high, while the Pittsburgh #8 and Ohio #6/#5 coal are relatively low*. The coals selected for the pollutant removal tests were based primarily on sulfur content and origin. Within those parameters, coals with high mercury concentrations were desired in order to provide increased measurement accuracy associated with the absolute concentrations and mercury removal. The mercury concentration in the Ohio and Pittsburgh coals are within ranges generally reported in the literature.[4] The concentration of mercury in the PRB coal is higher than typically reported in the literature.

4.6.3 Comparison of Gas Phase Mercury Speciation from Method 29 and the Ontario Hydro Method

Mercury vapor in the flue gas exists in both elemental (Hg^{o}) and ionic (Hg^{++}) forms. The ionic form is the more reactive of the two, so that ionic mercury is more readily removed in sulfur scrubbing systems. EPA Method 29 sampling has been validated for measuring metals concentration, including mercury, in the vapor state. With this technique, the metal vapors are trapped by the chemical solutions in the sample impinger bottles. The ability of Method 29 to distinguish between the different forms of mercury in the vapor state has been under question, and alternate methodologies (Ontario Hydro, for example) have been proposed to more accurately assess the concentration of the two forms of mercury.

In test series III and IV, triplicate measurements consisted of an EPA Method 29 sample train bracketed by two Ontario Hydro (OH) sample trains. A comparison of the ionic mercury concentration measured with the two techniques at the inlet and outlet of the IFGT facility are shown in Figure 4.18. The OH data are the average of two measurements and the uncertainty bars indicate the data range.

---

* Ohio #5/#6 denotes a blend of 80% Ohio #5 and 20% Ohio #6. The Ohio #6/#5 contained 80% #6 and 20% #5.

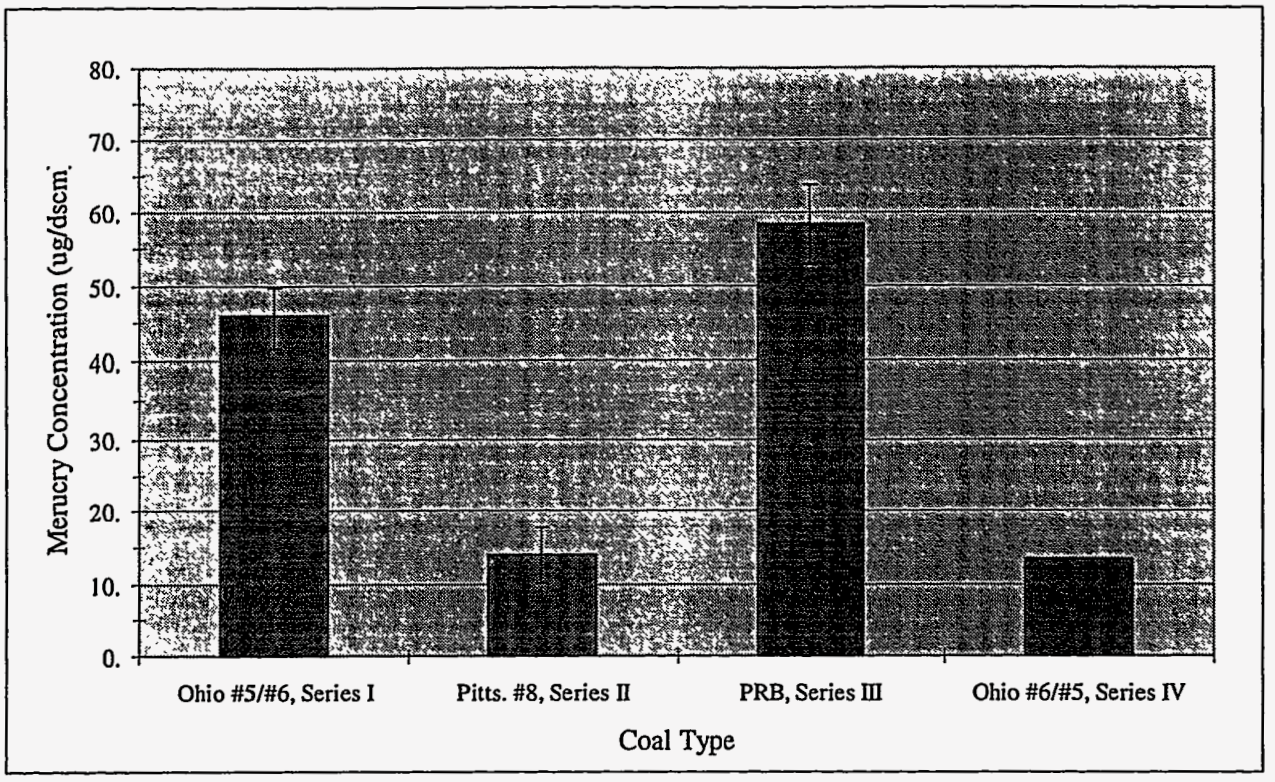

Figure 4.17 Flue Gas Mercury Concentration Resulting from 100% Release of Mercury in the Coal

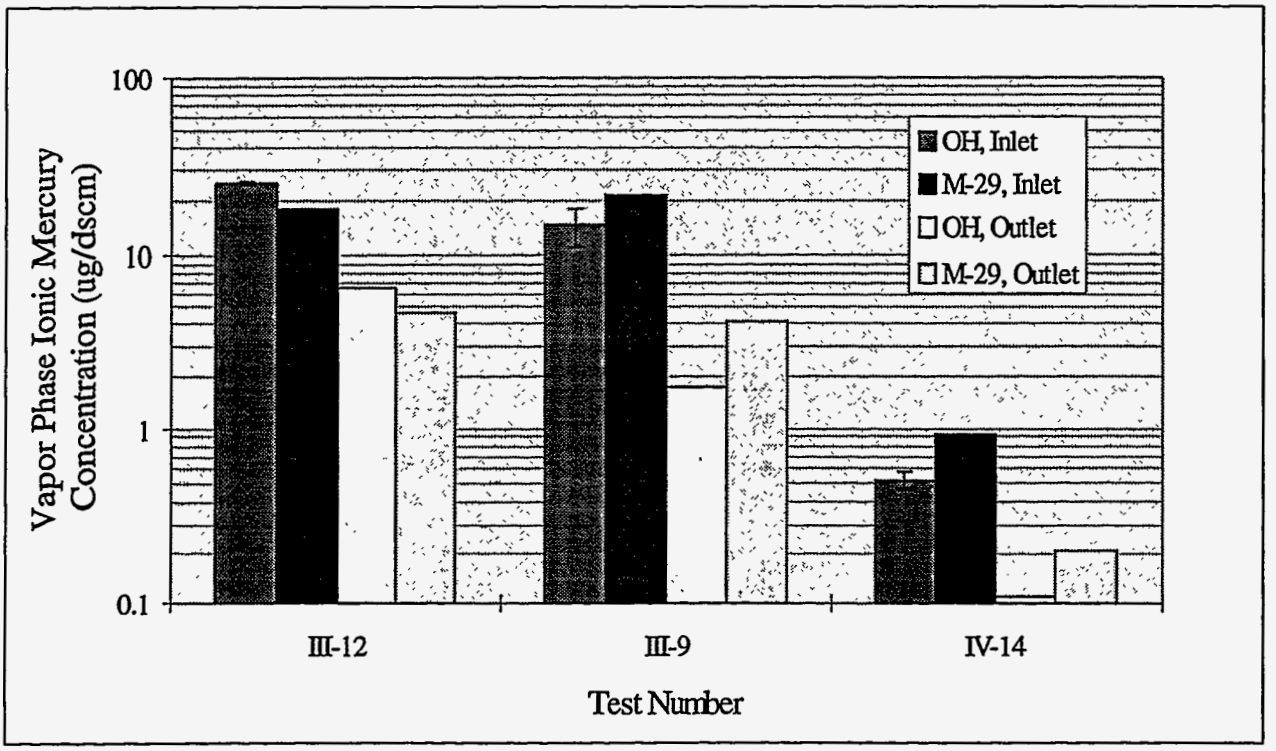

Figure 4.18 Comparison of Vapor Phase Ionic Mercury Measured Using Method 29 and Ontario Hydro (OH) Sample Trains

Figure 4.18 shows that at the inlet to the IFGT facility, the OH measurement of Hg^{++} exceeded the M-29 measurement of Hg^{++} in test III-12, while in test III-9 and IV-14, the M-29 measurement exceeded the OH measurement. In all three tests, the M-29 measurement is outside the range of the OH measurements.

Comparison of the OH and M-29 data at the outlet of the IFGT indicate the same trend, so that the relative change in Hg^{++} across the IFGT system is nearly the same for either technique. This indicates that the difference between the two measurement techniques may have been due to a real variation in Hg^{++} concentration in the flue gas over the six hour duration of the triplicate tests. The difference in the average ionic mercury concentration between tests series III and IV is due to the coal used for each test. Test III used a PRB coal while test IV used an Ohio coal.

Figure 4.19, is a corresponding comparison of the two measurement techniques for elemental mercury at the inlet and outlet of the IFGT facility. For tests III-12 and III-9 the elemental mercury concentration was quite high and the difference in concentration between the two measurement techniques at the inlet and outlet location are quite small. For test IV-14 the concentration of Hg^{o} was very low. The OH method provides a slightly larger measured value of Hg^{o} at both the inlet and outlet of the IFGT. The relative difference between the two techniques for this test is greater than for test series III, but the absolute difference is again very small.

Comparison of the OH and M-29 measurements of elemental and ionic mercury show only relatively small differences, and the difference is consistent at the inlet and outlet measurement locations. For this reason, no further distinction will be made between the two techniques with respect to the total concentration of mercury or the speciated forms of mercury. The data from the two measurement techniques were averaged to determine test average mercury concentrations and removal efficiencies.

4.6.4 Mercury Partitioning

Mercury is a relatively volatile element that can exist in the flue gas as a vapor and can also be attached to particulate carried by the flue gas. Figure 4.20 shows the concentration of mercury in the flue gas at the inlet to the IFGT facility as vapor, and that contained on the particulate, for all of the tests. The particulate and vapor forms are both in the common basis of ug/dscm. Expressed in this form, it is understood that the particle phase mercury concentration in the flue gas depends not only on the mercury concentration in the fly ash, but also the fly ash concentration in the flue gas.

Figure 4.20 shows that for test series I and III most of the mercury is partitioned to the vapor phase and is very repeatable from test to test. In test series II the total vapor phase concentration was below reportable limits, while in test II-4C the particulate concentration is larger than for any other test. In test IV-14 the vapor phase concentration is about the same as the particulate phase. For the data shown in Figure 4.20, the particle loading to the IFGT facility was about the same for all tests.

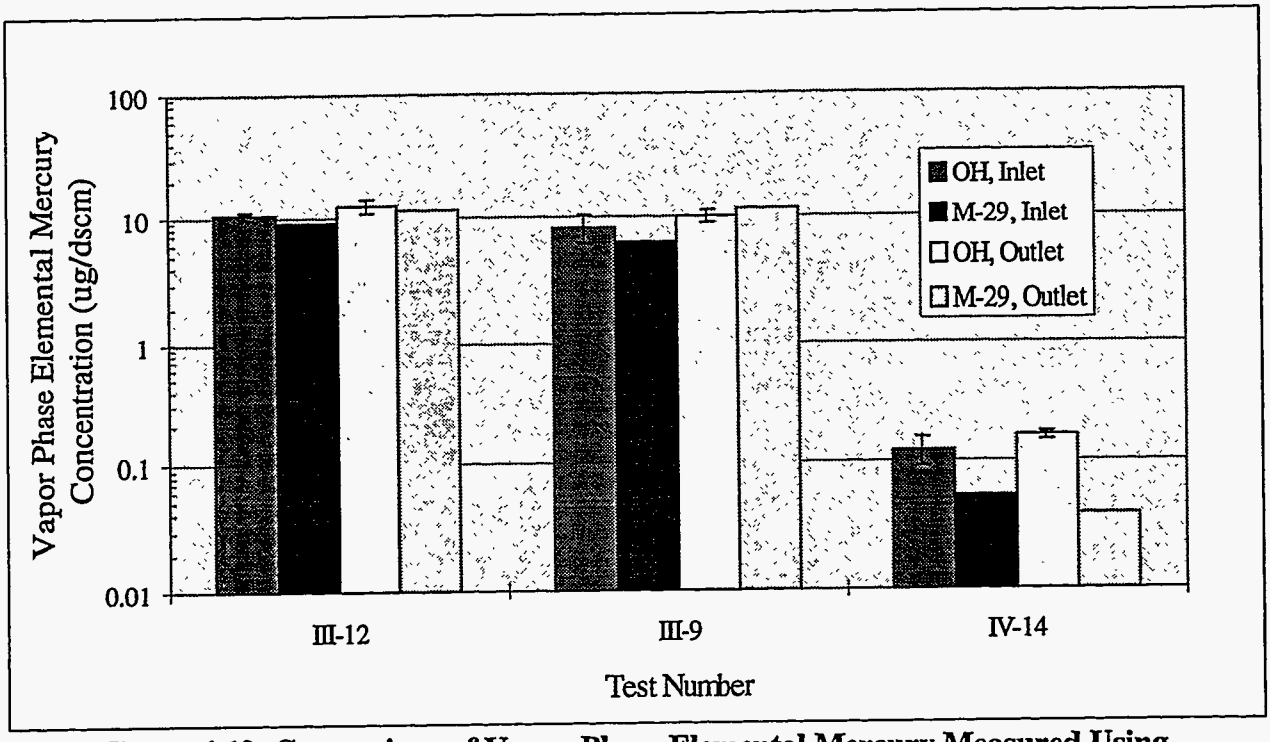

Figure 4.19 Comparison of Vapor Phase Elemental Mercury Measured Using Method 29 and Ontario Hydro Sample Trains

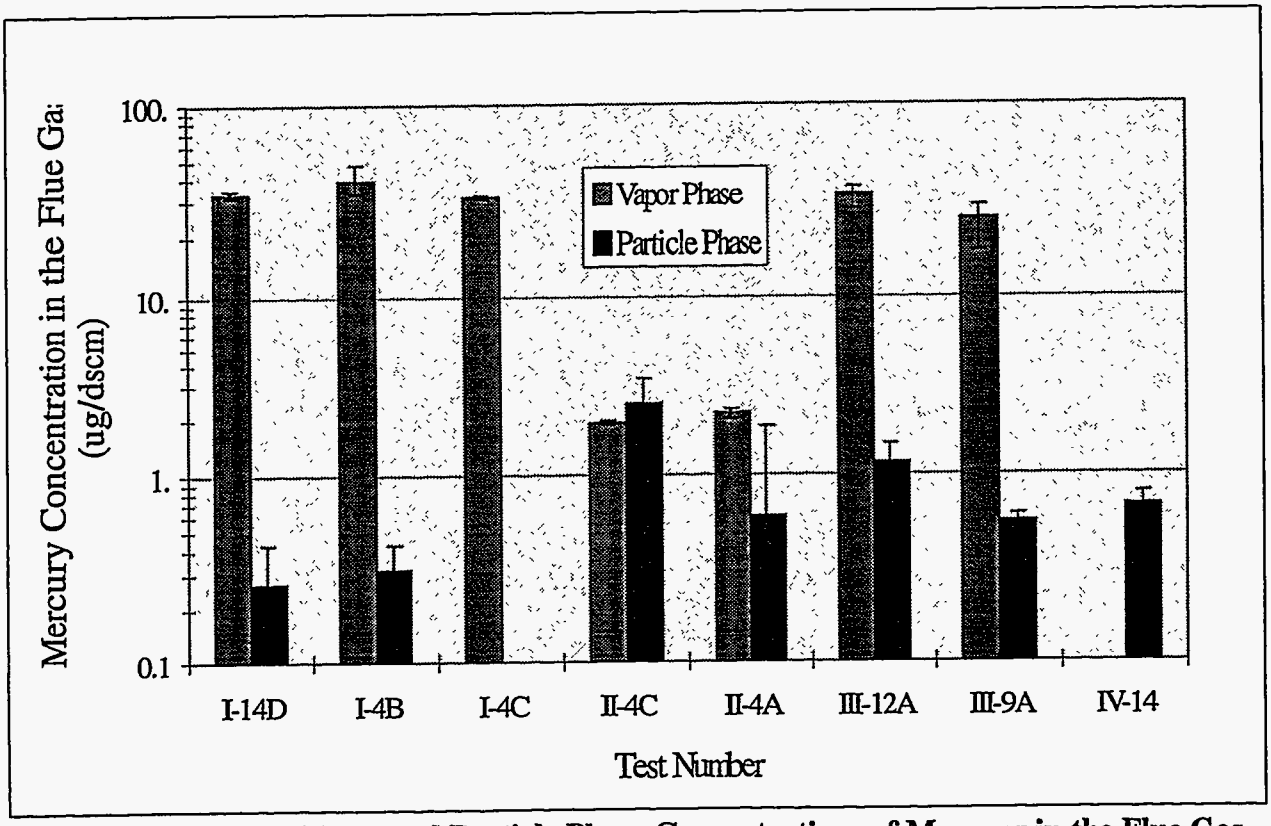

Figure 4.20 Vapor Phase and Particle Phase Concentrations of Mercury in the Flue Gas

The differences in particle phase concentration shown in Figure 4.20 is primarily due to differences in mercury concentration in the fly ash, and not particle loading. The cause of the variation from one test series to the next is not known, but is likely dependent on the coal type. Field measurements of mercury concentrations at utility power plants have traditionally shown wide variation.[5] Precautions were taken during the tests to ensure that combustion conditions were duplicated for each of the four tests. This included the same burner, excess air, load, primary and secondary air temperatures, coal grind (fineness), downstream equipment and operating procedure.

4.6.5 Vapor Phase Mercury Removal

Figure 4.21 shows the triplicate average ionic mercury concentration at the inlet to the IFGT facility and the calculated removal efficiency for each test. The vertical bars on the concentration data indicate the range of the triplicate measurements. The vertical bars on the removal efficiency is the estimated uncertainty based on the standard deviation in the triplicate measurements.

For test series I, III, and IV the ionic mercury removal efficiencies ranged from 75% to 85%, while for test series II the removal efficiency averaged less than 0%. Removal efficiencies on the order of 70% to 90% for ionic mercury are to be expected.[6] The measured concentrations for test II are just above reportable limits, and so may be subject to relatively large error. However, the measured concentrations for test IV-14 are similarly low, and are in agreement with the data for test series I and III. The data and analysis procedures from test series II have been reviewed and a cause for the abnormal results could not be found. However, the data are not in agreement with that from the other three test series and are not in agreement with data reported in the literature, and so should be considered questionable.

Figure 4.22 shows the average concentration and removal efficiency of elemental mercury for each test. The removal data averages from about 0% to -35% and is independent of mercury concentration or coal type. Elemental mercury removal data is not presented for test series II as the concentrations were below reportable limits.

The indicated increase in elemental concentration across the IFGT facility was not limited to triplicate averages at the inlet and outlet. Essentially all paired inlet/outlet measurement of elemental mercury indicated some increase in concentration. This effect may be real, if captured ionic mercury is reduced to elemental mercury and subsequently evolved from the scrubbing solution. This effect may also be an artifact of the sample trains used to measure ionic and elemental mercury.

Removal efficiencies of about 0% for elemental mercury are in general agreement with published data for other flue gas treatment equipment, primarily wet scrubbers.[7] An anticipated benefit from low temperature operation of the IFGT facility was not realized. The outlet flue gas temperatures for the data in Figure 4.22 ranged from about 27°C to 37°C (80°F to 98°F), which is well below the normal operating temperature for wet scrubbers.

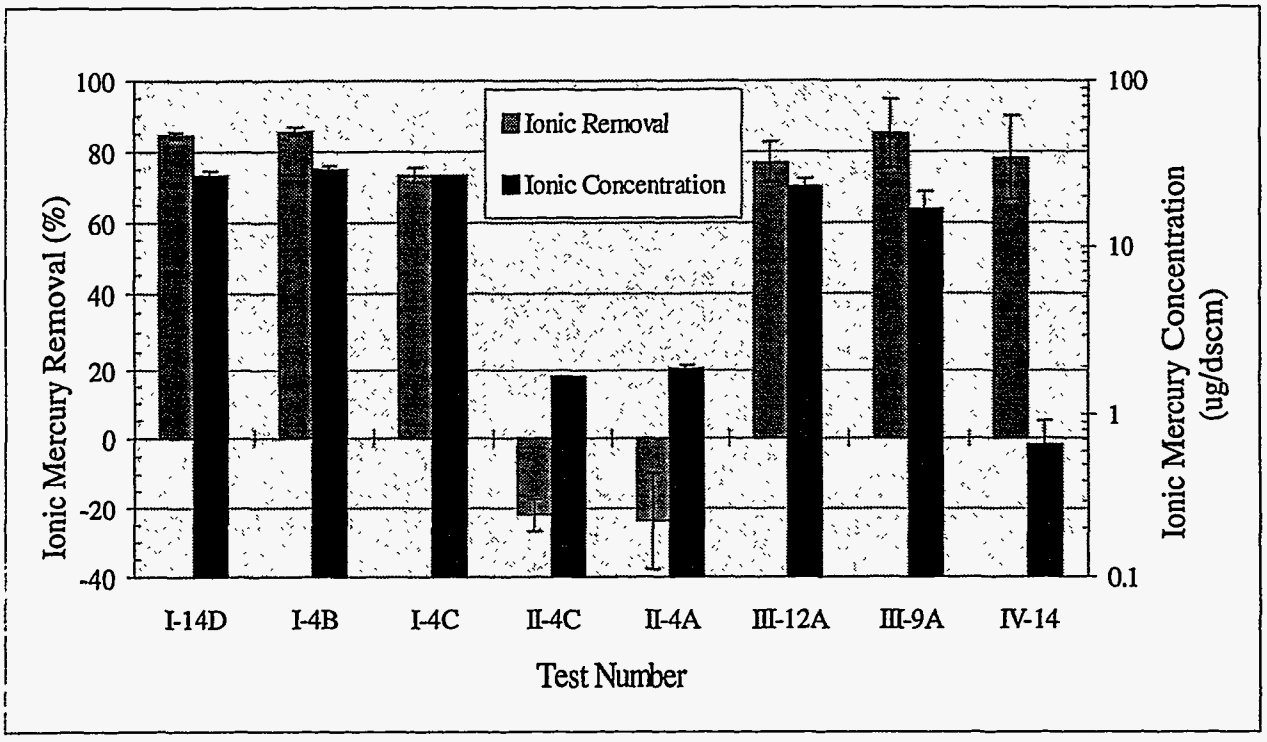

Figure 4.21 IFGT Removal Efficiency for Ionic Mercury (Left y-axis) and Ionic Mercury Concentration (Right y-axis)

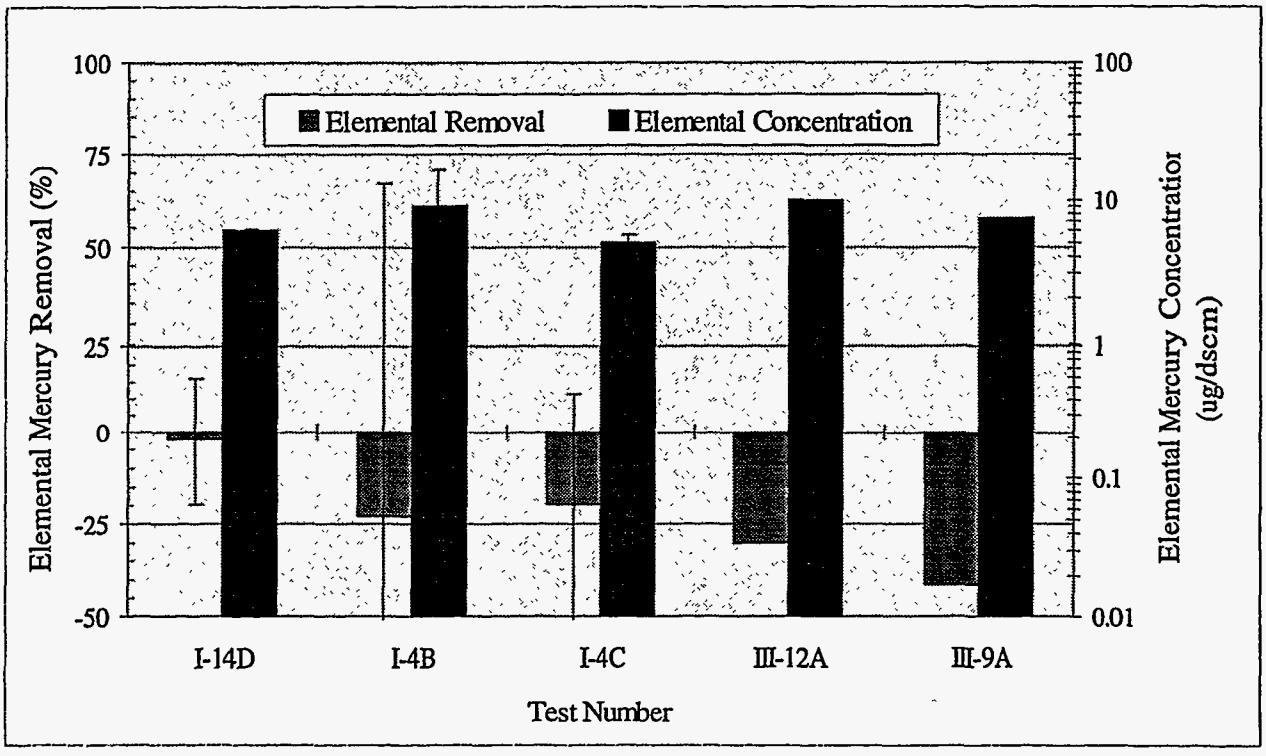

Figure 4.22 IFGT Removal Efficiency for Elemental Mercury (Left y-axis) and Elemental Mercury Concentration (Right y-axis)

4.6.6 Particle Phase Mercury Removal

The particle phase mercury concentration and removal efficiency for each of the tests are shown in Figure 4.23. Data are shown only for those tests in which the mercury concentration was above reportable limits. Three of the tests show an average removal efficiency of about 75%. Of the two tests that have lower removal efficiencies, test III-12A was conducted at partial load, and the lower mercury removal (42%) was due to a lower particulate removal efficiency (77%). The cause of the low removal efficiency of test III-9A is unknown. As indicated by the uncertainty limits, the measured concentrations of particulate mercury in the triplicate tests varied significantly.

The particle phase mercury removal is less than the overall particulate removal because the mercury concentration in the particulate at the outlet of the IFGT facility averaged 3 to 5 times greater than at the inlet. This indicates that the mercury tends to be concentrated in the sub-micron particulate, which is less effectively removed by the IFGT process.

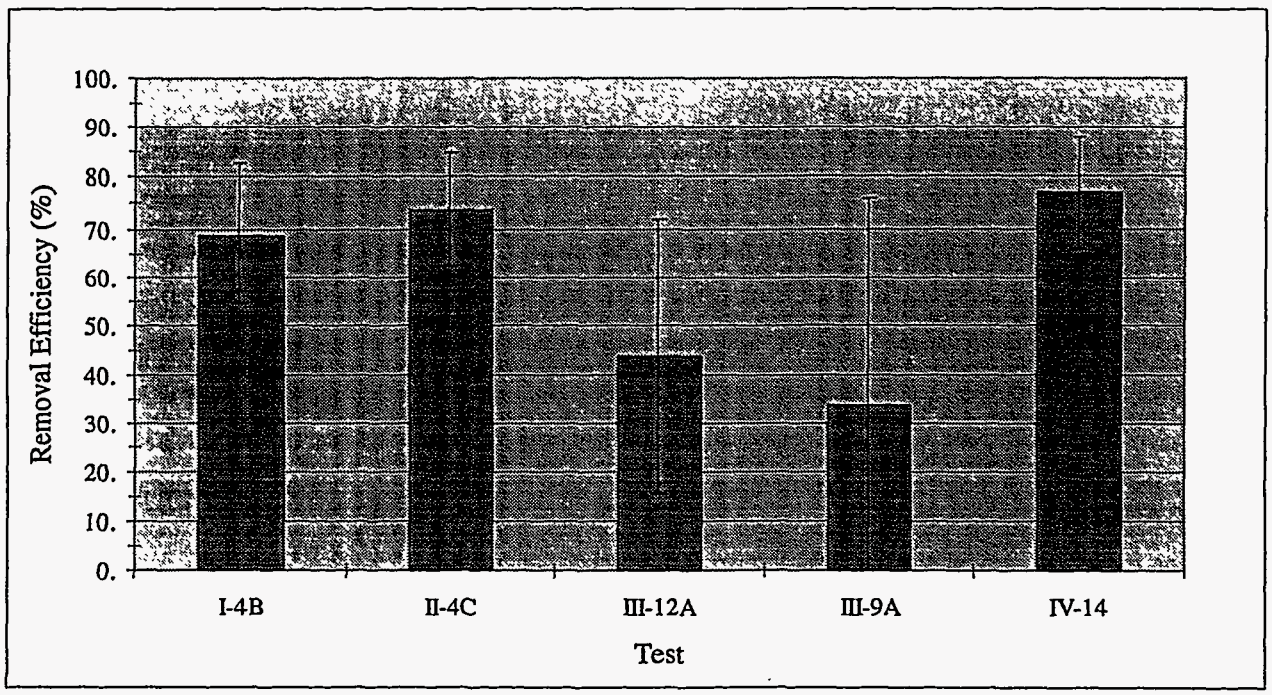

Figure 4.23 Removal Efficiency for Particle Phase Mercury

4.7 Trace Element Removal

4.7.1 Trace Element Measurement and Detection Limits

The trace element content of the vapor and particle phases entering the CHX® were measured in each of the four test series. Triplicate two hour tests were conducted at each test condition. In the first two test series, element concentrations were measured exclusively using EPA Method 29 sample trains. During the third and fourth test series the triplicate measurements consisted of two Ontario Hydro sample trains bracketing a single Method 29 sample train. The sample time for the Method 29 and Ontario Hydro trains were two hours for each of the triplicate tests. The Ontario Hydro sample trains were used primarily to obtain comparative mercury speciation data.

The concentration of trace elements in the recovered impingers and the concentration of trace elements in digested particulate samples were measured using graphite furnace atomic absorption (GFAA). Table 4.9 lists the limits of detection of the trace elements for the gas phase, fly ash, and coal samples that are typical for the four test series for the M-29 sample train. Also shown are the minimum reportable detection limits which have been defined as 10 times the detectable limit or 1.0 ug/dscm, whichever is greater for gas phase concentrations.

Table 4.9 Detection and Reporting Limits for Trace Elements

Element	Vapor Phase Limits		Particle Phase Limits		Coal
	Detection Limit (ug/dscm)	Reporting Limit (ug/dscm)	Detection Limit (ug/dscm)	Reporting Limit (ug/dscm)	Detection Limit (ppm)
Arsenic	0.117	1.2	0.064	1.0	0.20
Barium	1.173	11.7	0.643	6.4	2.00
Beryllium	0.059	1.0	0.439	4.4	0.10
Cadmium	0.012	1.0	0.026	1.0	0.02
Chromium	0.117	1.2	0.064	1.0	0.40
Cobalt	0.235	2.4	0.161	1.6	0.20
Lead	0.117	1.2	0.142	1.4	0.20
Manganese	0.117	1.2	0.101	1.0	0.40
Nickel	0.235	2.4	0.161	1.6	0.20
Selenium	0.117	1.2	0.142	1.4	0.20

Although Ontario Hydro trains have not been validated for trace elements other than mercury at this time, vapor phase trace elements were also measured in the Ontario Hydro impingers for test series III. The detection limits for vapor phase metals from OH sample trains are about 5 times

greater than for the M-29 sample trains shown in Table 4.9. For test series III and IV the vapor phase concentration of all trace elements except mercury were below reportable values for both the OH sampling methods, so that an accurate comparison of the two techniques using this data cannot be made.

4.7.2 Vapor Phase Trace Element Removal

Most of the trace elements are non-volatile and condense to a solid state at relatively high temperatures. Generally, trace elements measured in the vapor phase were below the reportable limits of detection at the inlet to the CHX®. This was especially true for the Pittsburgh and PRB coals for which gas phase concentrations of trace elements was very low. The exceptions are arsenic and selenium which occurred in fairly high concentration for several of the coals tested. Significant quantities of lead, nickel, and manganese were occasionally measured, but the repeatability of the concentration data as determined by the triplicate measurements was poor.

Figure 4.24 shows the concentrations and removal efficiency for arsenic for test series I and IV that used the Ohio coals. The uncertainty bars on the concentration represent the range of triplicate measurements, while the uncertainty bars on removal efficiency represents a root mean square (rms) uncertainty based on triplicate concentration measurements. The concentration of arsenic for the Pittsburgh and PRB coals were below reportable limits, and are not shown. For the tests shown in Figure 4.24, the arsenic concentration varied from 20 to 70 ug/dscm, and the removal efficiency was greater than 95%. The removal efficiency for test IV-14A with a mag-lime reagent is no different than for the other tests in which soda ash reagent was used.

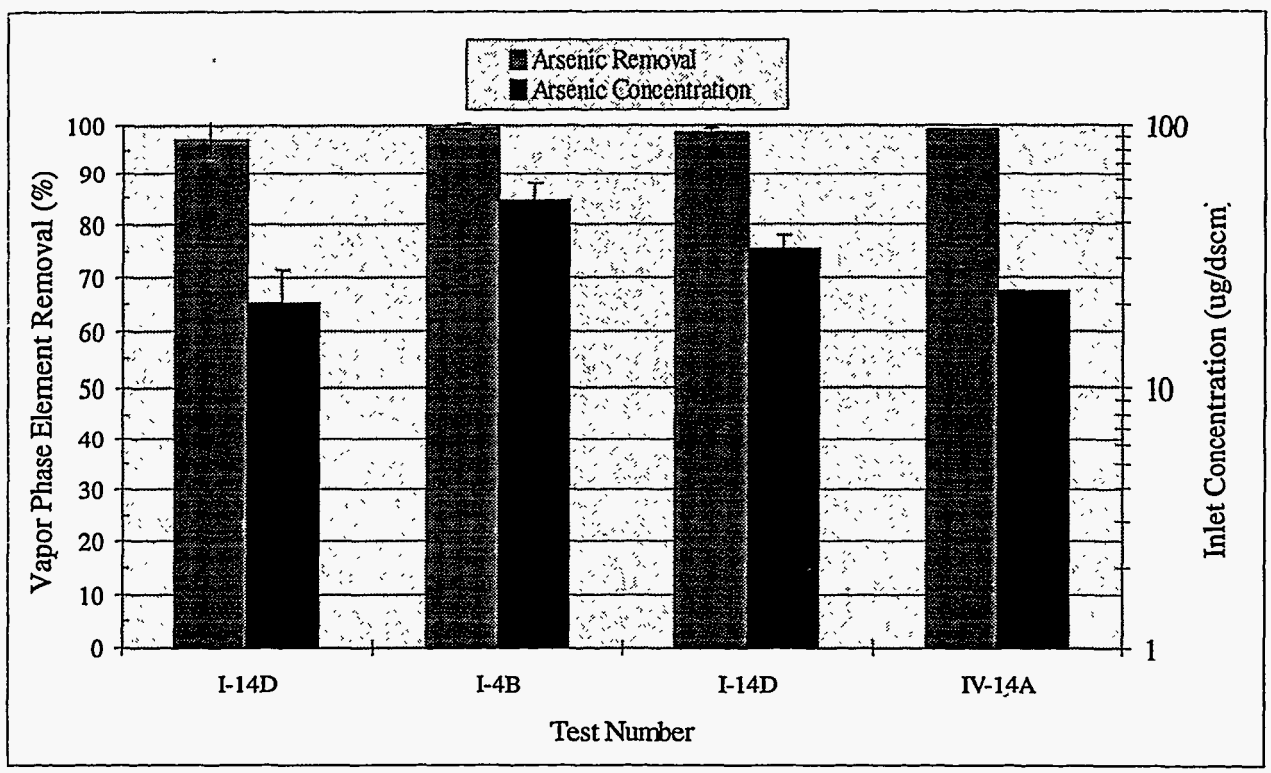

Figure 4.24 IFGT Removal Efficiency for Vapor Phase Arsenic (Left y-axis) and the Inlet Concentration (Right y-axis)

Figure 4.25 is a similar figure showing the concentration and removal efficiency for vapor phase selenium. Reportable quantities of selenium were measured in the Pittsburgh coal (series II) as well as for the Ohio coals (series I and IV). For test series I and test II-4C the selenium concentration and removal efficiency are both quite high. For test II-4A, the removal efficiency is about 50%, but the concentration is just above the reportable limit, and the uncertainty in the removal efficiency is quite large.

Test IV-14A represents a single Method 29 sample. The removal efficiency is lower than for tests with comparable concentrations. The lower removal efficiency for this test may be due to the mag-lime reagent that was used. All other tests were conducted with sodium based reagent.

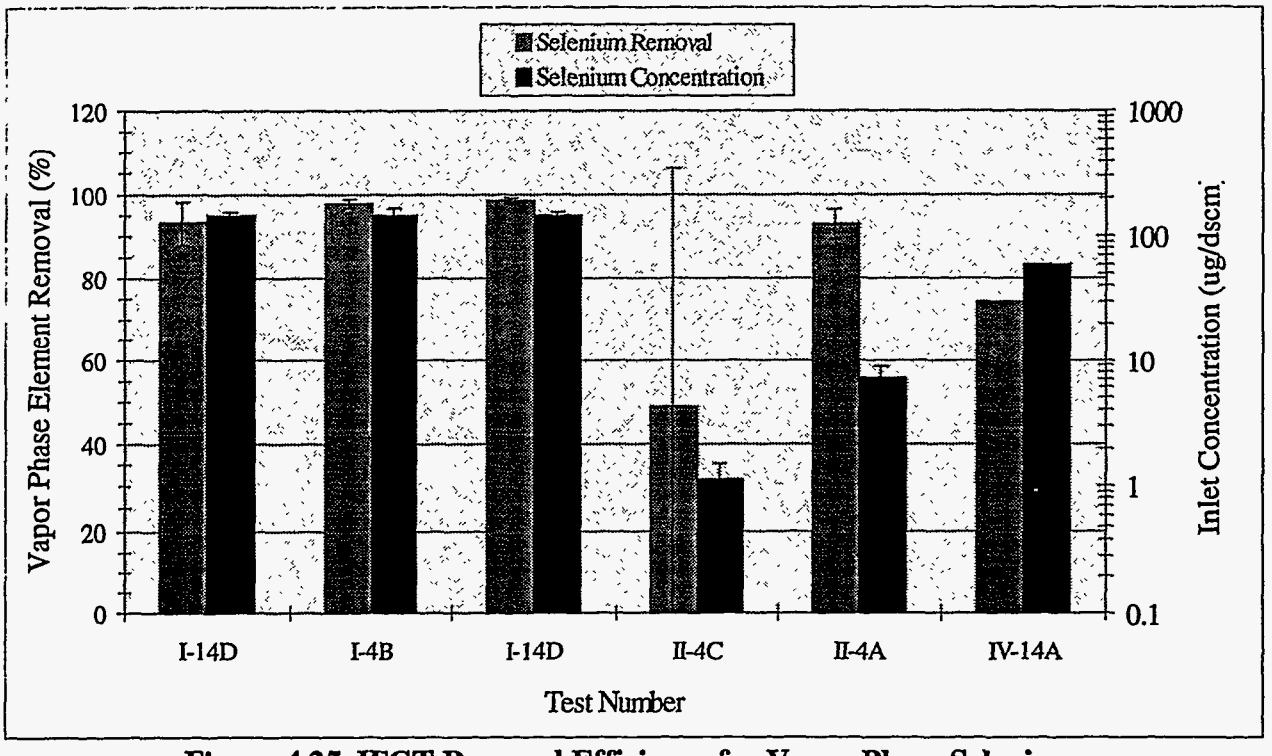

Figure 4.25 IFGT Removal Efficiency for Vapor Phase Selenium (Left y-axis) and the Inlet Concentration (Right y-axis)

4.7.3 Particle Phase Trace Element Removal

When expressed on a gas phase basis, the concentration of an element contained on particulate depends on both particulate concentration in the flue gas and the element concentration in the particulate. It is the product of these two numbers which represents the total quantity of the element in the flue gas.

Figure 4.26 shows the particle phase concentration of the elements in the flue gas at the inlet for three tests that represent the three different coals. For these three tests the particle loading at the inlet to the CHX® was relatively constant, so most of the test to test variation shown in the figure is due to variation of the elemental concentration in the particulate.

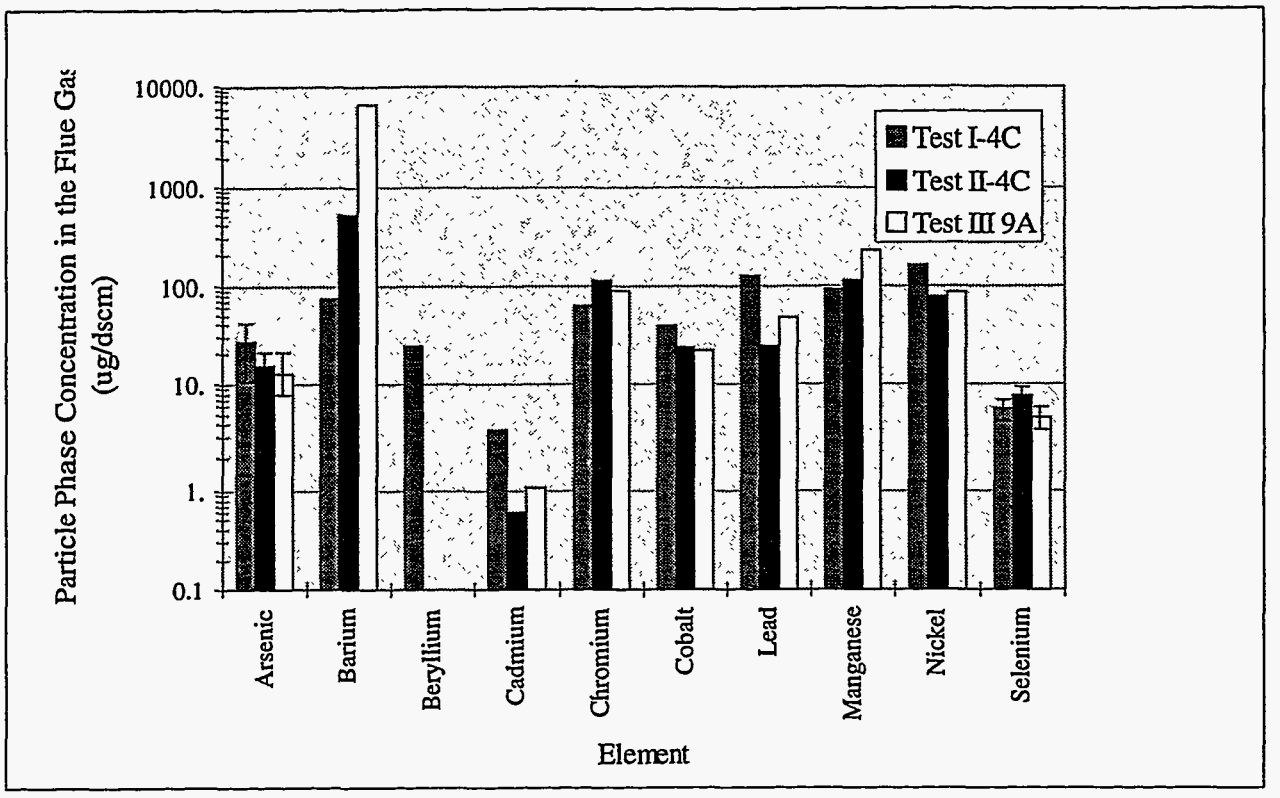

Figure 4.26 Particle Phase Elemental Concentration at the IFGT Inlet

Chromium has the lowest concentration of all of the elements measured, and is just above reportable limits. For most of the elements the variability with coal type (Ohio, Pittsburgh and PRB) is less than the variability from element to element. The exception is barium which had a very high concentration for test series III (PRB coal).

Figure 4.27 shows the element removal efficiency for the particle phase data. Measured data from all full-load tests are included in this figure. The particle phase removal efficiencies range from about 20% for cadmium to 100% for Beryllium. In general, although the concentration of cadmium in the particulate was above reportable limits, the triplicate measurements indicated a large variability.

For all elements except beryllium, the removal efficiency for the element is less than the removal efficiency measured for the particulate. For the tests shown in Figure 4.27, particle removal efficiencies ranged from 87% to 96%. The reduced efficiency for the removal of these elements compared to removal of the total particulate is caused by enrichment in the fine particulate.

With the exception of beryllium, all elements indicated a higher concentration in the fly ash at the outlet of the IFGT system than at the inlet to the IFGT system. This is illustrated by Figure 4.28 which shows the ratio of the element concentration in the particulate at the inlet of the CHX® to that at the outlet. As shown, the element concentration in the fly ash at the outlet is generally 2 to 10 times that at the inlet. Since the median particle size of the flyash at the outlet is about one-fifth of that at the inlet (1 micron vs 5 microns) this indicates that the fine

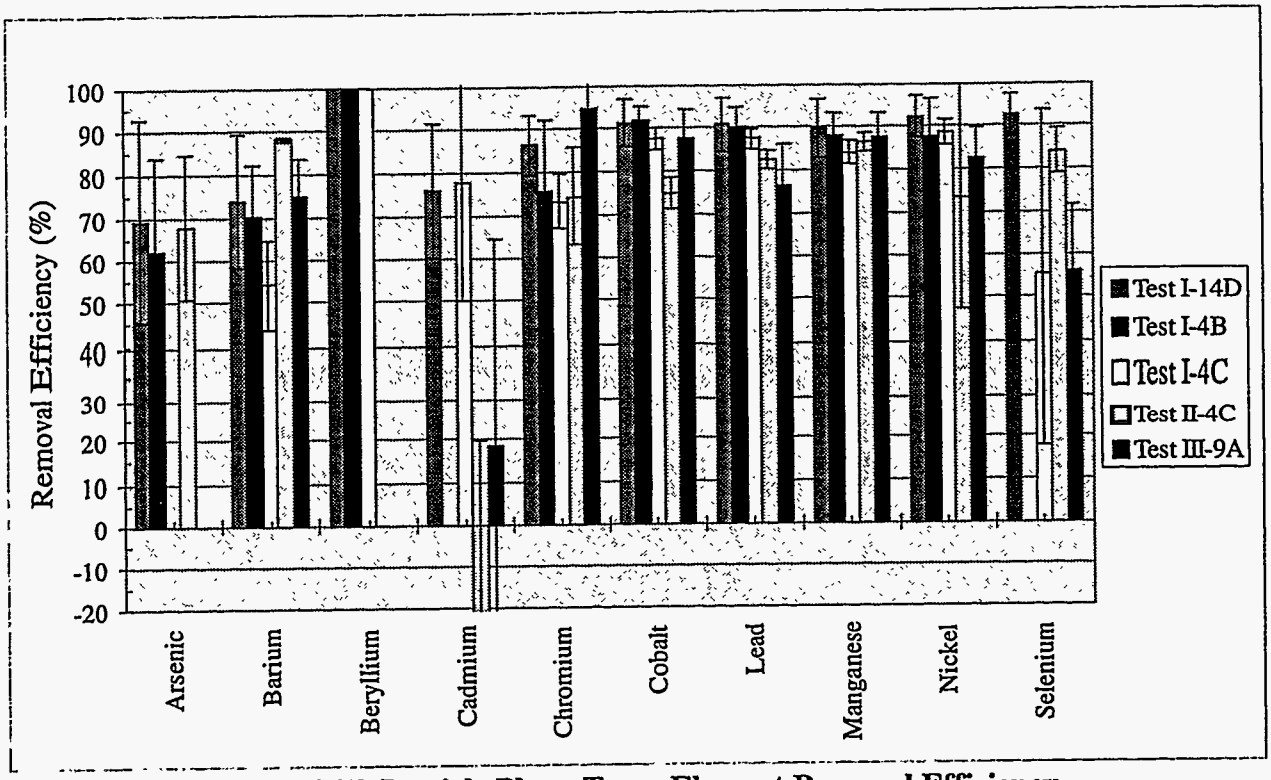

Figure 4.27 Particle Phase Trace Element Removal Efficiency

particulate contain proportionately higher concentrations of these elements. The removal of the element is less than the removal of the total particulate because the fine particulate, of which only 60% is removed, contains a disproportionate amount of the element.

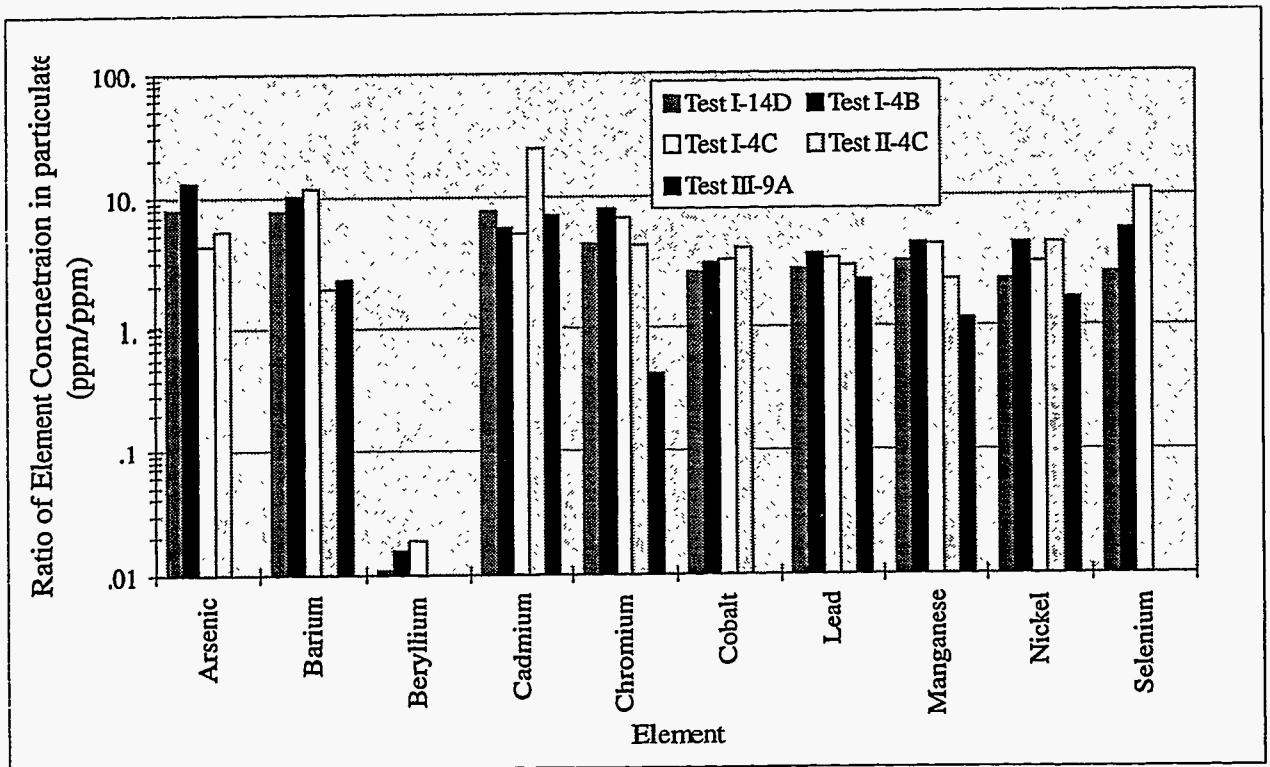

Figure 4.28 Ratio of Element Concentration in the Fly Ash at the IFGT Outlet to the Inlet

4.8 NO_x Removal

NO_x concentrations at the inlet and outlet of the IFGT facility were measured during test series I. Although removal of NO was not anticipated, NO_2 removal with the sodium based reagent was possible. The NO_x measurements in Test Series I were performed to determine if any measurable reduction in NO_x occurred in the IFGT process.

Figure 4.29 shows the calculated NO_x removal efficiencies for all of measured data. Within the experimental error of the measurements, NO_x removal averaged 0% for all of the tests. Based on these results, NO_x measurements were suspended for the remaining tests.

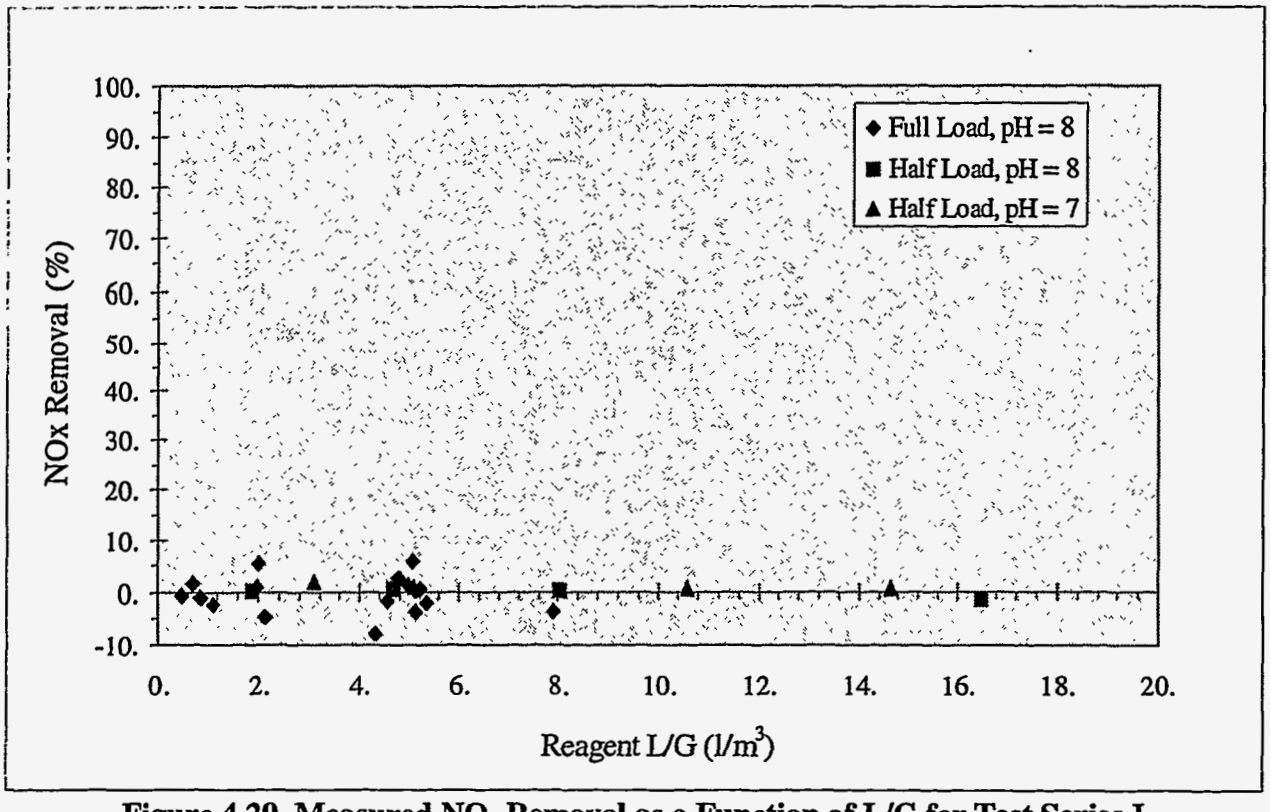

Figure 4.29 Measured NO_x Removal as a Function of L/G for Test Series I

4.9 Wear Tests at ECTC

4.9.1 Operation Summary and Discussion

Over the course of the wear tests, the CHX® pilot test unit was operated "at conditions" for 6,240 hours. During this time, all major design conditions operating ranges were met and maintained. A summary of the major operating conditions and the actual operating ranges is given in Table 4.10.

Table 4.10 Summary of CHX® Operating Conditions at the ECTC

Operating Parameter	Range or Value
Inlet Gas Flow	1275 scmh (750 scfm)
Inlet Gas Temperature	150°C (300°F)
Inlet Water Temperature	55 to 60°C (130 to 140°F)
Outlet Gas Temperature	82 to 93°C (180 to 200°F)
Outlet Water Temperature	76 to 80°C (170 to 175°F)
Inlet Particulate Loading (EPA M5 average)	25 mg/dscm (0.022 lb/10^6 Btu) 2,060 hours 400 mg/dscm (0.35 lb/10^6 Btu) 4,180 hours
Tube Wash Cycle	20 minutes every 8 hours

The particulate loading to the inlet of the CHX® test unit is reported as an average unit because the loading was increased partway through the test. The above value represents an average of the measured values after the change in particulate loading. A graphical summary of the CHX® inlet particulate loading over the course of the test program is shown in Figure 4.30. The particulate loading data presented in Figure 4.30 was obtained using an Environmental Systems P-5A *in situ* particulate monitor. The P-5A monitor was operated on a continuous basis and served as a qualitative indicator for the particulate loading level to aid ECTC personnel in maintaining a steady particulate loading to the CHX®. EPA Method 5 particulate sample trains were performed periodically to confirm the particulate loading. Particulate loadings from the EPA Method 5 sample trains are considered to be the official particulate loading data for Task 3.

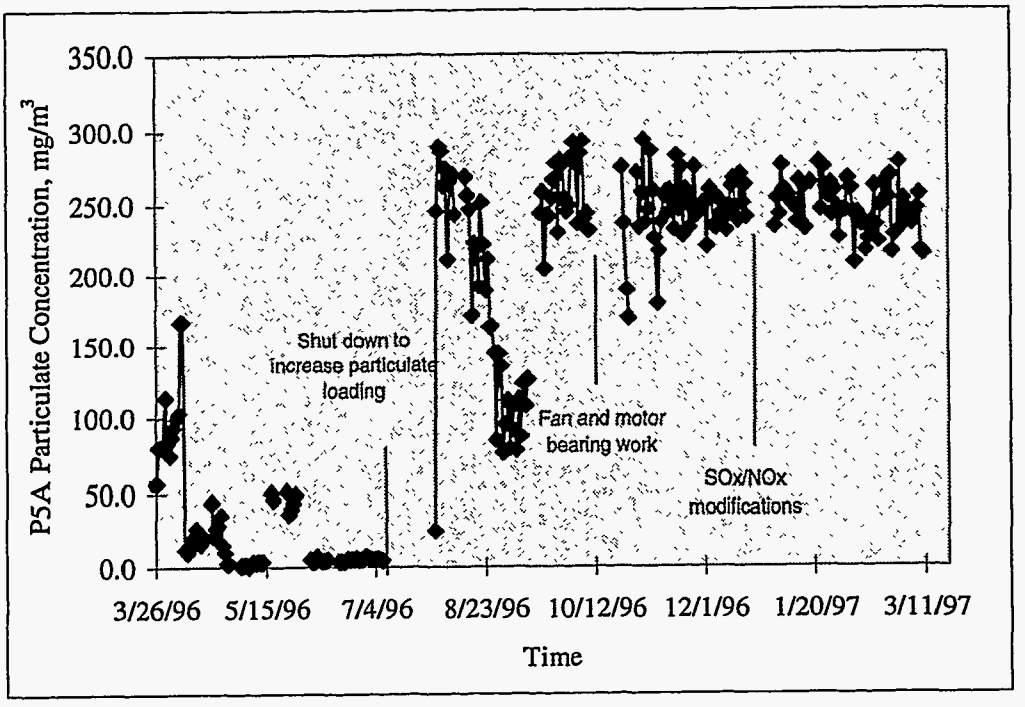

Figure 4.30 P-5A Measurements of Particulate Concentration During the One Year Wear Test

Visual inspections of the top surface of the CHX® heat exchanger were made both before and after scheduled tube washings during each inspection trip. In every case, the "dirty" inspection revealed a uniform coating of fly ash on each tube with no apparent bias from one tube to another. This coating covered the top (leading) half of each tube. Minimal fly ash was found on the bottom (trailing) half. After washing, the "clean" inspection revealed essentially complete removal of the fly ash coating, with only isolated areas (<5% total visible surface area) retaining some of the fly ash. Photographs of typical "dirty" and "clean" tubes may be found in Figures 4.31 and 4.32, respectively. The clean area in the center of Figure 4.31 is due to inadvertent contact with the tube surface prior to being photographed.

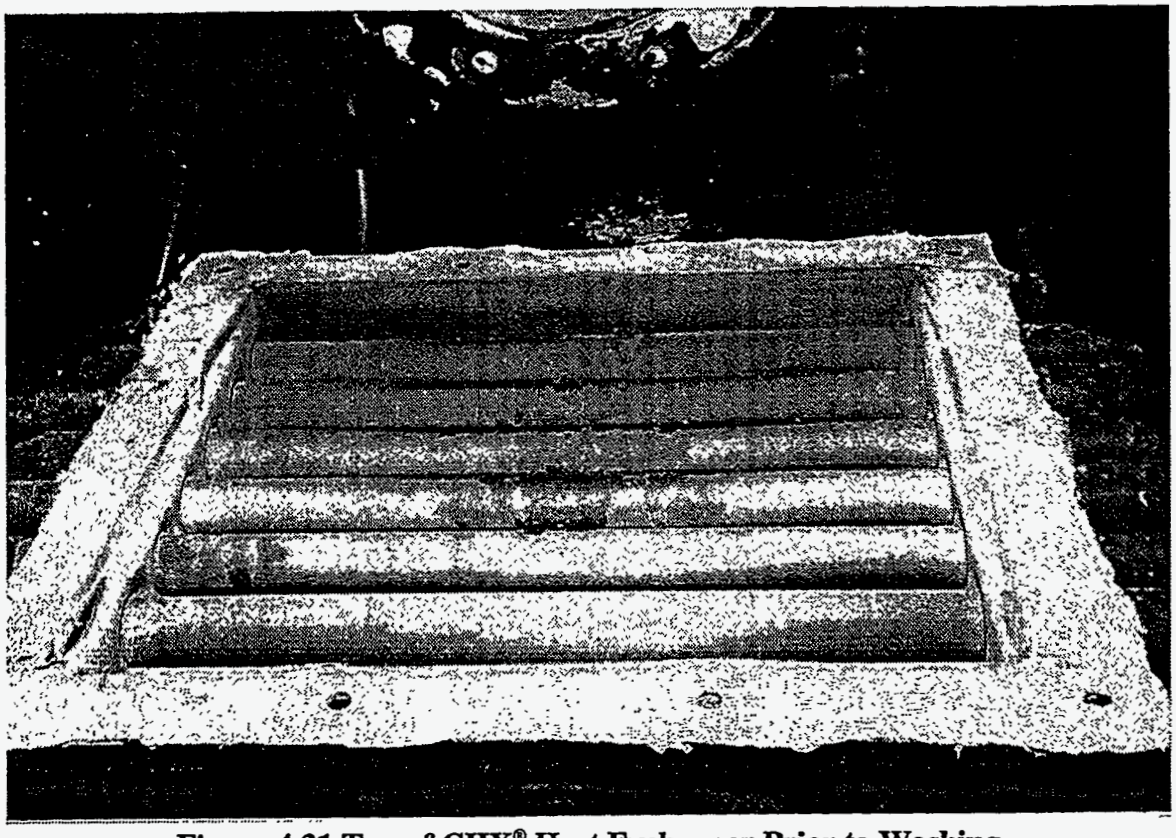

Figure 4.31 Top of CHX® Heat Exchanger Prior to Washing

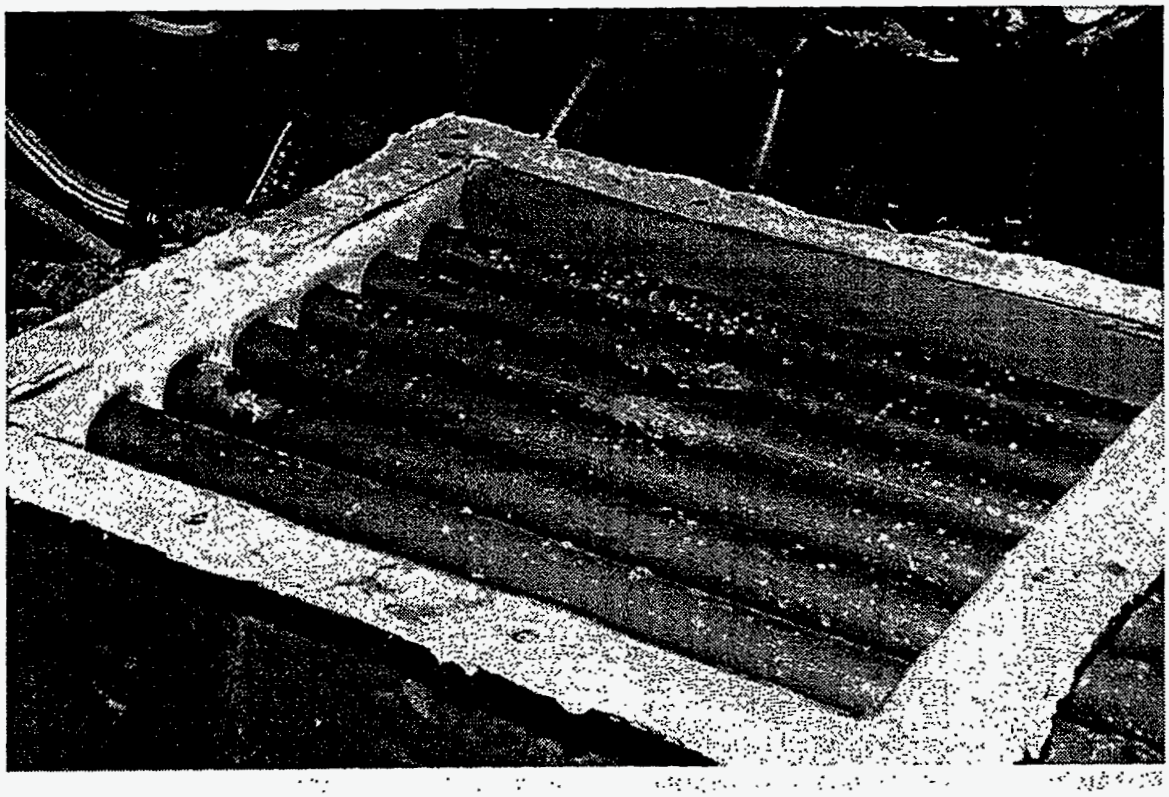

Figure 4.32 Top of CHX® Heat Exchanger After Washing

After approximately 5,000 hours of operation, several fly ash deposits were found in the heat exchanger which were unaffected by the wash cycle. These deposits began approximately halfway down the heat exchanger, on the tubes closest to the walls, and continued to the bottom of the heat exchanger. These deposits can be seen in Figure 4.33. The most likely cause for these deposits is inadequate wash water flow rate. The initial wash water setup consisted of one

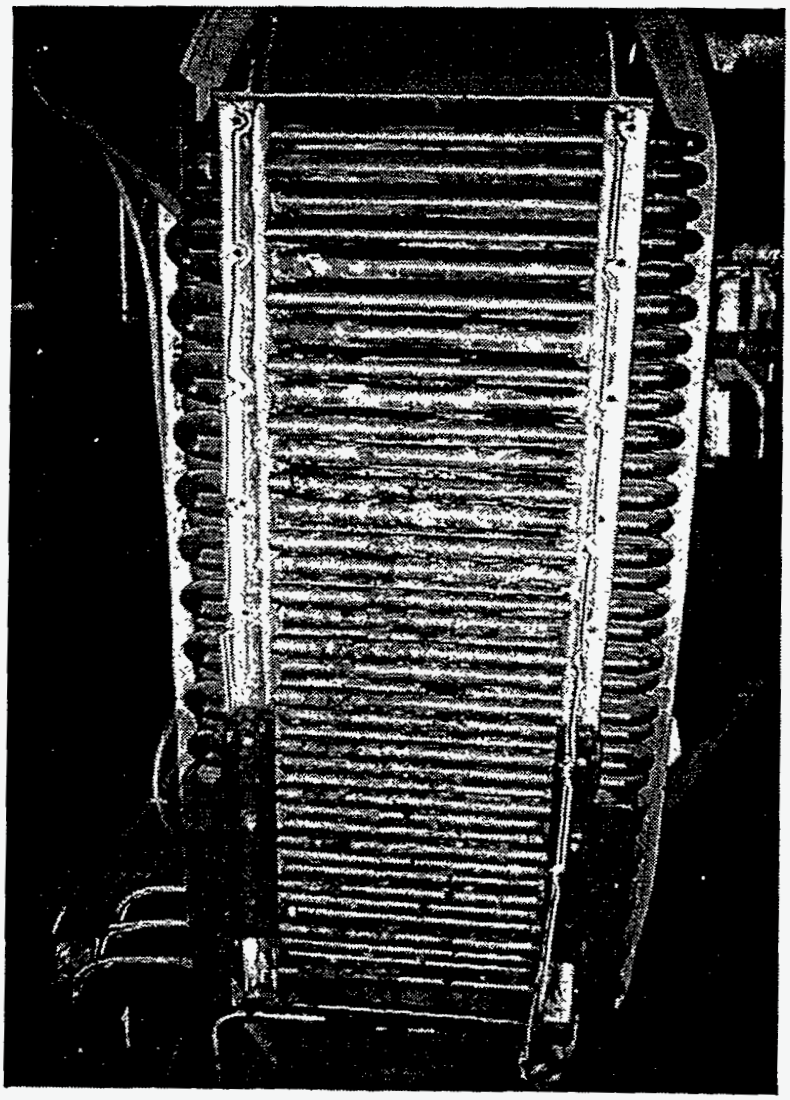

Figure 4.33 Fly Ash Deposits on the Tubes in the CHX® Heat Exchanger

(1) spray nozzle with a nominal flow rate of 3.8 lpm (1 gpm) which operated for 20 minutes every 8 hours. This is the standard wash cycle for oil-fired applications. While the top few rows of tubes were effectively cleaned, being subjected to the most energetic cleaning, the tubes further down in the heat exchanger were essentially cleaned by wash water dripping from the tubes above. Any deposits which were not removed, but only wetted, then served as sites for additional fly ash deposition. Based on these findings, a new wash nozzle manifold, consisting of three (3) equally spaced 3.8 lpm (1 gpm) nozzles, was installed for the remainder of the test. This new manifold was also operated for 20 minutes, effectively tripling the wash water flow rate.

The effect of the modified wash water manifold can be seen in Figures 4.34 and 4.35. In Figure 4.34, the percent solids of the wash water effluent is shown for the two manifold setups. For the original setup (1 nozzle), it can be seen that the percent solids concentration levels off at the end of the wash cycle, indicating that less than complete solids removal is occurring. With the modified manifold (3 nozzles), not only is the percent solids concentration continually decreasing, the initial and final concentrations are higher (and lower, respectively), indicating more complete solids removal.

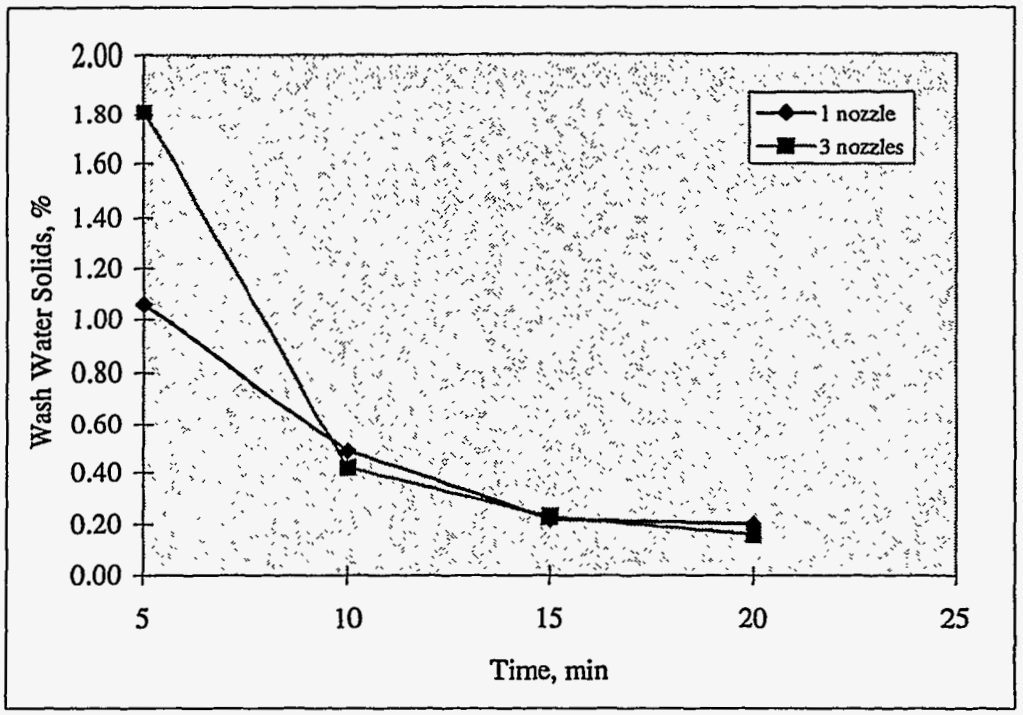

Figure 4.34 Wash Water Solids Concentration

In Figure 4.35, the heat exchanger differential pressure drop is shown as a function of time for the last four extended operating periods. The first three periods were conducted with one wash nozzle in service, the last with the three-nozzle manifold. In each of the first three operating periods, the differential pressure drop increased by approximately 100 Pa (0.4 in. H_2O) and was increasing, while the pressure drop increase for the last period was approximately 50 Pa (0.2 in. H_2O) and essentially steady.

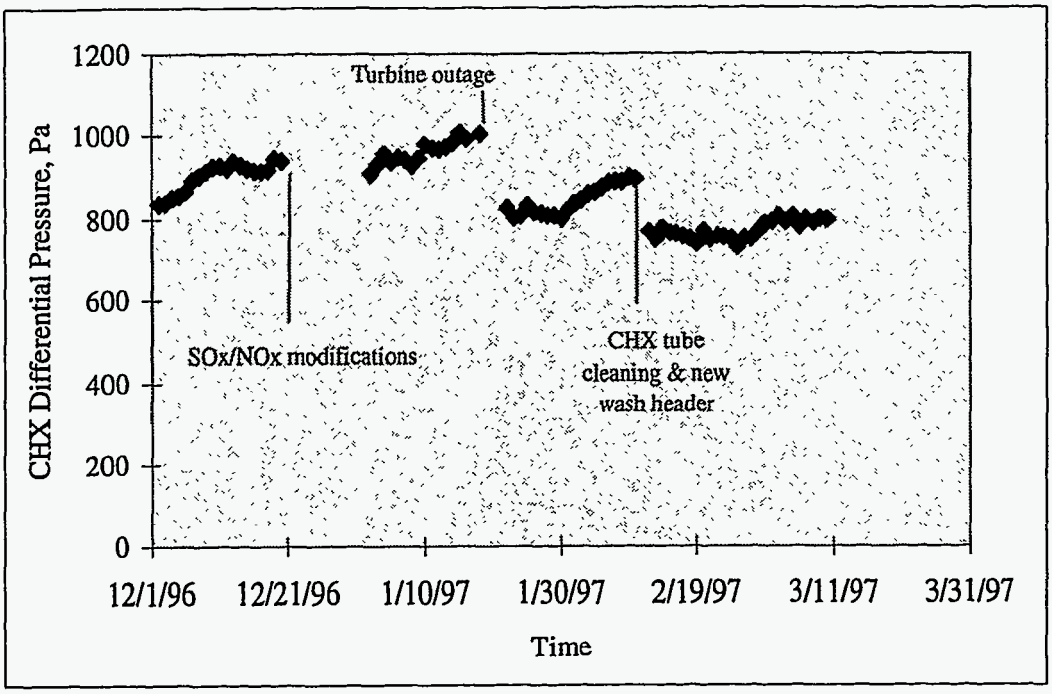

Figure 4.35 Differential Pressure Across the CHX® Unit as a Function of Time

4.9.2 Wear Performance Discussion

The primary goal of Task 3 was to determine the amount of wear, if any, incurred by the Teflon® internals of the CHX® pilot unit's heat exchanger (specifically the heat exchanger tube surfaces), while operating under typical flue gas conditions. As mentioned in Section 4.2, three measurement techniques were employed in an effort to determine the amount and type of wear. This section will focus on the results from two of the techniques (eddy current film thickness and surface replication). The third technique (vertical and horizontal tube dimensions) is not included in this discussion for the reasons outlined in Section 4.2.

Teflon® Film Thickness Measurements

Six complete sets (including measurements taken prior to flue gas exposure) of film thickness measurements were obtained during the course of the test program. Each set consists of 90 data points for the top row of tubes (3 angles * 6 tubes * 5 locations) and 30 data points for the second row of tubes (1 angle * 6 tubes * 5 locations). Tabular summaries of each of the data sets are located in Appendix A of Addendum II. All film thickness data presented in the tables and in graphical form have been normalized.

Results of the film thickness measurements indicated that no significant reduction in tube film thickness occurred during the course of the test program. Figures 4.36 and 4.37 illustrate this finding. The data presented in Figures 4.36 and 4.37 represent the average tube values for measurements taken in the vertical position for tubes 1 through 6 and tubes 7 through 12, respectively.

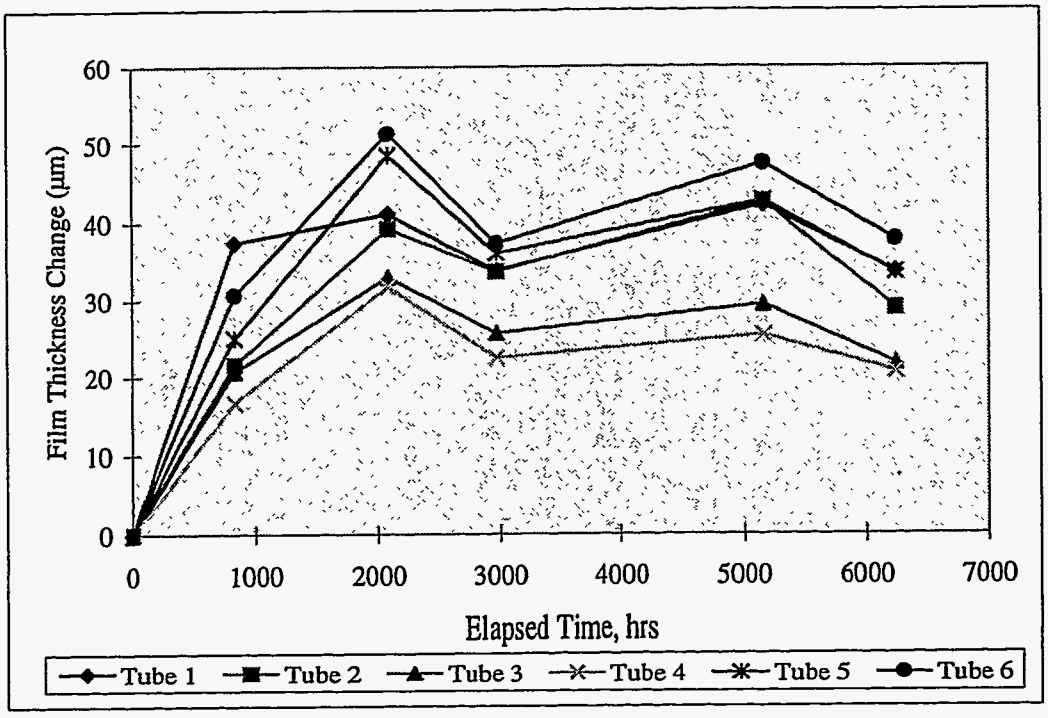

Figure 4.36 Cumulative Change in Teflon® Film Thickness as a Function of Time for Tubes 1 through 6

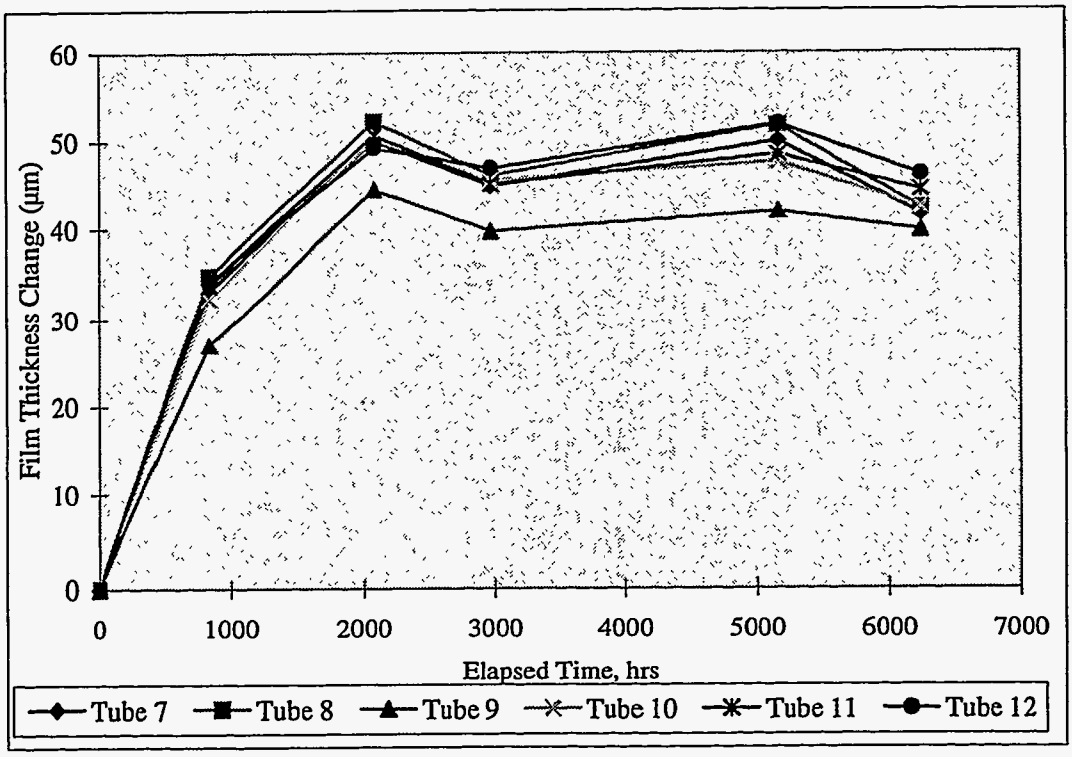

Figure 4.37 Cumulative Change in Teflon® Film Thickness as a Function of Time for Tubes 7 through 12

As illustrated in the two figures, after an initial increase in film thickness, no significant decrease was observed for any of the measured tubes. The increase in film thickness observed during the first two inspection trips is most likely due to the relaxation of surface stresses in the Teflon® film. These surface stresses result from the manufacturing process, and stress relaxation occurs when the Teflon® film is heated. The amount of increase ranged from 30.5 to 50.8 μm (1.2 to 2.0 mils), representing a 7 to 10% increase for a nominal 508 micron (20 mil) film.

As mentioned in Section 4.2, thickness measurements were also obtained for angles of +45° and -45° from the vertical at each of the measurement locations. These off-angle measurements were conducted to expand the amount of film surface being inspected and thus offer a more complete picture of any potential wear patterns and tendencies. In addition, the flue gas velocity at these locations was higher, creating the potential for greater abrasive wear than on the top surface of the tubes. In Figures 4.38 and 4.39, film thickness data is plotted as a function of both time and measurement angle for tubes 1 and 5, respectively. Due to the flue gas flow pattern from the inlet plenum to the first row of tubes, tubes 1 and 5, respectively, were chosen as representative of minimal and maximal potential wear sites. Tube 6, having the greatest potential for wear in the top row, was not chosen for this comparison due to instrument positioning problems during inspection, resulting in greater measurement variation. Plots for the other 4 tubes from the top row may be found in Appendix G of Addendum II.

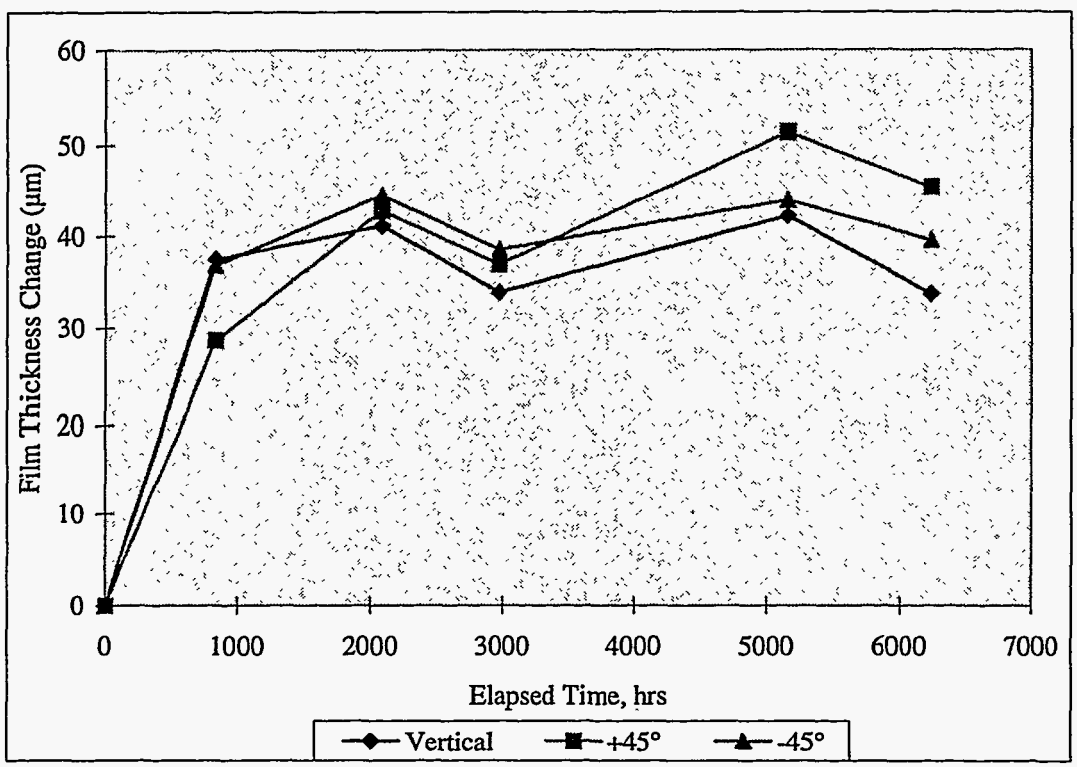

Figure 4.38 Cumulative Change in Teflon® Film Thickness as a Function of Time and Angular Position -- Tube 1

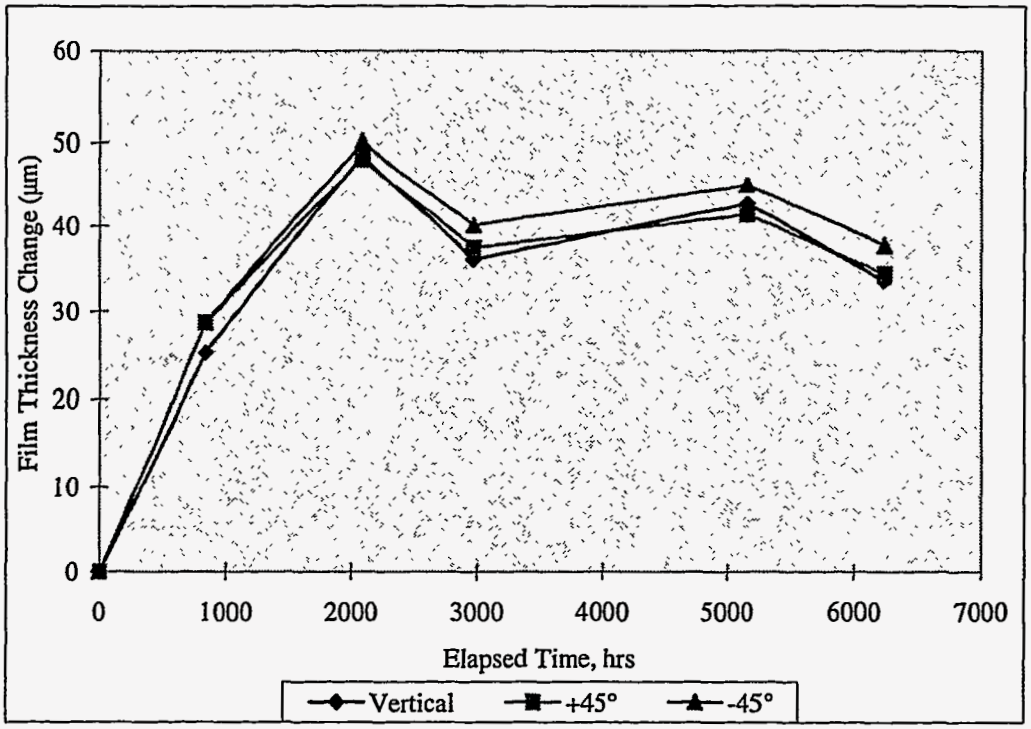

Figure 4.39 Cumulative Change in Teflon® Film Thickness as a Function of Time and Angular Position -- Tube 5

In each of the figures it can be seen that there were no significant differences in film thickness changes as a function of angular position, suggesting that high flue gas velocity areas, such as those between tubes, do not incur increased amounts of abrasive wear. Similar results were observed for the other 4 tubes in the top row of the heat exchanger. Although there appears to be a slight (10.2 µm [0.4 mil]) decrease in film thickness for tube 5, this amount is within the absolute accuracy range (+/- 1% of reading) of the thickness gage for a nominal 508 µm (20 mil) film.

Teflon® Surface Replications

Six sets (including replications made prior to flue gas exposure) of film surface replications were obtained during the course of the test program. Each set consists of 5 film replications made in the locations shown in Figure 3.1. The goal of making the surface replications was to record and observe any microscopic changes to the Teflon® tube surface which may not be evident to the naked eye or detected with the eddy current film thickness technique. As mentioned in Section 4.2, each replication was inspected under a microscope and then photographed at two different magnifications (25X and 200X). Comparisons were then made between the pre-test, intermediate and post-test replications to determine the location and amount of microscopic surface wear. Representative examples of the surface replications are shown in Figures 4.40 through 4.42. Figure 4.40 represents a typical tube surface prior to exposure to flue gas, Figure 4.41 shows the surface of tube 1, and Figure 4.42 the surface of tube 6, both at the conclusion of the test program. The microphotographs in each of the three figures were taken at a magnification of 200X.

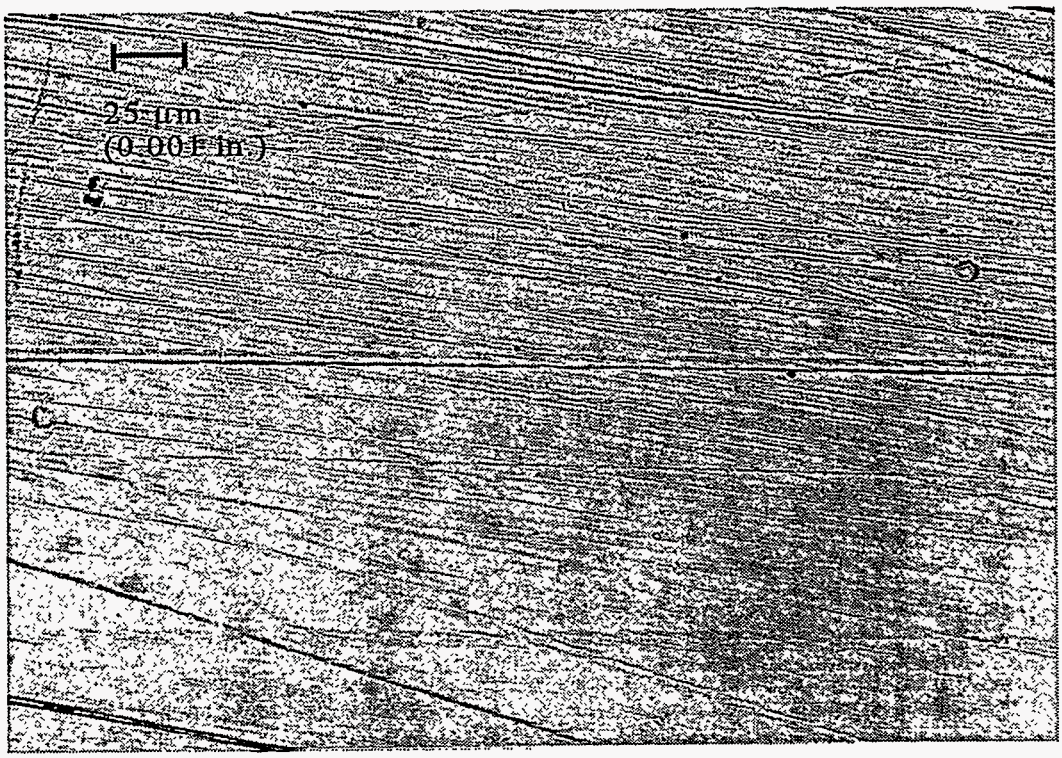

Figure 4.40 Microphotograph of Clean Tube Surface

In Figure 4.40 the surface of the Teflon® film is extremely smooth, with only minor striations running axially (lengthwise). These striations result from the manufacturing process. In Figure 4.41 (tube 1), minimal surface damage is visible. This is not unexpected in that the predicted flue gas flow pattern to the top row of tubes has a region of low flow at this tube. The vertical

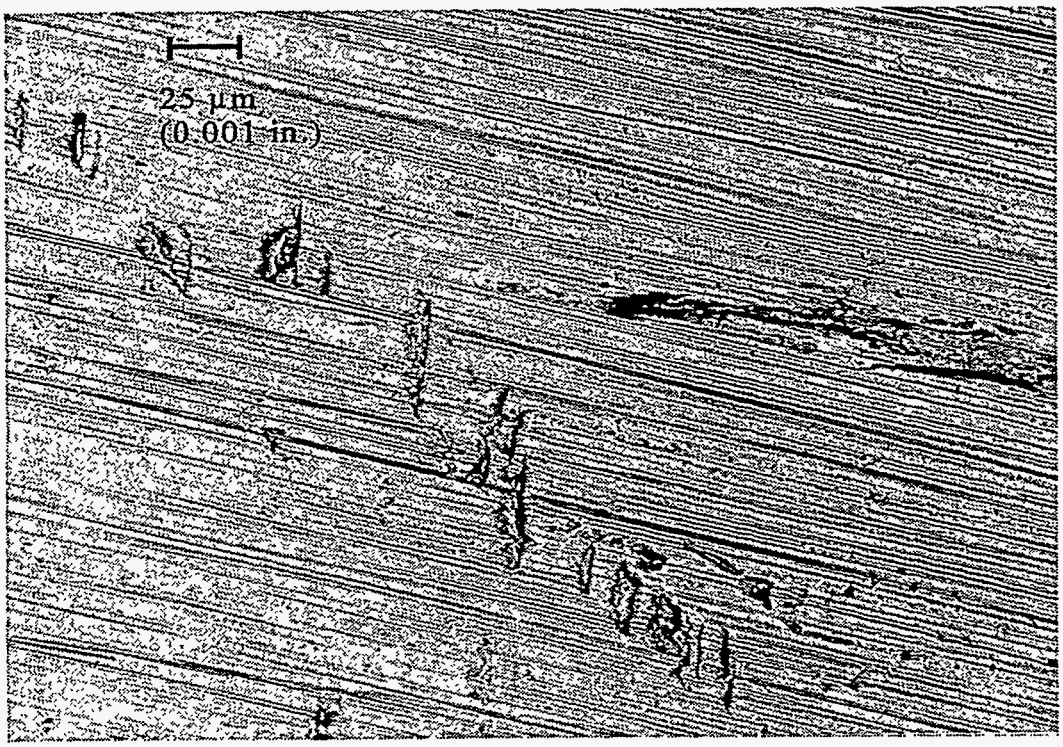

Figure 4.41 Microphotograph of Tube 1 -- End of Test

marks running from the lower right to upper left are cuts in the surface made by the calipers used to make the tube dimensional measurements (see Section 4.2). In Figure 4.42 (tube 6) some minor wear damage is visible. This also is not unexpected, since this tube was expected to see the most flue gas (and fly ash). The wear damage appears to be very fine and uniform, but very small (μm range), resembling small, circular depressions. Typically, details for any given object are visible to the naked eye down to about 200 μm (8 mils). At a magnification of 200X, this translates to a size of approximately 38.1 mm (1.5 inches) on the microphotograph. For comparison, the dark oval in the center of the Figure 4.42 is approximately 12.7 mm (0.5 inches) long, or approximately 63 μm (2.5 mils).

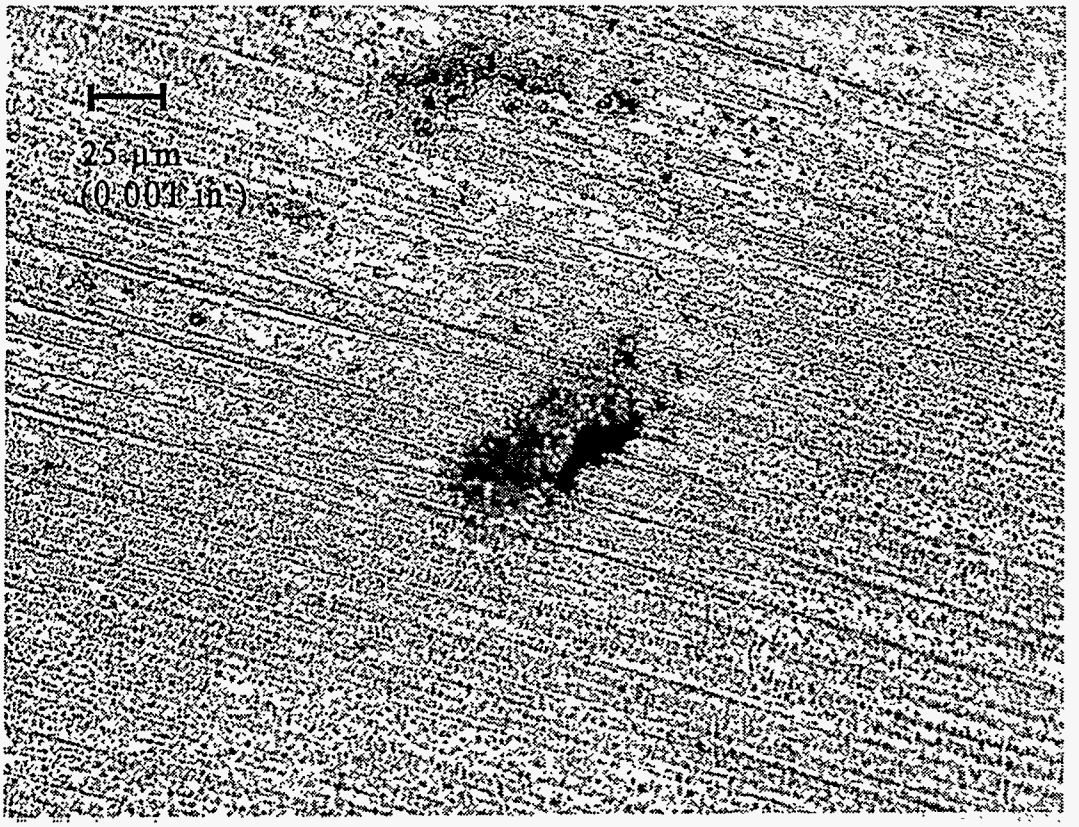

Figure 4.42 Microphotograph of Tube 6 -- End of Test

5.0 ECONOMIC ANALYSIS OF FGD TECHNOLOGIES

For the IFGT technology to be commercially viable, its effective pollution removal capability must be achieved at a competitive cost. A cost analysis of an IFGT system was developed based on the results of the pilot IFGT tests conducted in Task 2. The results of the analysis are presented in Table 5.1. This report summarizes the economic analysis methodology and discusses the results for a limestone based wet Flue Gas Desulfurization (LWFGD) system, the sodium-based IFGT system, and a mag-lime-based IFGT system.

The IFGT system used in this analysis consists of eight modules in both the first and second heat exchanger stages. One-half of the first heat exchanger consists of the standard copper-nickel and Teflon® coated water heating tubes. One-half of the first stage heat exchanger and all of the second stage consists of Teflon®-covered aluminum tubes that are open to the atmosphere. The capital, design, erection and operation costs of two IFGT systems were compared to the cost of a LWFGD system. The IFGT systems are with a soda ash reagent and mag-lime reagent.

Although the IFGT system can remove several pollutants, the analysis assumes the equipment is installed only for SO_2 removal. Credit is not taken for removal of particulate, other acid gases, ammonia, or trace elements. Credit is taken for heat recovery by the IFGT system. For this analysis it is assumed that the IFGT recovers 3% of the furnace heat release and that this heat can be returned to the power cycle, providing a 1% improvement in cycle efficiency. Credit is not taken for the reduction in emissions that result from the increase in cycle efficiency and are based on the amount of emissions per unit of electrical energy generated.

Economic analyses are sensitive to the assumptions that are used as a basis for comparison. Because the IFGT system design is based on industrial size, the capacity of the largest single unit at this time, is smaller than nearly all utility power plant scrubbers. However, for this analysis a 100 MW_e plant was assumed, requiring three IFGT units in parallel. This was compared to a single LWFGD system of the same flue gas capacity. In addition to plant size, the economic comparison assumes the plant burns a 1.5% sulfur coal, the plant thermal efficiency is 33%, and that the flue gas enters the FGD equipment at 300 F and 6% excess oxygen.

The cost components that were evaluated and the basis of the evaluation is as follows:

Capital – the cost of <u>all</u> equipment required to operate the units, gas flange to gas flange, and from receipt of the reagent to the discharge of the byproduct effluent. It includes the <u>increase</u> in the cost of the fan and motor required to offset the pressure drop through the FGD equipment. Capital cost also includes all wiring, instrumentation and controls required to operate the equipment. For each of the three FGD scenarios, B&W Inc. estimated these costs using the same procedures that are used to cost commercial offerings.

Design and Erection (D/E) - the design and erection costs were estimated at 55% of the capital cost.

Operating Power – This includes the power required to operate all the FGD auxiliary equipment.

Fan Power – The increase in fan power (kW/in W.G.) required to overcome the pressure loss through the FGD system.

Reagent – The reagent cost is sensitive to geographic location in the United States. For this estimate a representative reagent cost was used excluding shipping. The molar calcium-to-sulfur ratio used for the limestone system evaluation was 1.08. For the sodium-based IFGT system, the sodium-to-sulfur ratio used was 2.2. For the mag-lime-based IFGT the (calcium + magnesium)-to-sulfur ratio used was 1.05

By-Product Disposal – For limestone reagent it is assumed that the byproduct is dewatered and disposed in a lined landfill. The cost per pound is based on the cost of the landfill sufficient for the estimated plant life. Credit is not taken for a gypsum grade byproduct sold to wallboard manufacturers. For soda ash and mag-lime, the disposal cost represents the cost of an evaporation pond to handle the effluent for the same time period.

Heat Recovery – It is assumed that 3% of the furnace heat release is removed from the flue gas and is recovered into the plant steam cycle, resulting in a 1% improvement in cycle efficiency.

Electricity cost – Electricity is evaluated at $0.055/kW for both electricity consumed and electricity saved.

The annualized and life cycle costs associated with these components for the three FGD scenarios are shown in Table 5.1. All costs shown in the Table including the annualized and life cycle costs are in current dollars.

Comparison of the costs for the three scenarios shows the following:

Capital cost - the IFGT system is less costly than the LWFGD system by about $5 million and the total installed cost is less costly by about $7.5 million. This is due to the very few auxiliary systems required by soda ash and mag-lime systems compared to limestone systems that require a large amount of auxiliary equipment.

Power Consumption – The power consumption by the IFGT auxiliary systems is one tenth to one-fifth of that required by the LWFGD auxiliary equipment. This is entirely offset by the increase in fan power required by the higher pressure drop of the IFGT system. The total power consumption of the soda ash IFGT is slightly less than the limestone process while the mag-lime IFGT is slightly greater.

Reagent cost – the annualized cost of soda ash is nearly $2 million more than limestone, while mag-lime is about $0.4 million more. The reagent cost is a significant portion of the total annualized operating cost for the IFGT systems.

Byproduct disposal – soda ash and mag-lime disposal costs are both about $.13 million greater than the limestone process wastes. LWFGD. This is due entirely to limestone dewatering which reduces the byproduct volume by about 50%.

Annual operating cost – The annual operating cost for the soda ash exceeds the limestone process $2 million, while mag-lime costs are $0.65 million more. The cost differential is almost entirely due to reagent cost.

Heat Recovery – The annual cost recovery for a 1% improvement in cycle efficiency achieved with the IFGT is $0.48 million.

Total Annual Cost – the total annual cost of the mag-lime IFGT (operating, annualized D/E and heat recovery) is about $.22 million less than LWFGD, while the soda ash IFGT is about $1.1 million more.

Life Cycle Cost – The total life cycle cost of the mag-lime IFGT is $4.4 million less than for LWFGD. This represents about a 10% savings. The slightly greater operating cost associated with mag-lime IFGT is offset by the much lower D/E cost. The life cycle cost of the soda-ash IFGT is $23 million greater than LWFGD. All of the greater cost is attributable to the cost of the reagent.

As shown by the above analysis, a mag-lime IFGT system can provide a less expensive alternative to sulfur removal than LWFGD at a 100 MW scale. The power cost for both systems is about the same, while the higher cost of the mag-lime is nearly offset by heat recovery. What could be the most attractive feature of the mag-lime system is the relatively low initial cost of the system. The total D/E cost for LWFGD is equivalent to $212/kW, while the mag-lime system is equivalent to $136/kW, installed. As the plant size increases, the cost per installed kW decreases for LWFGD so that for a 1200 MW plant the cost of installed LWFGD is about $90/kW. IFGT units larger than 35 MW have not yet been designed. Some reduction in installed kW is expected with increased size, but the magnitude is not known. Based on past analyses of LWFGD, the installed cost of the two units will be about equivalent for a plant size of about 400 MW.

Table 5.1 provides a comparison of three scenarios for flue gas desulfurization. This is the first rigorous evaluation of the cost of IFGT compared to LWFGD. In addition to providing cost comparison Table 5.1 also indicates the costly components of the IFGT system, indicating areas of improvement. For the IFGT systems, fan power to overcome gas side pressure drop is the most expensive component of operating power. The pressure loss in an IFGT can be easily reduced by reducing the surface area of the tubes in the first or second stage. This is equivalent to reducing the number of heat exchanger modules in each stage from the standard eight to seven or six. In this analysis, the surface area is not required for heat transfer. This surface may be required to maintain effective particulate removal (if needed) or SO2 removal, and this will have to be determined.

Table 5.1 Preliminary Economic Comparison

COMPARISON VARIABLES	LIMESTONE WET FGD SYSTEM	SODA ASH BASED IFGT SYSTEM	MAG-LIME BASED IFGT SYSTEM
COST (U.S. Dollars)			
Captial Cost	$13,671,269	$8,745,157	$8,773,721
Erection Cost	$7,519,198	$4,809,836	$4,825,547
Total Design & Erection (D/E Cost)	$21,190,467	$13,554,993	$13,599,268
POWER			
Gas Side Pressure Drop (in. WG)	8.86	11.00	12.20
ID Fan Power (kW/in WG)	200	200	200
Increased ID Fan Electricity (kW)	1772	2200	2440
Auxiliary Power Consumption (kW)	657	49	129
Total Power Consumption (kW)	2429	2249	2569
Annual Cost ($/Year)	$819,205	$758,498	$866,421
REAGENTS			
Consumption (lb/hr)	4,335	4,262	2,187
$ / ton	$5.44	$110.00	$57.00
Annual Cost ($/YR)	$72,304	$1,437,402	$382,204
BY-PRODUCT DISPOSAL			
Product (Lb/Hr)	9,244	20,554	20,069
Disposal Cost ($/lb)		$0.0014	$0.0014
Operating - hours per year	6132	6132	6132
Annual Cost ($/YR)	$0	$175,192	$171,058
ANNUAL OPERATING COST			
Reagent	$72,304	$1,437,402	$382,204
Power	$819,205	$758,498	$866,421
By-Product Disposal	$0	$175,192	$171,058
Annual Cost ($/YR)	$891,508	$2,371,091	$1,419,683
HEAT RECOVERY			
Annual Heat Recovery	$0	$481,800	$481,800
TOTAL COSTS (Annual)			
Heat Recovery	$0	($481,800)	($481,800)
Operating Cost	$891,508	$2,371,091	$1,419,683
D/E Cost (Annualized at 15.2%)	$2,728,488	$1,745,343	$1,751,044
Total Cost (Annual)	**$3,619,996**	**$3,634,635**	**$2,688,927**

Basis
Plant Load Factor = 70%
Plant Life = 30 years
Capital Levelization Factor = 15.2%
Cost of Electricity = $0.055/kW

6.0 CONCLUSIONS

The work performed under Tasks 2 and 3 of this Phase I contract have shown the IFGT to be a potentially viable new technology for the abatement of both major and minor gaseous and particulate pollutants from fossil fired boilers. The Task 2 tests demonstrated that the IFGT was capable of removing several pollutants in an efficient and low cost manner. The wear tests conducted in Task 3 showed that no significant wear problems were implicit with the use of Teflon® covered heat exchanger tubes. The preliminary economic comparison of the IFGT when compared to the dominant commercial FGD LSFO process compared very favorably. Some of the more important conclusions drawn from this work are summarized below.

SO_2 Removal

The IFGT process has exceeded the goal for SO_2 removal, providing greater SO_2 removal than a conventional wet scrubber operating at similar L/G. The sodium carbonate reagent is highly reactive and has sufficient dissolved alkalinity to remove all of the SO_2 in high sulfur flue gas even at very low liquid-to-gas ratios. Greater than 95% removal of SO_2 at L/Gs less that one tenth of that required by conventional LSFO systems shows that the surface area of the tubes in the second stage provides more than adequate gas-liquid contact for SO_2 absorption.

The 50% SO_2 removal using lime slurry and the 88% removal efficiency of the mag-lime slurry reflects the diminished absorption capacity of these reagents. The estimated removal efficiencies for a 0.75% sulfur coal are estimated to be approximately 70% for lime and 95% with mag-lime.

The SO_2 removal tests using calcium based reagents confirm that they are potentially acceptable alternatives to the sodium based reagents. This is significant from the standpoint of operation costs, disposal costs, and environmental issues. Calcium based byproducts are environmentally benign and are potentially saleable.

Particle Removal

At full load, the particle removal efficiency of the IFGT process exceeded goals. The overall removal efficiency depends on the particle size distribution of the fly ash entering the IFGT system. Removal efficiency for particulate greater than 2.5 microns averaged 98%. More significantly, the removal efficiency for particulate smaller than 2.5 microns averaged 76%. These fine particulate, referred to as PM2.5, will be regulated in the near future, and while the exact nature of the regulations are not yet defined, the IFGT process provides the capability to address these forthcoming regulations. The test data show that while the removal efficiency is dependent on the size distribution of the coal, it is otherwise independent of coal type.

Particle removal was achieved at an inlet particle loading up to 800 mg/dscm. For a typical utility coal-fired boiler this represents about 10% to 15% of the fly ash removed by particulate clean-up devices. Higher particulate loading is possible, but the point at which high particle loading affects the performance (removal efficiency or cleaning) of the IFGT has not been determined. Although the IFGT process may not be capable of handling the full particulate loading from a boiler, it can provide relief from operational problems and upsets associated with particle removal devices. In the case of an ESP, the IFGT could augment or replace some of the

particulate removal capability of the ESP. In the case of a baghouse, an IFGT could accommodate an increase in particulate loading due to damaged bags, providing more flexibility to plant operation.

The IFGT system was operated at particle loading up to 800 mg/dscm without problems in handling or disposing of the particulate from the system. The fly ash retained on the heat exchanger tubes was easily rinsed by increasing the flow rate of rinse water above the design value of about 60 liters per minute per square meter (1.5 gpm/ft^2). The design value is based on experience with oil and gas-fired units, and the increase in flow needed for the higher loading of coal fly ash is expected.

Mercury

The goal for vapor phase mercury removal of 90% was not achieved. Measured removal efficiencies for vapor phase mercury ranged from +69% to -23% and was significantly dependent on relative amounts of ionic and elemental mercury. Ionic mercury removal ranged from 75 to 85%. There was no measurable removal of elemental mercury. In fact, some tests indicated an increase in elemental mercury across the IFGT. This result could be an artifact of sampling techniques or could be caused by reduction of ionic mercury in the aqueous phase and subsequent evolution of elemental mercury.

The inability to remove elemental mercury in the IFGT system indicates that flue gas temperature is not a significant factor in the removal of this specie. The flue gas temperatures in the IFGT were about 15°C (27°F) cooler than in wet FGD systems, while the measured removal efficiencies closely parallel results obtained in other studies.

Ionic mercury removal was essentially the same for all tests, and no clear trend with operating condition over the range tested was evident. If the effects of operating condition are small, they could easily be masked by the overall accuracy of the measurements. The removal efficiency for ionic mercury parallels that obtained in conventional wet FGD systems that operate with different scrubbing chemistry, pH and L/G.

Full-load particulate mercury removal ranged from 55% to 80%. This is less than the total particle removal efficiency. The cause of the difference is the enrichment of mercury in the fine particulate and the fact that the fine particulate removal for the IFGT is less than the overall removal.

Chloride and Fluoride

The goals for chloride and fluoride removal from the flue gas were met with the IFGT system. Except for one outlier (Test I-4A) the chloride removal averaged 98.2% over all tests. Fluoride removal ranged from 83% to 99% for the coals and operating conditions tested. Many chloride and fluoride compounds tend to be highly soluble in aqueous solutions and the high measured removal efficiencies were expected.

NO_x

NO_x removal measured in test series I averaged essentially 0%, and so these measurements were suspended for the balance of the tests. Either the sodium reagent was not effective at removing the NO_2, or the NO_2 component of total NO_x was too small to detect any change in concentration of total NO_x.

Ammonia

Ammonia removal ranged from 50% to 90% depending primarily on the scrubbing solution pH, dissolved solids, and the flue gas outlet temperature. Although there are no Federal regulations for ammonia removal, state and local emissions limits typically range from 2 to 10 ppm. The IFGT can effectively remove ammonia to these concentrations, thereby providing the means to more completely remove NO_x with SCR and SNCR systems.

Trace Elements

The test data showed that arsenic and selenium were the only vapor phase trace metals that were consistently detected. Other elements were occasionally detected in reportable quantities but measurement repeatability was poor. The removal efficiencies for arsenic and selenium averaged greater than 95%.

Heat Recovery

Heat recovery averaged 5.0% of furnace heat release with an inlet flue gas temperature of 120°C (250°F), an outlet flue gas temperature of 35°C (95°F) and a cooling water inlet temperature of 30°C (86°F). At these conditions the outlet flue gas temperature is at or above the water vapor dew point and all of the heat recovery is in the form of sensible heat. For inlet flue gas temperatures of 150°C (300°F), which is more typical for back-end gas cleanup, the heat recovery would increase to 6% of the furnace heat release.

For utility power plants, the amount of useable heat that can be recovered from the flue gas will depend on the temperature at which heat is rejected in the power cycle. Typically, this is higher than the 30°C used in this test, and is closer to 60°C (140°F). With this restriction the energy that can be recovered into the power cycle is reduced to about 3% of the furnace heat release.

This energy recovery is significantly less than the 8% to 12% that can be recovered in gas-fired industrial processes. In industrial processes the cooling water temperature can be as low as 10°C (50°F), the flue gas temperature in excess of 175°C (350°F) and the water vapor dew point near 60°C (140°F). Still, a 3% energy recovery can provide a 1% increase in generated electricity. For a 100 MW plant this is equivalent to approximately $.5 million per year. This improvement in efficiency can partially offset the operating cost of the IFGT equipment.

Wear

The single-stage pilot CHX® unit installed at the ECTC operated for over 6,200 hours. Visual inspections, film thickness measurements, and film surface replications were performed at various times during the test program. No significant wear was detected on any of the tube surfaces. Specific conclusions about the wear test results include the following:

Particulate Deposition: At higher particulate loadings, deposition can be a problem, particularly if inadequate wash water flow rates are used. Wetted ash surfaces which are not removed during washing become sites for additional ash deposition, resulting in increases in heat exchanger pressure drop. Installation of the modified, 3-nozzle manifold (and subsequent increase in flow rate) seemed to alleviate this problem. For oil applications, the "design" wash schedule is 40.75 l/min/m^2 (1 gpm/ft^2) for 10 minutes. Based on the results from this test program, this rate will need to be increased for higher particulate loadings such as coal-fired utility applications.

Film Thickness: No significant decrease in film thickness was detected during the course of the test program. After an initial increase in film thickness resulting from surface stress relaxation during heating, film thicknesses remained essentially constant. Some locations exhibited a slight decrease (0.4 mils) in thickness, but this amount is within the absolute accuracy range (+/- 1% of reading) of the thickness gage. Measurements at various angular positions around the circumference of the tubes also showed no significant wear, even in areas of high flue gas velocity.

Film Surface: Surface replications taken during the course of the test program revealed only minor, microscopic wear damage to the surface of the Teflon® film, and only on tubes subjected to the highest flue gas flow rates. The wear damage appeared to be on the m. level and was very fine and uniform, resembling round depressions in the film surface. At this scale, this type of wear damage should pose no problems for long-term operation of a large-scale unit.

Predicted Teflon® Film Life: Based on the measurement data, the Teflon® coating on the heat exchanger tubes should have a life expectancy of greater than 10 years. If the 0.4 mil decrease observed for some tube locations is correct, 10 years of operation would yield an approximate decrease in film thickness of 4 mils from a nominal film thickness of 20 mils. It would be more probable that any tube replacement would be due to other operational problems (e.g., scale buildup, temperature excursions due to cooling water failure, etc.). For comparison, operation at a particulate loading of 400 mg/dscm (0.35 lb/10^6 Btu) for 6 months is equivalent to 10 years at 20 mg/dscm (0.017 lb/10^6 Btu).

Comparative Economic Analysis

The comparative economic analysis performed as part of this program is sufficiently promising to give encouragement for the continued pursuit if the development of the IFGT concept to commercial reality.

Based on the results of Phase I testing we can conclude that the overall objectives of Phase I, have been met. Specifically,

- The pollutant removal performance of the IFGT process for pollutants that are currently regulated, or for which regulations are being considered, have been characterized for a range of operating conditions and for a range of coal types.

- Most of the pollutant removal goals for the IFGT process were demonstrated. Removal of vapor phase mercury, and the elemental form of mercury in particular was less than originally expected, but in general agreement with data for other types of flue gas treatment equipment.

- Tests with calcium-based reagents have shown that they are a feasible alternative to sodium reagent for low sulfur coals. Process modifications to permit higher L/Gs or greater dissolved alkalinity in the reagent will likely provide 90%+ SO_2 removal for higher sulfur coals.

- The increase in SO_2 transfer units with L/G for both soda ash and calcium reagents was less than expected, and indicates a possible mal-distribution between the liquid scrubbing solution and the flue gas. This mal-distribution is most likely associated with the region near the walls of the second-stage heat exchanger. This type of wall effect is common in small pilot-scale facilities. Larger test facilities provide performance results more representative of commercial scale equipment.

- The IFGT is an effective particulate removal device, removing over 98% of particulate greater than 2.5 microns and 76% of particulate smaller than 2.5 microns. The removal of the fine particulate is especially important in view of impending regulations on PM 2.5.

- The IFGT is effective at removing vapor phase selenium and arsenic, the only trace elements that were repeatably measured in significant quantities in the flue gas.

- The operating temperatures and water vapor content of the flue gas for utility power boilers will typically limit heat recovery to about 3% of the boiler heat release. This heat recovery can increase plant efficiency, providing a substantial economic benefit and reducing emission of pollutants on the basis of energy produced.

- The Integrated Flue Gas Treatment process successfully removes multiple pollutants (SO_2, HCl, HF, particulate, ammonia, arsenic, selenium, and mercury) in a single device.

- At least ten year life of the Teflon® covering of the heat transfer surface is achievable.

- Magnesium enhanced lime is more cost effective than soda ash for use with the IFGT.

7.0 REFERENCES

1. Fogiel, M., "The Essentials of Transport Phenomena II," The Research and Education Association, 1987.

2. Holman, J.P., "Heat Transfer - Fourth Edition," McGraw Hill, 1976.

3. Johnson, J.W., "A Computer-Based Cascade Impactor Data Reduction System," Southern Research Institute, March 1978, EPA-600/7-78-042.

4. U.S. Geological Survey Coal Quality (COALQUAL) Database: Version 1.3, OPEN FILE-REPORT 94-205, 1994.

5. EPRI, "Electric Utility Trace Substances Synthesis Report - Volume 3," EPRI TR-104614-V3, 1994.

6. Peterson, J.R., et al, "Mercury Emissions Control By Wet FGD Systems: EPRI Pilot-Scale Results," EPRI, DOE, EPA 1995 SO_2 Control Symposium.

7. Sloss, L.L., "Mercury Emissions and Effects - The Role of Coal," IEA Coal Research Report ISBN 92-9029-258-X, 1995.

8.0 BIBLIOGRAPHY

P.V Danckwerts., "Gas-Liquid Reactions," McGraw-Hill, 1970.

J.B. Jarvis, et al, " The Effect of High Total Dissolved Solids on Wet Lime-Limestone Flue Gas Desulfurization Systems," EPRI TR-100242, 1991.

J.F. Zemaitis, et al, " Handbook of Aqueous Electrolyte Thermodynamics," AICHE, 1986.

9.0 LIST OF ACRONYMS AND ABBREVIATIONS

ARC	Alliance Research Center
B&W Inc.	Babcock and Wilcox Inc.
CHX®	Condensing Heat Exchanger (trademarked product name)
ECTC	Environmental Control Technology Center
EPRI	Electric Power Research Institute
FGD	Flue gas desulfurization
IFGT	Integrated flue gas treatment (trademarked product name)
MTI	McDermott Technology Inc.
PRB	Powder River Basin
USDOE	United States Department of Energy
USEPA	United States Environmental Protection Agency